

NASA Contractor Report 187086

11N-20  
190197  
98P

## SPDE/SPRE Final Summary Report

George Dochat  
*Mechanical Technology Incorporated*  
*Latham, New York*

(NASA-CR-187086) SPDE/SPRE FINAL  
SUMMARY REPORT (Mechanical  
Technology) 98 p

N94-15482

Unclas

September 1993

63/20 0190197

Prepared for  
Lewis Research Center  
Under Contract NAS3-23883

**NASA**

National Aeronautics and  
Space Administration



## TABLE OF CONTENTS

SECTION	PAGE
LIST OF FIGURES .....	v
LIST OF TABLES .....	vii
1.0 INTRODUCTION .....	1
2.0 SPDE OVERVIEW .....	3
2.1 SPDE Design .....	3
2.2 SPDE Testing in 1986 .....	4
2.3 SPDE Accomplishments .....	15
3.0 SPRE OVERVIEW .....	17
3.1 Engine and Test Configuration .....	17
3.2 Test Procedure .....	20
3.3 Test Results .....	20
4.0 HYDRODYNAMIC BEARING EVALUATION .....	25
4.1 Test Results .....	26
4.1.1 Rig Tests .....	26
4.1.2 Engine Tests .....	27
4.2 Conclusions .....	28
4.3 Recommendations .....	29
5.0 SPRE LINEAR ALTERNATOR DYNAMOMETER EVALUATION .....	31
5.1 Test Results .....	31
5.1.1 Locked Plunger Test .....	31
5.1.2 Open-Circuit Voltage Test .....	32
5.1.3 Alternator Performance Test with a Nonmagnetic Adjacent Structure .....	32
5.1.4 Alternator Performance Test with Magnetic Adjacent Structure .....	34
5.2 Conclusions .....	35
6.0 SPRE HEAT PIPE HEATER HEAD .....	37
6.1 Heater Head Design .....	37
6.2 Thermal Analysis .....	40
6.3 Stress Analysis .....	42
6.3.1 Creep Analysis .....	42
6.3.2 Outer Shell Fatigue Evaluation .....	43
6.3.3 Heat Pipe Penetration Fatigue Evaluation .....	43
6.3.4 Heat Well Stress Analysis .....	43
6.4 Recommendations .....	47
APPENDIX A: SPDE INSPECTION AND BUILD SUMMARY .....	49
APPENDIX B: SPDE DATA SUMMARY REPORTS .....	55
APPENDIX C: SELECTED SPDE PLOTS PRODUCED FROM APPENDIX B DATA .....	67
APPENDIX D: SPRE HIGH-EFFICIENCY ALTERNATOR TEST .....	77
REFERENCES .....	103

~~FIG 1.1.1~~ INTENTIONALLY BLANK

THE FOLLOWING INFORMATION IS FOR YOUR INFORMATION ONLY. IT IS NOT TO BE USED FOR ANY OTHER PURPOSE.

THIS INFORMATION IS FOR YOUR INFORMATION ONLY. IT IS NOT TO BE USED FOR ANY OTHER PURPOSE.

THE FOLLOWING INFORMATION IS FOR YOUR INFORMATION ONLY. IT IS NOT TO BE USED FOR ANY OTHER PURPOSE.

**INTENTIONALLY BLANK**

PREPARED BY: [REDACTED]

## LIST OF FIGURES

NUMBER	PAGE
1	Space Power Demonstrator Engine .....3
2	SPDE Heater Head During Assembly .....7
3	Completed SPDE Heater Head Assembly with Regenerator Screens .....7
4	Completed SPDE Cooler Ready for Installation into Heater Head Assembly .....8
5	SPDE Post and Flange and Displacer .....8
6	Completed SPDE Displacer Drive Assembly on Assembly Stand .....9
7	SPDE Power Piston .....9
8	SPDE Power Piston Cylinder with Inner Alternator Stator Attached .....10
9	SPDE Alternator Stator .....10
10	SPDE Installed in Test Cell .....11
11	Hot Engine Test: Piston PV Power .....12
12	Hot Engine Test: Stroke Ratio .....12
13	Hot Engine Test: Displacer-to-Piston Phase Angle .....13
14	Space Power Research Engine .....19
15	SPRE Test: Piston PV Power .....22
16	SPRE Test: Engine PV Efficiency .....23
17	SPRE Test: Electrical Power Output .....24
18	SPRE Test: Alternator Power vs. Piston PV Power .....24
19	Cylinder No. 1 Configuration .....26
20	Cylinder No. 2 Configuration .....27
21	Locked-Plunger: Voltage vs. Current .....32
22	Alternator Open-Circuit Voltage at 21-mm Plunger Stroke .....33
23	Predicted vs. Measured Alternator Efficiency with Nonmagnetic Adjacent Structure .....33
24	Predicted vs. Measured Alternator Performance with Nonmagnetic Adjacent Structure at Frequencies to 87 Hz .....34
25	Alternator Performance Comparison with Magnetic and Nonmagnetic Adjacent Structure .....35
26	Top View — SPRE Head .....38

PRECEDING PAGE BLANK NOT FILMED

## LIST OF FIGURES (Continued)

NUMBER	PAGE
27	SPRE Heat Exchangers .....39
28	Material Creep Properties .....40
29	SPRE Wall Temperature Analysis .....41
30	High-Cycle Fatigue at Low Temperature .....44
31	High-Cycle Fatigue at High Temperature .....44
32	Predicted Stress vs. High-Cycle Fatigue at High Temperature .....45
33	Creep SPRE Heater Wells Assuming Compressive Creep is the Same as Tensile Creep .....46

## LIST OF TABLES

NUMBER	PAGE
1	SPDE Design Point Operating Parameters .....5
2	SPDE Materials .....5
3	SPDE Engine Geometry .....6
4	HFAST Comparison with Actual Performance at Selected SPDE Operating Points .....14
5	SPRE Engine Geometry .....18
6	SPRE Acceptance Test Points .....21
7	Tuning Capacitors Required at Various Operating Pressures .....22
8	Hydrodynamic vs. Hydrostatic Bearing Losses .....28





## 1.0 INTRODUCTION

To support the objectives of the SP-100 program in assessing the applicability of power conversion technologies to a space-based power generating system, NASA-Lewis Research Center (NASA-LeRC) awarded an initial 17-month contract, NAS3-23883, to Mechanical Technology Incorporated (MTI) to design, fabricate, and test a space power demonstrator engine (SPDE). The goal of the SPDE program was to demonstrate the feasibility of free-piston Stirling engine (FPSE) power converter systems for space applications. The FPSE power converter offers the potential for extremely long life, high reliability, and excellent efficiency at low hot-to-cold temperature ratios, and can provide this efficiency at a relatively low heater head temperature. All of these attributes are attractive to a space power conversion system.

MTI's SPDE design consisted of two identical submodules in an opposed configuration. The SPDE was on test in 16 months and was operated at full design conditions. The engine was developed over the next year to achieve the majority of its design goals. When the engine development was complete, MTI and NASA-LeRC decided to separate the submodules of the engine to accelerate continued development of space power converter technology. The SPDE submodules were named space power research engines (SPREs), with SPRE-I located at NASA and SPRE-II located at MTI.

The purpose of this report is to summarize MTI's test and development activities within the SPDE/SPRE program. Section 2.0 presents an overview of the SPDE portion of the program. Section 3.0 describes results of SPRE testing, and Section 4.0 presents results of testing performed on SPRE power piston hydrodynamic bearings.

Initial SPDE tests indicated that the linear alternator efficiency shortfall of 70% (versus 90% design) was attributed to the magnetic structure surrounding the alternator. The SPRE alternator was tested on a linear dynamometer with both magnetic and nonmagnetic structures. Section 5.0 contains the results of this testing.

Finally, Section 6.0 describes MTI's design of a heat pipe heater head that would integrate with the SPRE and is a potential approach for a heat input system in advanced engines. This heat pipe design provides a design against which alternative designs can be measured.

216 INTENTIONALLY BLANK

## 2.0 SPDE OVERVIEW

The objective of the SPDE program was to design, build, and demonstrate with full-scale hardware the key technology issues that would permit selection of the FPSE generator as the space power conversion system. Key technology issues to be demonstrated included:

- 25-kW<sub>e</sub> power output
- 25% system efficiency (electric power out/heat into the head)
- 8 kg/kW<sub>e</sub> (17.6 lb/kW) specific power
- Temperature ratio of 2.0
- Hot-end temperature of 630 K, cold-end temperature of 315 K
- Successful application of hydrostatic internal gas bearings
- Dynamic balance (less than 0.08 mm) vibration amplitude along any axis.

### 2.1 SPDE Design

The SPDE consisted of two identical 12.5-kW<sub>e</sub> FPSE submodules (shown in Figure 1) in an opposed (heater head to heater head) in-line configuration. Each submodule contains a linear, monocoil permanent-magnet alternator. The submodules are standard, spring-to-ground, virtual-rod-displacer engines with helium as the working fluid. The engine heater and cooler are annular, tube-in-shell units, with the engine working fluid passing through the tubes. The regenerator is an annular, stacked screen matrix sandwiched between the heater and cooler.

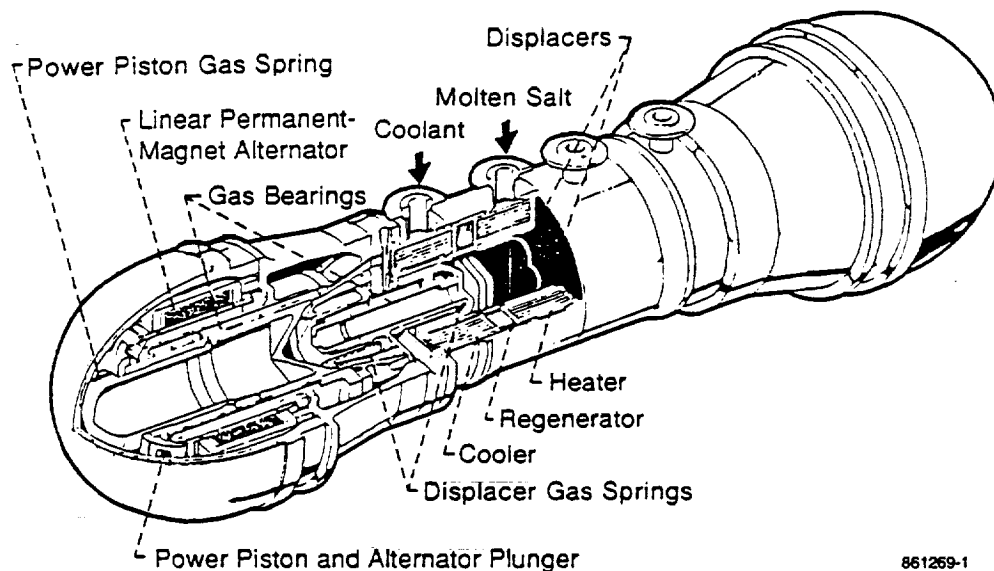


Figure 1. Space Power Demonstrator Engine

The permanent-magnet alternator is a moving magnet design in which the magnets are carried on a lightweight, nonmagnetic, nonconducting cylindrical carrier. The magnet carrier operates between an inner and outer laminated Hyperco stator. The submodule output coils are connected in series. Thermal power is supplied to the SPDE by pumping a hot (~630 K) molten salt heat-transfer fluid through the shell of each tube-in-shell heater unit. Similarly, thermal power is rejected from the module to water circulated through the shell of each tube-in-shell cooler. The electrical output of the module is rectified to dc and is dissipated through a 25-kW<sub>e</sub> resistance unit.

The SPDE is designed for steady-state operation at the design point and, as such, has no control system. Variations in power are accomplished through temperature changes in the external heating/cooling systems and load applied to the system.

Table 1 presents SPDE design parameters; Table 2 lists the SPDE materials; and Table 3 presents the SPDE engine geometry. A more complete description of the design is contained in Brown (1987)\*. Major hardware components of the SPDE, as fabricated, are shown in Figures 2 through 9. Typical engine build sheets for the SPDE are provided in Appendix A.

The SPDE initial assembly and initial hot low-pressure run were performed in June 1985. As shown in Figure 10, the engine was installed in the test cell horizontally and was suspended from the ceiling by four straps, such that dynamic balance of the opposed piston configuration could be directly observed.

In early SPDE tests, the measured indicated power was ~15% below design predictions at 75 bar mean pressure. However, at full pressure, 150 bar, the power was 50% below the predicted level. Disassembly of the engine showed that the stacked, unsintered regenerator screens were badly damaged. Metallurgical analysis of the screens indicated relative motion between the screens and the regenerator housing walls. Subsequent investigation revealed that the manufacturer had rolled the screens to 75% of the desired thickness, which resulted in a loose packing of the screens in the regenerator housing. The action of the reversing flow in the engine was determined to be the cause of the damage. The screens were replaced by a sintered 25 $\mu$ m wire felt metal regenerator with a tight fit in the regenerator housing. In addition to replacing the screens with the felt metal, wire stand-offs were added to prevent direct contact of the regenerator with the heater or cooler (i.e., provided a small plenum between the regenerator and heater and the regenerator and cooler). This change improved the flow distribution. Engine tests with the new regenerator showed good correlation with predictions at both low and high mean pressure. Details of early SPDE tests are given in Dochat (1987). Evaluation of the regenerator screen failure is contained in Hull (1987).

## 2.2 SPDE Testing in 1986

For thermodynamic characterization of the SPDE, engine parasitic losses were evaluated in a series of cold tests (temperature ratio = 1.0). Alternators motored the pistons with the displacers either held fixed at their top-dead-center position or free to move. With the displacers held fixed, the power needed to drive the pistons equaled the engine parasitic losses (predominately the pressure-induced hysteresis and leakage losses). A comparison of measured and predicted indicator power over ranges of mean pressure and piston stroke showed that these losses were close to predictions.

---

\* References are located following Appendix D.

TABLE 1 — SPDE DESIGN POINT OPERATING PARAMETERS

Design Parameter	Value
Frequency	105.0 Hz
Mean Pressure	150.0 bar
Heater Wall Temperature	630.0 K
Cooler Wall Temperature	315.0 K
Displacer Stroke Amplitude (XD)	8.97 mm
Piston Stroke Amplitude (XP)	10.16 mm
Phase Angle XD Relative to XP	65° *
Compression-Space Pressure Amplitude	14.38 bar

\*During early testing of the SPDE, displacer gas spring volume was changed by adding a stuffer to achieve a phase angle of about 90° for maximum power.

91TR13

TABLE 2 — SPDE MATERIALS

Component	Material
Displacer Dome and Radiation Shields	Inconel-718
Support Cone	Beryllium
Displacer Rod	Beryllium
Gas Spring Piston and Cylinder	Beryllium/Steel
Flange and Post	Steel
Heater and Cooler Tubes	Inconel-718
Heat Exchanger Structure	Inconel-718
Power Piston and Cylinder	Beryllium/Steel
Plunger Carrier	Titanium
Pressure Vessel	Low-Alloy Steel
Alternator	Epoxy Hyperco, Copper

91TR13

TABLE 3 — SPDE ENGINE GEOMETRY

<b>Displacer</b>	
Hot side diameter (m):	$1.143 \times 10^{-1}$
Hot side area (m <sup>2</sup> ):	$1.0261 \times 10^{-2}$
Cold side area (m <sup>2</sup> ):	$9.9725 \times 10^{-3}$
Maximum amplitude (m):	$1.24 \times 10^{-2}$
Displacer mass (kg):	1.701
<b>Piston</b>	
Diameter (m):	$1.4478 \times 10^{-1}$
Piston area (m <sup>2</sup> ):	$1.6463 \times 10^{-2}$
Maximum amplitude (m):	$1.53 \times 10^{-2}$
Piston mass (kg):	9.967
<b>Heater</b>	
Number of heater tubes:	1632
Length (m):	$9.02 \times 10^{-2}$
Inner diameter (m):	$1.27 \times 10^{-3}$
Wall Thickness (m):	$5.08 \times 10^{-4}$
<b>Regenerator</b>	
Frontal area (m <sup>2</sup> ):	$2.39 \times 10^{-2}$
Length (m):	$2.463 \times 10^{-2}$
Wire diameter (m):	$2.54 \times 10^{-5}$
Porosity (%):	83.8
Type of Matrix:	Felt metal
<b>Cooler</b>	
Number of tubes:	1548
Length (m):	$9.5 \times 10^{-2}$
Inner diameter (m):	$1.52 \times 10^{-3}$
Wall Thickness (m):	$5.08 \times 10^{-4}$
<b>Cold Connecting Duct</b>	
Volume (m <sup>3</sup> ):	$3.52 \times 10^{-4}$
Surface area (m <sup>2</sup> ):	$1.00 \times 10^{-1}$
Hydraulic diameter (m):	$1.37 \times 10^{-2}$
Effective length (m):	$7.85 \times 10^{-2}$
<b>Expansion Space</b>	
Mean volume (m <sup>3</sup> ):	$6.82 \times 10^{-4}$
Wetted area (m <sup>2</sup> ):	$1.374 \times 10^{-1}$
<b>Compression Space</b>	
Mean volume (m <sup>3</sup> ):	$4.47 \times 10^{-4}$
Wetted area (m <sup>2</sup> ):	$1.11 \times 10^{-1}$
<b>Appendix Gap</b>	
Diameter (m):	$1.143 \times 10^{-1}$
Minimum gap (m):	$1.58 \times 10^{-4}$
Maximum gap (m):	$3.21 \times 10^{-4}$
Effective gap (m):	$2.25 \times 10^{-4}$
Effective length (m):	$1.15 \times 10^{-1}$

ORIGINAL PAGE  
BLACK AND WHITE PHOTOGRAPH



Figure 2. SPDE Heater Head During Assembly

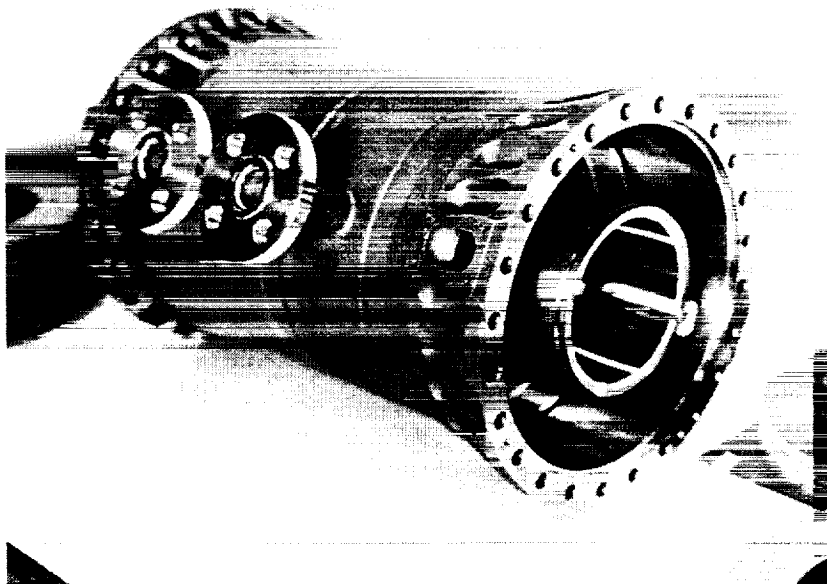


Figure 3. Completed SPDE Heater Head Assembly  
with Regenerator Screens

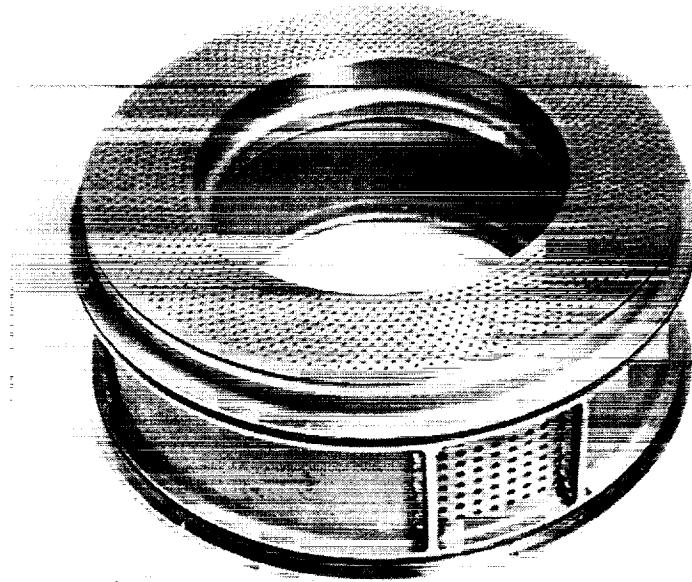


Figure 4. Completed SPDE Cooler Ready for Installation into Heater Head Assembly

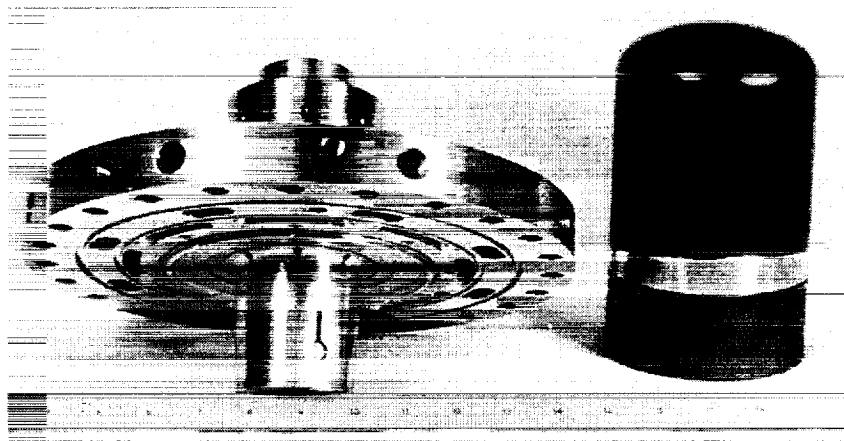


Figure 5. SPDE Post and Flange and Displacer



ORIGINAL PAGE  
BLACK AND WHITE PHOTOGRAPH

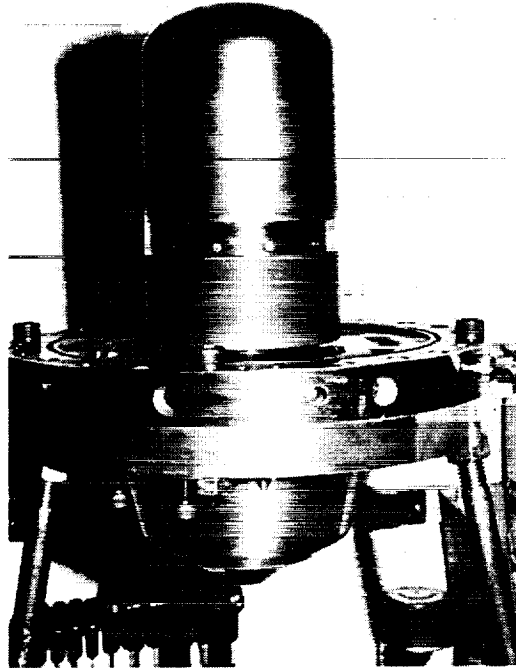


Figure 6. Completed SPDE Displacer Drive Assembly  
on Assembly Stand

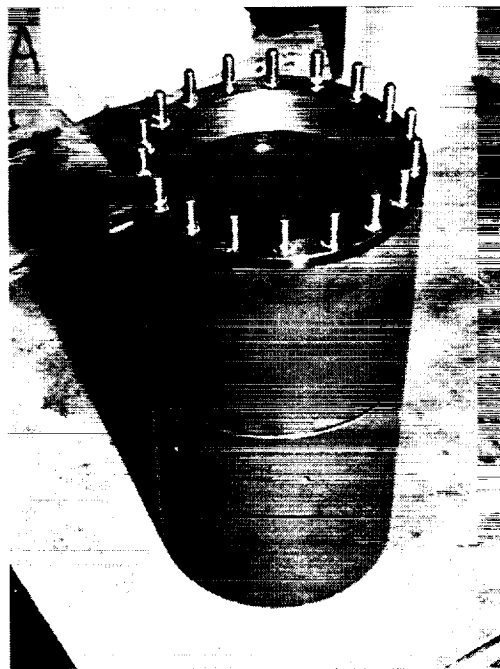


Figure 7. SPDE Power Piston

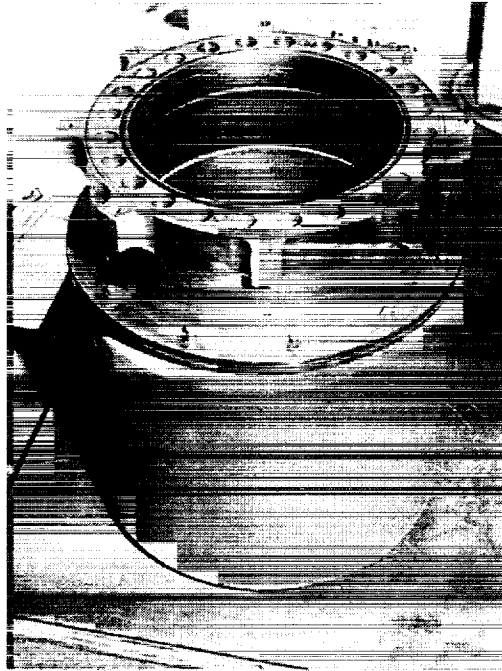


Figure 8. SPDE Power Piston Cylinder with Inner Alternator Stator Attached

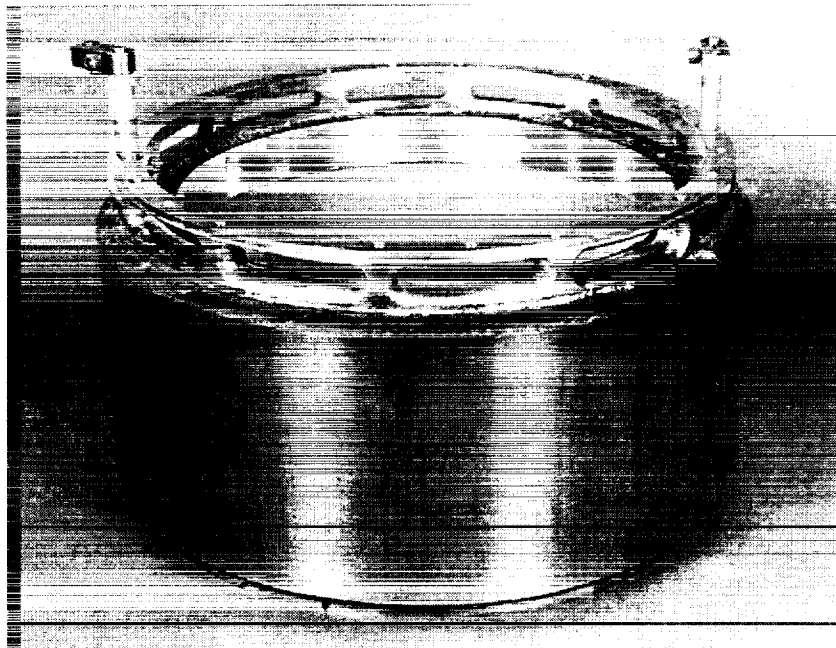


Figure 9. SPDE Alternator Stator

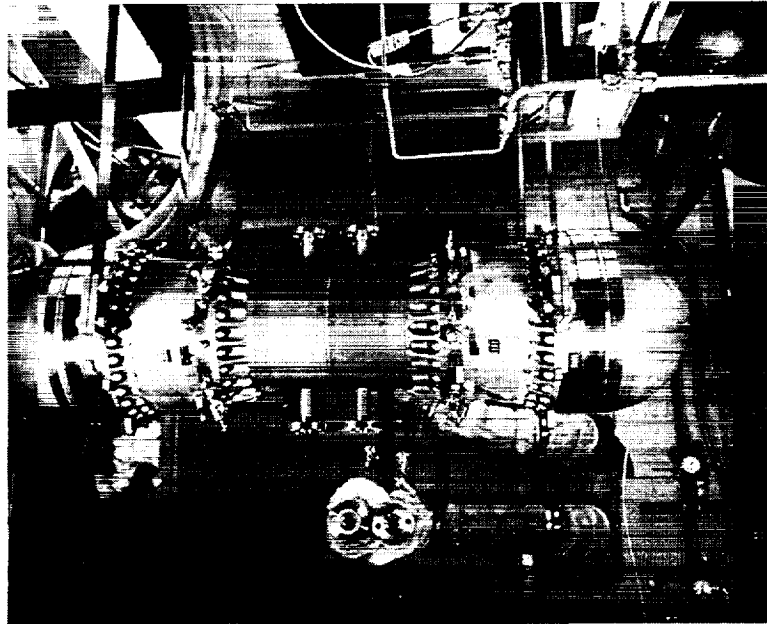


Figure 10. SPDE Installed in Test Cell

Parasitic losses associated with the moving displacer (i.e., heat exchanger pressure drop losses, flow-induced hysteresis losses, and mixing losses) were evaluated by repeating the tests with the displacer unlocked and reciprocating, and with the heat exchanger temperature ratio maintained at unity. These tests confirmed that the engine parasitic losses were close to predicted values. Details of these early parasitic loss tests are presented in Dochat (1986).

During the remainder of 1986, power module performance was characterized over a full range of operating conditions. Tests were conducted at heat exchanger temperature ratios of 1.6 to 2.0, mean pressures of 75 to 150 bar, and piston strokes of 10 to 20 mm (design stroke). Appendix B provides a summary of the data obtained after repairing the regenerator and completing the diagnostic tests. Appendix C contains selected data plots of the information contained in Appendix B. As shown in the Appendix B data and the Appendix C plots, the highest piston PV power was 25 kW which was obtained on 10/24/1986, data file SP106E, (data point 38 in Appendix B). MTI's harmonic code HFAST closely predicted engine performance. Figure 11 shows predicted and actual values for engine piston PV power, plotted as a function of power piston stroke amplitude at a temperature ratio of 2.0 and 150 bar mean pressure. Maximum measured piston PV power was 25 kW. Engine dynamics are shown in Figures 12 and 13, where the predicted and actual engine stroke ratio (defined as displacer amplitude divided by piston amplitude) and displacer-to-piston phase angle compare well.

Predictions were made with the HFAST code available at that time. The development of the MTI HFAST code is an ongoing effort supported by NASA-Lewis, and modifications are incorporated as a better understanding of loss mechanisms develops. Differences between tests and predicted data provide a starting point in our evaluation to obtain an improved analytical understanding. Complete documentation that highlights the HFAST code development history will be provided when the HFAST code is delivered to NASA. Table 4 compares HFAST to selected SPDE operating points. It is noted that the SPDE data that is presented at a temperature ratio of 2.0 is, in fact, operating closer to a temperature ratio of 2.1 due to an error in the physical fluid properties that was not corrected until after the completion of the SPDE program.

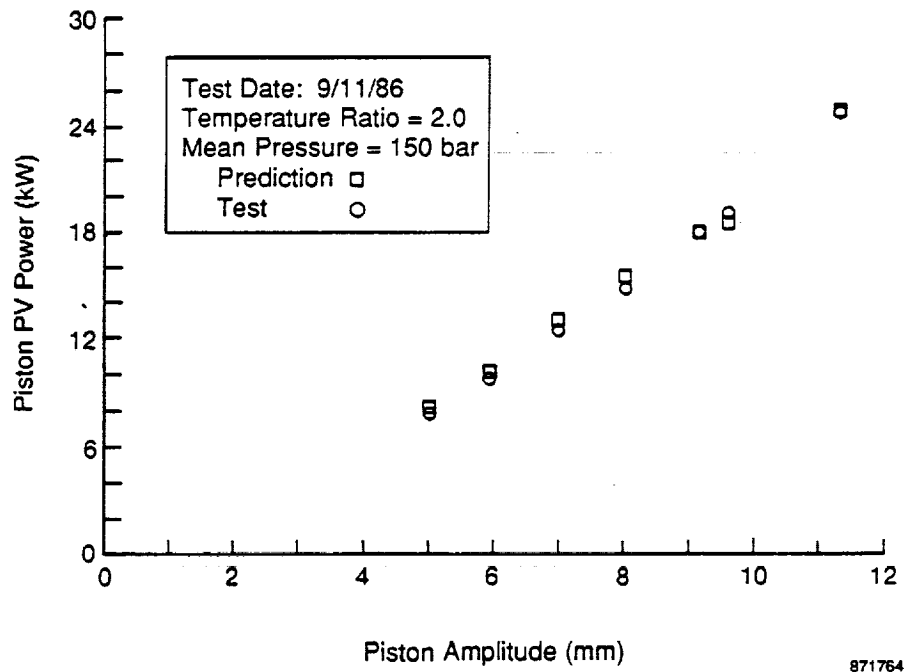


Figure 11. Hot Engine Test: Piston PV Power

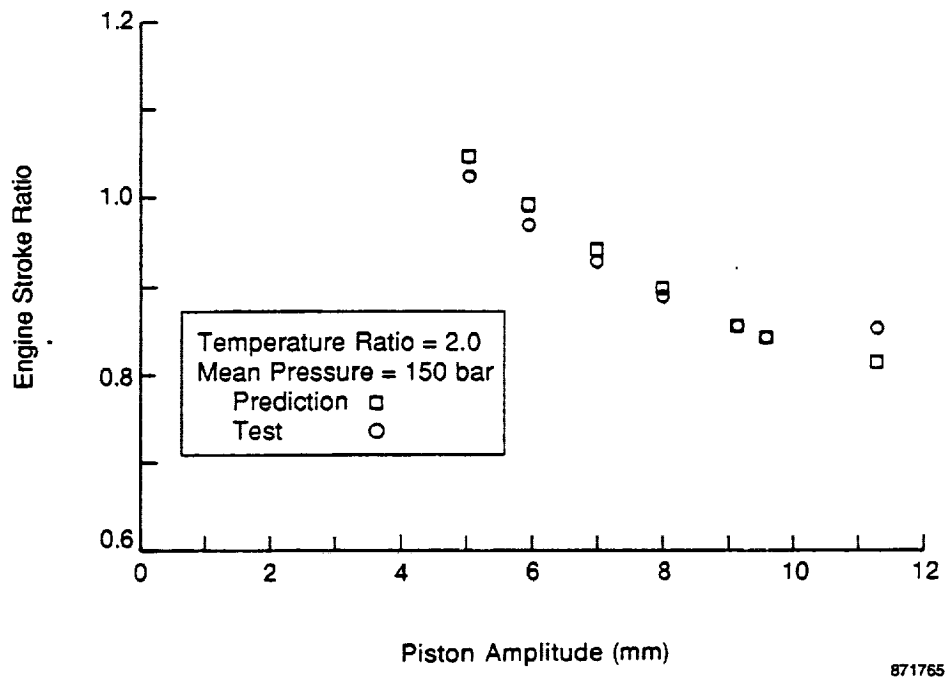


Figure 12. Hot Engine Test: Stroke Ratio

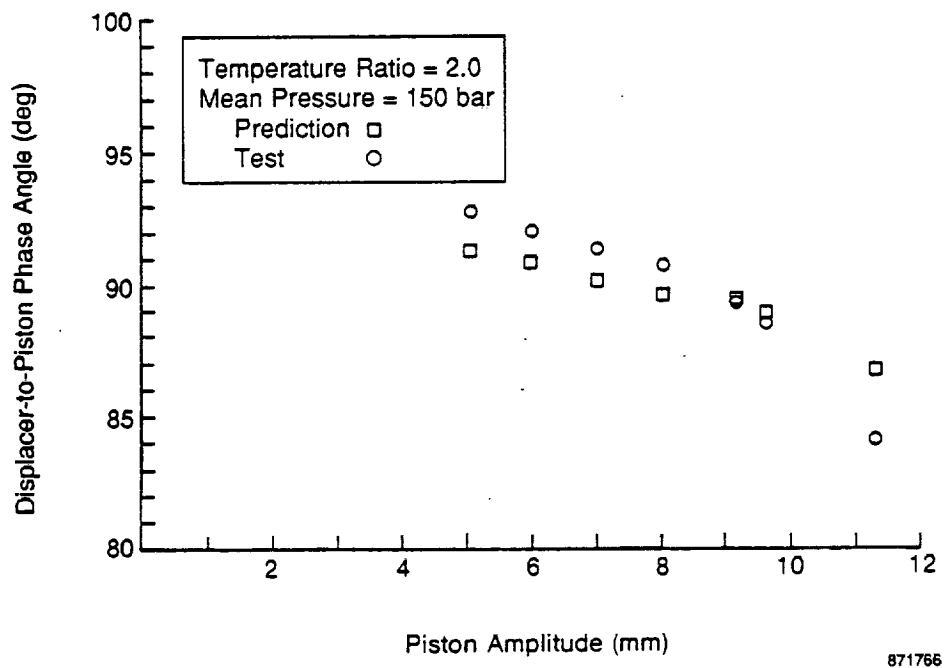


Figure 13. Hot Engine Test: Displacer-to-Piston Phase Angle

TABLE 4 — HFAST COMPARISON WITH ACTUAL PERFORMANCE AT SELECTED SPDE OPERATING POINTS

Scan No.	Operating Conditions						Performance				
	Temperature Ratio††	Mean Pressure (bar)	Frequency (Hz)	Piston Amplitude (mm)	Stroke Ratio*	Displacer Phase Angle	Pressure Ratio** (%)	Compression Space Pressure Angle	Piston PV Power (kW)	Heat In (kW)	Heat Out (kW)
27	2.018	150.3	100.7	5.01	1.02	92.83	5.85 (6.09) <sup>†</sup>	-9.7 (-10.34)	7.82 (8.572)	40.8 (37.2)	27.9 (28.1)
30	2.002	150.4	100.4	5.93	0.968	92.05	6.80 (7.14)	-8.77 (-9.36)	9.71 (10.76)	50.0 (46.9)	34.6 (35.4)
34	1.995	150.3	100.1	6.98	0.927	91.42	7.92 (8.35)	-8.1 (-8.66)	12.44 (13.65)	61.3 (59.4)	45.5 (44.9)
39	1.986	150.3	99.79	8.00	0.887	90.75	9.06 (9.51)	-7.45 (-7.99)	14.73 (16.40)	7.89 (72.2)	56.2 (54.8)
42	1.965	150.3	99.55	9.13	0.854	89.30	10.29 (10.75)	-6.95 (-7.25)	17.85 (19.16)	91.8 (87.3)	67.3 (67.0)
43	1.953	150.2	99.44	9.57	0.843	88.52	10.77 (11.22)	-6.78 (-6.95)	19.02 (20.08)	99.4 (93.4)	69.6 (72.1)

91TR13

$$*\text{Stroke Ratio} = \frac{\text{Displacer Amplitude}}{\text{Piston Amplitude}}$$

$$**\text{Pressure Ratio} = \frac{\text{Compression Space Pressure Amplitude}}{\text{Mean Pressure}}$$

† (HFAST Prediction)

†† Due to an error in coolant fluid properties, actual temperature ratios were closer to 2.1.

### 2.3 SPDE Accomplishments

Major SPDE accomplishments achieved by October 1986 are listed below:

- Achieved operation at design stroke, pressure, and temperature
- Demonstrated 25-kW piston PV power versus 28.8-kW goal
- Achieved 22% piston PV efficiency versus 28% goal
- Demonstrated 17-kW<sub>e</sub> power versus 25-kW<sub>e</sub> goal
- Demonstrated excellent dynamic balance
- Measured 0.03-mm casing motion amplitude at design point versus 0.08-mm maximum permissible
- Achieved stable operation over entire operating range
- Obtained good data correlation with MTI's HFAST Stirling engine harmonic code.

At the completion of the SPDE testing and demonstration program, the SPDE linear alternator, as installed, was operating at 70% efficiency versus a design of 90%. Subsequent SPDE alternator bench tests indicated the electrical output power shortfall was due primarily to eddy current losses in the alternator support structure, not the alternator itself.

The SPDE was the first engine designed at a temperature ratio of 2.0. The development and validation of analytical codes were significant results of the SPDE program. Thermodynamic efficiency at 22.5% versus a 28% efficiency goal was demonstrated. Improved analytical codes indicated that changes in regenerator porosity and aspect ratio, as well as modifications to heater and cooler geometries, would significantly improve efficiency. These changes will not be made to the SPRE, but will be incorporated into the first test article in any follow-on program. Therefore, the knowledge gained during the SPDE program is directly transferable to future generations of Stirling space engines.





### 3.0 SPRE OVERVIEW

The SPRE module incorporates a 12.5-kW SPDE submodule with a flat closure plate welded to the pressure vessel to form the expansion space. The SPRE engine geometry is presented in Table 5. The only changes from the SPDE engine geometry are the volume and wetted area of the expansion space. HFAST was used to analyze SPRE performance; a reduction in expansion space volume, as compared to the SPDE increased engine power. Displacer gas spring seal clearances were also improved. To reduce the vibrations of the resultant single-cylinder engine, a dynamic vibration absorber was designed as an attachment to the engine. The absorber was assembled and has been successfully tested at both 75- and 150-bar mean pressure and frequency conditions. SPRE tests were conducted, however, with the engine connected to a seismic mass.

The acceptance testing conducted on SPRE-I prior to shipment to NASA-LeRC ran smoothly. The measured PV and electrical power were slightly above the highest previous data; 13 kW PV and 8 kW electrical were measured. Although there were no formal acceptance criteria required for this test, PV and electrical power of greater than one-half the SPDE power was the informal goal. This performance was achieved. This section summarizes the principal dynamic and thermodynamic performance results of the testing. A complete description can be found in Rauch, 1987.

#### 3.1 Engine and Test Configuration

Acceptance test hardware included the SPRE-I engine, an electrical load configured for rectified ac operation, and a seismic mass coupled to the engine heater. The remaining support equipment and facilities were the same as those used for previous SPDE and SPRE tests.

The SPRE configuration is shown in Figure 14. During checkout tests, a crack developed in the displacer bearing plenum cover. This caused larger than normal midstroke bias in the displacer position and higher losses in the aft displacer gas spring. This bias restricted the operating range of stroke and pressure and was the primary problem resulting from this failure. For the final acceptance test run, the original plenum (P/N 1015C03-0121) was replaced with a stronger, redesigned plenum (P/N 1015C03-315). The new plenum reduced the aft gas spring volume by approximately 14.75 cm<sup>3</sup>.

The spool that connects the engine to the seismic mass was redesigned to correct problems identified during the previous checkout testing. The present spool is made of steel, which has a similar thermal expansion to the Inconel (Inco)-718 heater and has therefore eliminated bending stresses in the hot-end spool bolts. The spool wall thickness was reduced to address a concern that thermal stresses in the spool may cause high stresses in the welds. The hot-end spool bolts were replaced with bolts that have constant strength up to 1460 K. The mating surface of the mass was machined flat and certified grade-8 bolts replaced bolts of undocumented pedigree at the mass or cold end of the spool. All spool bolts were torqued to 60 in./lb with nuclear-grade, antiseize lubricant during assembly. The spool bolts require periodic checks to protect against loosening.

Two minor discrepancies exist in the engine hardware. First, the cooler used in the SPRE has a minor leak in one tube joint. Therefore, gas bubbles may be observed in the coolant outlet and the cooling system must be vented to prevent pressure buildup. Second, during the final assembly, new bolts were used for fixturing the flange and post to the heater head. These bolts were slightly too long and one bolt galled during removal. In the process of retapping the hole to clean it out, the tap broke, and rather than remove the tap, the remaining bolts were used for the assembly. As time permits, removal of the tap is recommended.

TABLE 5 — SPRE ENGINE GEOMETRY

<b>Displacer</b>	
Hot side diameter (m):	$1.143 \times 10^{-1}$
Hot side area (m <sup>2</sup> ):	$1.0261 \times 10^{-2}$
Cold side area (m <sup>2</sup> ):	$9.9725 \times 10^{-3}$
Maximum amplitude (m):	$1.24 \times 10^{-2}$
Displacer mass (kg):	1.701
<b>Piston</b>	
Diameter (m):	$1.4478 \times 10^{-1}$
Piston area (m <sup>2</sup> ):	$1.6463 \times 10^{-2}$
Maximum amplitude (m):	$1.53 \times 10^{-2}$
Piston mass (kg):	9.967
<b>Heater</b>	
Number of heater tubes:	1632
Length (m):	$9.02 \times 10^{-2}$
Inner diameter (m):	$1.27 \times 10^{-3}$
Wall Thickness (m):	$5.08 \times 10^{-4}$
<b>Regenerator</b>	
Frontal area (m <sup>2</sup> ):	$2.39 \times 10^{-2}$
Length (m):	$2.463 \times 10^{-2}$
Wire diameter (m):	$2.54 \times 10^{-5}$
Porosity (%):	83.8
Type of matrix:	Felt metal
<b>Cooler</b>	
Number of tubes:	1584
Length (m):	$9.5 \times 10^{-2}$
Inner diameter (m):	$1.52 \times 10^{-3}$
Wall Thickness (m):	$5.08 \times 10^{-4}$
<b>Cold Connecting Duct</b>	
Volume (m <sup>3</sup> ):	$3.52 \times 10^{-4}$
Surface area (m <sup>2</sup> ):	$1.00 \times 10^{-1}$
Hydraulic diameter (m):	$1.37 \times 10^{-2}$
Effective length (m):	$7.85 \times 10^{-2}$
<b>Expansion Space</b>	
Mean volume (m <sup>3</sup> ):	$7.61 \times 10^{-4}$
Wetted area (m <sup>2</sup> ):	$1.473 \times 10^{-1}$
<b>Compression Space</b>	
Mean volume (m <sup>3</sup> ):	$4.47 \times 10^{-4}$
Wetted area (m <sup>2</sup> ):	$1.11 \times 10^{-1}$
<b>Appendix Gap</b>	
Diameter (m):	$1.143 \times 10^{-1}$
Minimum gap (m):	$1.58 \times 10^{-4}$
Maximum gap (m):	$3.21 \times 10^{-4}$
Effective gap (m):	$2.25 \times 10^{-4}$
Effective length (m):	$1.15 \times 10^{-1}$

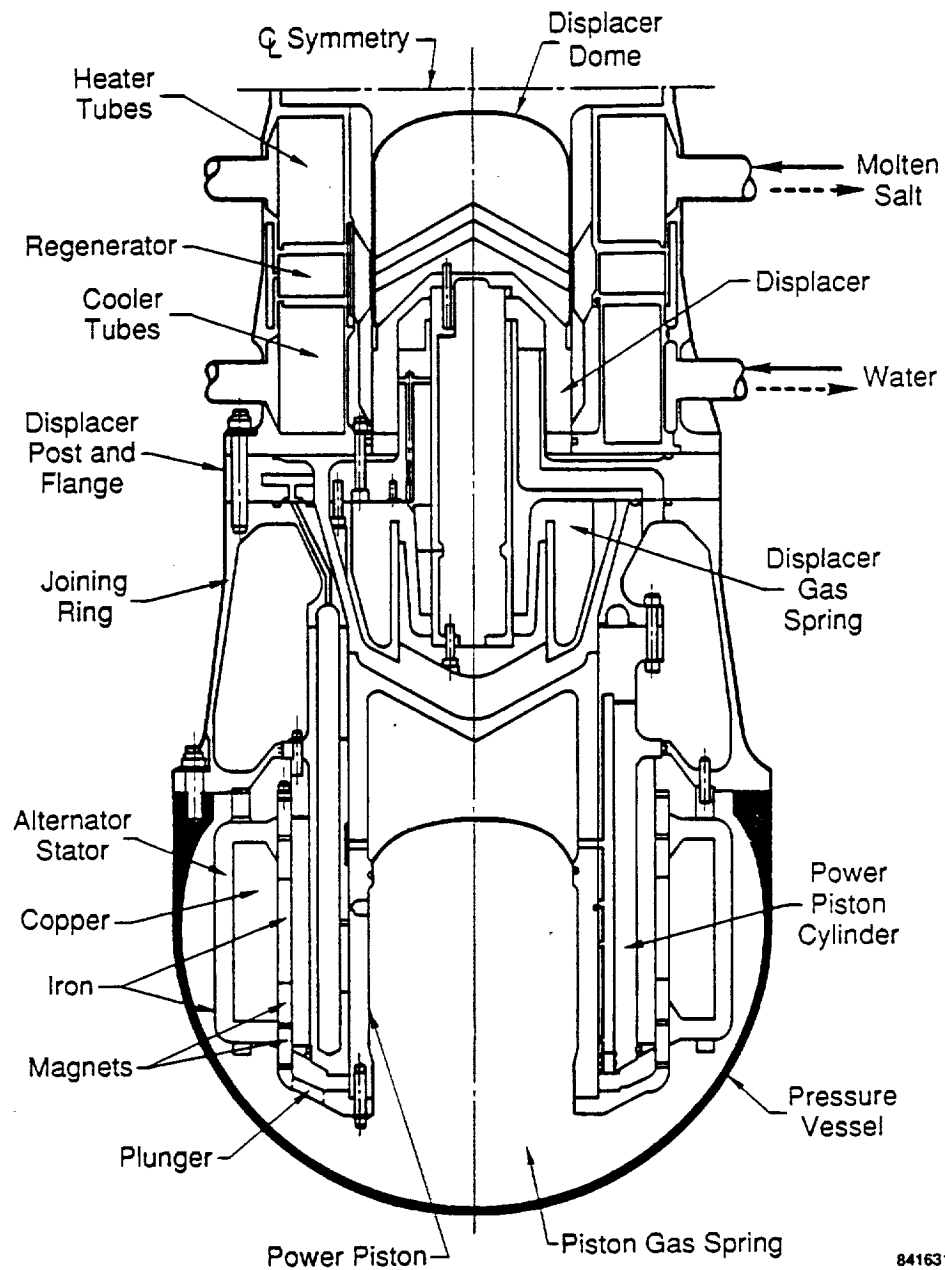


Figure 14. Space Power Research Engine (One-Half of Space Power Demonstrator Engine)

### 3.2 Test Procedure

The SPRE was tested following established procedures. SPRE acceptance test points are shown in Table 6. Three or more complete scans at each of the test points were obtained and then averaged to provide data. The first test point is representative of the NASA start point since NASA will use line voltage at 60 Hz to start the engine. MTI uses a power supply and therefore starts the engine at approximately 70 Hz and 75 bar.

The engine was started at a mean pressure of 75 bar and a temperature ratio of 1.6 (point 2) and then heated to a temperature ratio of 2.0 (points 3 and 4). During startup, data at temperature ratios of 1.6 and 1.8, and 10-mm piston stroke were obtained. The stroke was then varied from 10 to 18 mm at 75 bar, obtaining data points 4 through 8. The stroke was reduced to 12 mm and the pressure was increased to 150 bar, obtaining data points 10 and 11 at 100 and 125 bar, respectively. The piston stroke was again varied from 12 to 20 mm, obtaining points 12 to 16. The pressure was reduced to 75 bar and point 9 at full stroke was obtained; the 75-bar curve was repeated in descending order from point 9 to point 4. Then, as the engine was being cooled down, data at temperature ratios of 1.6 and 1.8 and 12-mm piston stroke were obtained. The pressure was then reduced to 50 bar and a temperature ratio of 1.6, (point 1), and data were obtained at a slightly varying pressure to determine the pressure for 60-Hz operation. Most of the SPRE data was obtained using externally supplied pressure for the hydrostatic gas bearings.

The tuning capacitors were switched out (in) as the pressure, and therefore, frequency was increased (decreased). The 50-bar capacitors were switched out at 62 to 63 bar as the pressure was increased to 75 bar. Table 7 shows the switches required for discrete pressure increases. When the capacitors are switched out (increasing tuned pressure), the stroke drops 1 to 2 mm; when capacitors are switched in (decreasing tuned pressure), the stroke increases 1 to 2 mm.

During cooldown, the engine was run down to a temperature ratio of 1.29 at 50 bar. Salt dilution was stopped by a high-level switch at 386 K.

### 3.3 Test Results

As shown in Figure 15, the peak piston PV power achieved was 13 kW at the design conditions. This value is approximately 0.6 kW above the previous record. The PV power data trends were as expected. As various operating parameters were changed, the scatter was typically less than 0.5 kW. As the design stroke was approached at 150 bar, several points were recorded at 9.5- to 10-mm piston amplitudes. Data at 75 bar and a temperature ratio of 2.0 were obtained both before and after the higher pressure operation. The amplitude was increased from 5.0 to 9.0 mm before and decreased from 10.0 to 5.0 mm after the high-pressure data were obtained. The before-and-after 75-bar data differ by approximately 0.2 kW, which is probably due to the engine having not achieved true steady-state operation before the data were taken.

Engine efficiency, based on heat rejected, is plotted against power in Figure 16. The efficiency is relatively constant at 20 to 22% for a temperature ratio of 2.0. However, there is a slight upward trend with increasing piston stroke (and consequently, PV power) at constant 75- and 150-bar levels.

TABLE 6 — SPRE ACCEPTANCE TEST POINTS

Test Point	Mean Pressure (bar)	Temperature Ratio*	Piston Stroke (mm)**
1	50	1.6	10
2	75	1.6	10
3	75	1.8	10
4	75	2.0	10
5	75	2.0	12
6	75	2.0	14
7	75	2.0	16
8	75	2.0	18
9	75	2.0	20
10	100	2.0	12
11	125	2.0	12
12	150	2.0	12
13	150	2.0	14
14	150	2.0	16
15	150	2.0	18
16	150	2.0	20

\*Due to an error in coolant fluid properties, actual temperature ratios were higher (2.1 instead of 2.0).

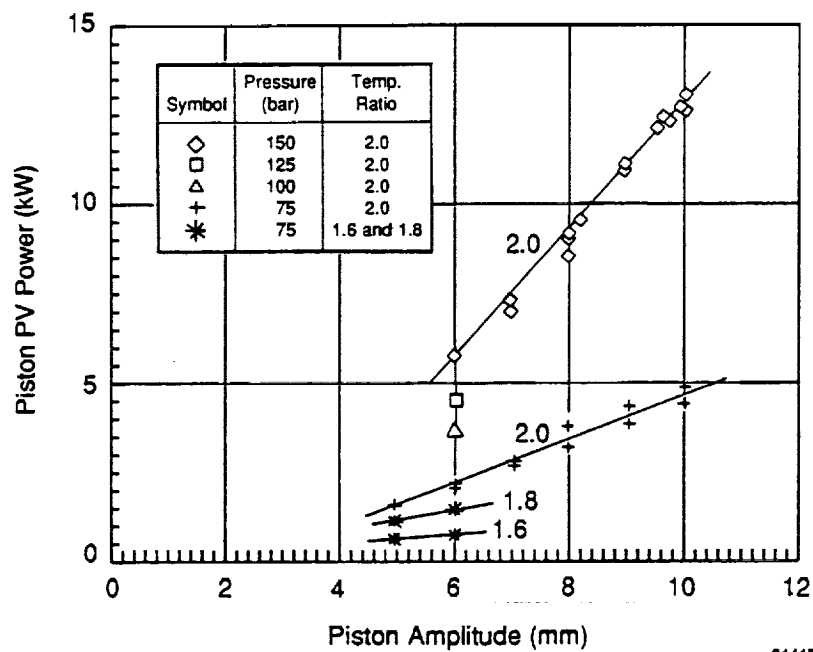
\*\*The data tables and plots report an amplitude equal to stroke/2.

91TR13

TABLE 7 — TUNING CAPACITORS REQUIRED AT  
VARIOUS OPERATING PRESSURES

Tuned Pressure (bar)	Switch Pressure (bar)	Total Capacitance ( $\mu$ f)
50	62 to 63	764
75	86 to 87	505
100	112 to 113	392
125	136 to 137	322
150	Not Switchable	292

91TR13



91415

Figure 15. SPRE Test: Piston PV Power

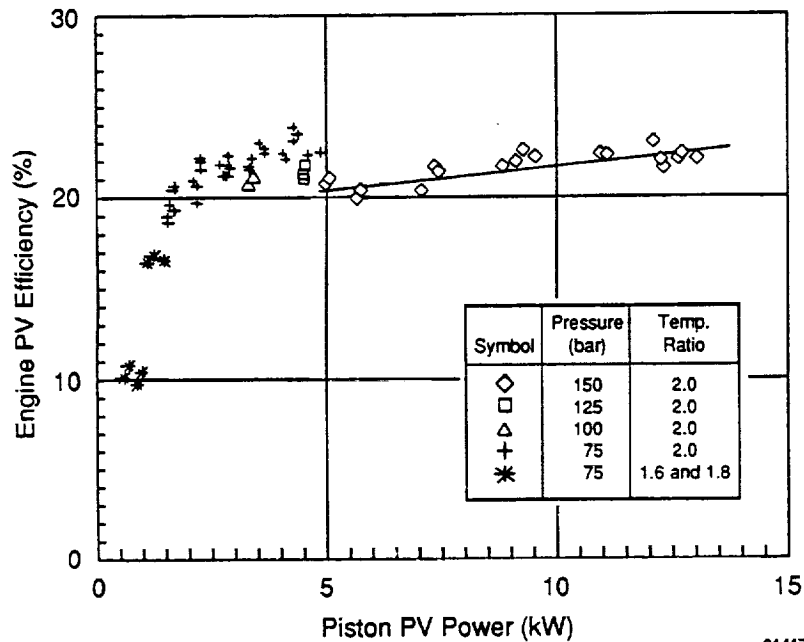


Figure 16. SPRE Test: Engine PV Efficiency

The electric output power, shown in Figure 17, generally follows the trend of PV power at a lower level. The losses in the piston gas spring and alternator account for the differences. The alternator output power plotted against piston PV power (see Figure 18) shows that the lower end efficiency is approximately 78% and 62% for 75- and 150-bar operation, respectively. Alternator efficiency at the peak power point is 70.6%. The 8.6 percentage point difference is due to power piston gas spring losses.

The acceptance test and shipment of the SPRE-I engine were successfully completed in May 1987. The engine, facility, and data acquisition all performed well, resulting in a complete set of consistent data. Also, the engine achieved the highest piston PV power and electrical output to date (13 kW and 8 kW<sub>e</sub>, respectively).

Subsequent to delivering the SPRE-I to NASA, it was determined that the method of calculating the cooler wall temperature was in error and, hence, the temperature ratio was approximately 2.1 versus the 2.0 as reported in the test data.

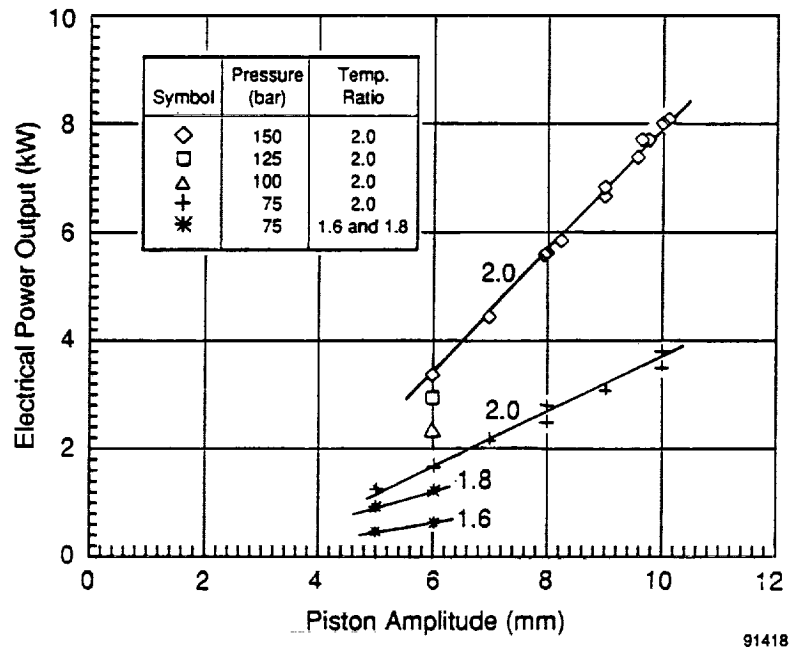


Figure 17. SPRE Test: Electrical Power Output

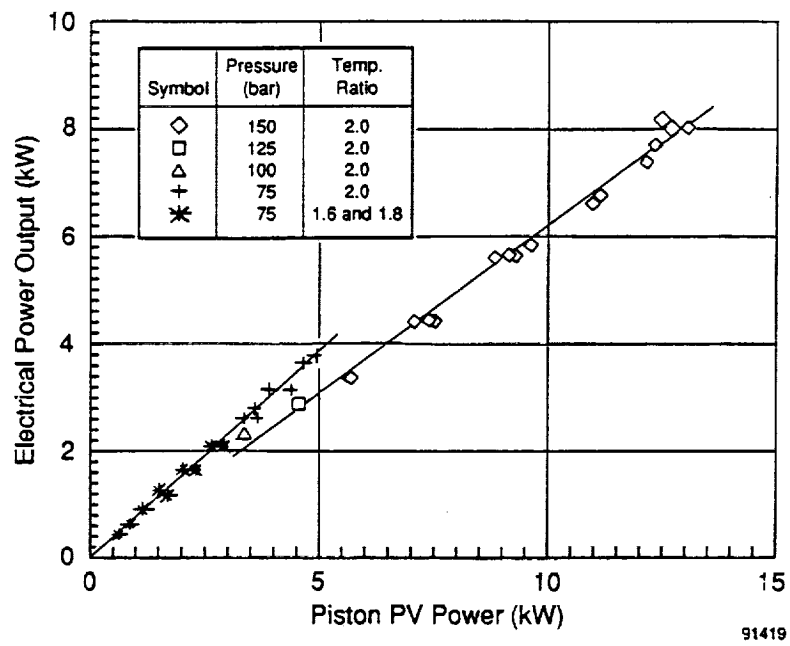


Figure 18. SPRE Test: Alternator Power vs. Piston PV Power



#### 4.0 HYDRODYNAMIC BEARING EVALUATION

The purpose of the testing effort was to develop a hydrodynamic bearing configuration that would operate stably at engine design conditions, and to demonstrate hydrodynamic bearing operation in the running SPRE. A gas hydrodynamic bearing that operates at 150-bar mean pressure, both rotates and reciprocates, and has time-varying gas pressure waves acting on its ends (such as in an FPSE) had not been studied before.

The SPRE uses hydrostatic bearings to provide radial support for the displacer and the power piston. The term "hydrostatic" indicates that the bearing pressure profile, which generates the load-carrying capacity, is primarily the result of high-pressure-supplied bearing pressure, applied either externally or internally. Gas is introduced from a high-pressure source (i.e., higher than engine mean pressure) into the bearing clearance between the cylinder and the reciprocating piston. From this point, the gas drains to the engine mean pressure volume. The high-pressure gas in the SPRE is designed to be supplied to the bearing from the power piston gas spring. The bearing supply plenum and the piston gas spring volume are connected by means of ports when the gas spring pressure is near its maximum.

Advantages of the hydrostatic bearing include its relatively high stiffness, its high stability, and its demonstrated operation. Disadvantages are its mechanical complexity and its significant impact on engine efficiency. Mechanical complexity arises from the need for numerous drillings, orifices, and supply and drain galleries. Engine efficiency is reduced because of the high-pressure amplitude requirement in the gas springs (approximately 7 bar), which results in significant thermal hysteresis and seal leakage loss.

Hydrodynamic bearings have the potential to simplify the bearing mechanical arrangement and reduce the losses mentioned above. The bearing load capacity (i.e., bearing pressure distribution) is generated by rotational motion of the bearing journal and, therefore, does not require an external pressure source. The disadvantage of the hydrodynamic bearing is that it is susceptible to whirl instability. The primary geometric and operating variables that affect stability are bearing surface geometry, clearance, rotational speed, load, journal mass and mass moment of inertia, and bearing end conditions.

Plain cylindrical bearings operating with no load are unstable. Bearing stability increases with an increase in load, and decreases with an increase in mean pressure and rotational speed. The instability of a plain cylindrical bearing is exhibited by an increase in the journal radial displacement at half the journal rotational frequency (i.e., half-speed whirl). Half-speed whirl instability can be eliminated by incorporating herringbone grooves on the surface of the journal or the cylinder. This technique has been proven effective for journals that only rotate and do not reciprocate.

MTI investigated implementation of a hydrodynamic gas bearing on the SPRE power piston. After an in-depth literature search, as well as consultation with MTI and world-renowned bearing experts (Professor Jorgen Lund of the University of Denmark, and Professor Coda Pan of Columbia University), a detailed experimental effort was laid out. This effort involved:

- Evaluation of plain cylindrical and herringbone groove bearings in a rig that imposed SPRE operating conditions
- Selection of the preferred bearing configuration based on the rig test results
- Demonstration of the selected bearing configuration in the running SPRE at design operating conditions.

The following subsections summarize results obtained from hydrodynamic bearing tests. A complete report of the hydrodynamic test evaluation is contained in Spelter (1989).

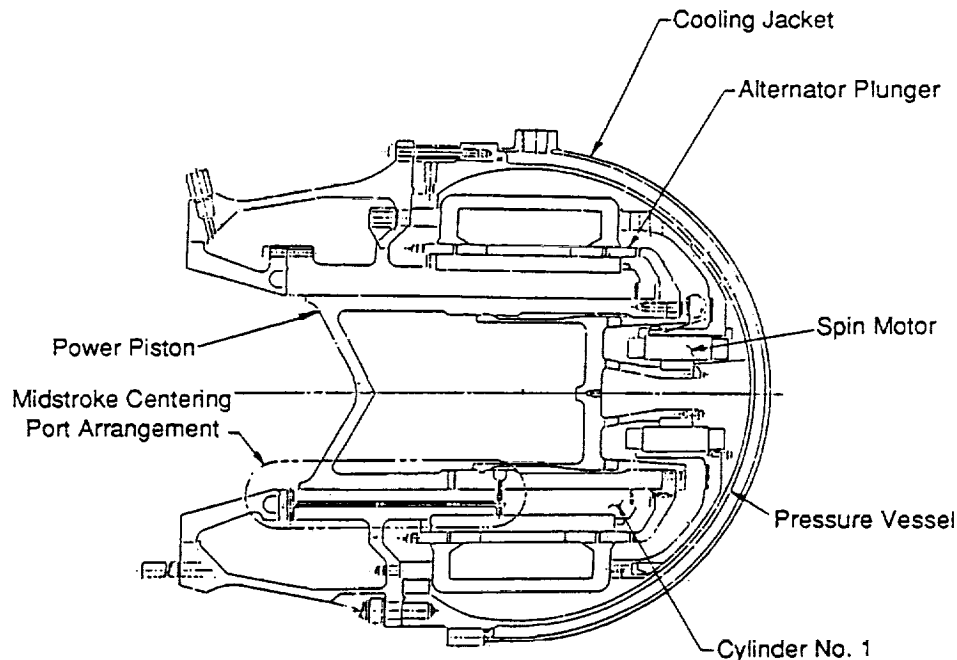
#### 4.1 Test Results

Tests were performed both on the bearing test rig and in the running SPRE. A hydrodynamic bearing configuration that would operate stably at engine design conditions was developed on the bearing test rig. Operation of the hydrodynamic power piston bearing was demonstrated in a running SPRE.

##### 4.1.1 Rig Tests

Hydrodynamic tests without piston reciprocation showed stable operation up to 165 bar mean pressure. At all operating mean pressures, a half-speed subharmonic component was seen in the proximity probe measurements of the radial motion of the power piston. Although half-speed subharmonic components were present in the proximity probe signals (indicating the presence of half-speed whirl), there was no indication from the spin motor current wave form of any continuous or intermittent contact between the piston and the cylinder.

Hydrodynamic tests with piston reciprocation were performed next. Initial tests with Cylinder No. 1 (see Figure 19), which has no bearing feed holes or drain grooves present, and a plain piston showed that half-speed whirl was again present. The power piston stroke could not exceed 12 mm at 75 bar mean pressure without spin motor stall. At a mean pressure of 150 bar, the spin motor stalled when the piston stroke reached 11 mm.



89474

Figure 19. Cylinder No. 1 Configuration

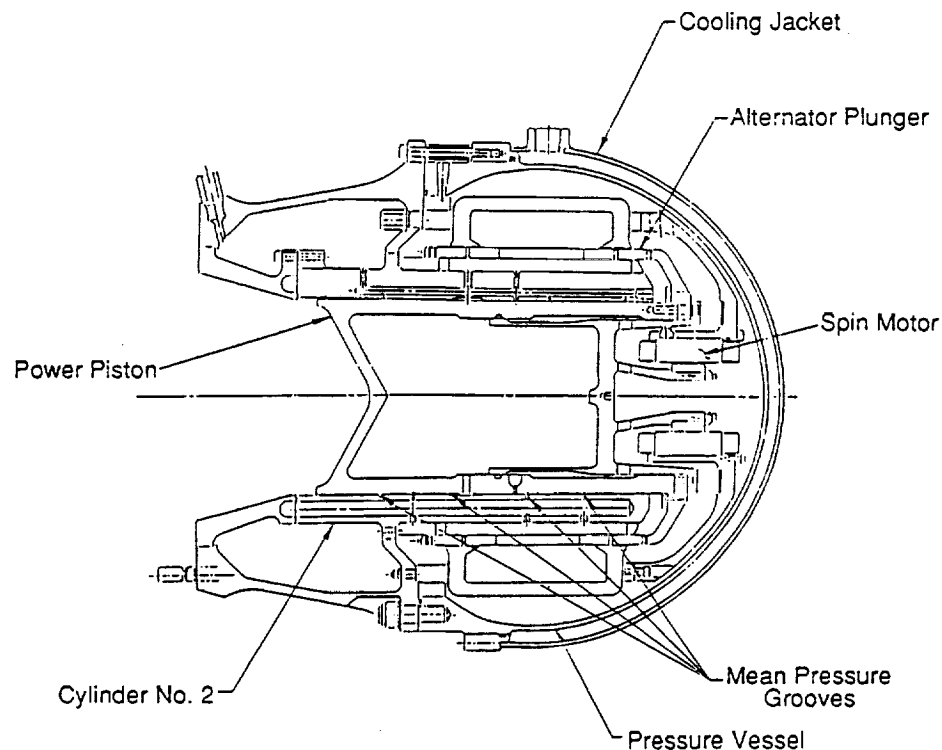
Using Cylinder No. 1 and a piston with herringbone grooves, 50% more stroke was achieved before motor stall occurred. In addition, no half-frequency subharmonic component was seen in the proximity probe signals at lower strokes (the half-frequency component was measured just before motor stall).

Based on several diagnostic tests performed, it was concluded that instability at large strokes was due to the large pressure gradient across the bearing length caused by the compression space and power piston gas spring pressure amplitudes. Based on these results, a potential stable hydrodynamic bearing configuration was identified as a plain journal and a cylinder with circumferential grooves to isolate the bearing region from the pressure fluctuations at the ends.

Tests with a plain beryllium piston and Cylinder No. 2, which has mean pressure grooves to isolate a greater length of the bearing from pressure variations (see Figure 20), showed stable operation at design conditions out to 20-mm stroke. Although stable bearing operation was achieved with this configuration, the frequency spectrum of the proximity probe signal still showed a half-speed subharmonic component.

#### 4.1.2 Engine Tests

Using the plain piston and Cylinder No. 2 configuration in the SPRE, stable hydrodynamic bearing operation was achieved in the running engine mode at the design operating conditions (i.e., engine heat exchanger temperature ratio = 2, mean pressure = 150 bar, operating frequency = 103 Hz, and piston stroke = 20 mm).



89473

Figure 20. Cylinder No. 2 Configuration

## 4.2 Conclusions

A power piston hydrodynamic gas bearing operating at 150-bar mean pressure, reciprocating at 103 Hz and with 20-mm stroke (full design stroke), and rotating at 730 rpm can operate stably in the running SPRE.

An important factor in achieving stable operation at design stroke was isolating a portion of the bearing length from pressure variations. A time-varying pressure gradient across the bearing length can destabilize hydrodynamic bearing operation.

The overall hydrodynamic bearing configuration loss was approximately 700 W, compared to 1700 W for the hydrostatic bearing configuration. Table 8 contains a detailed breakdown of the losses. The potential to reduce losses by designing for hydrodynamic bearings versus hydrostatic bearings is primarily due to the reduction in the power piston gas spring hysteresis loss with the hydrodynamic bearings, which amounted to 320 W for the hydrodynamic bearings versus 1500 W for the hydrostatic bearings. This was made possible by designing the piston gas spring with a 3-bar pressure amplitude versus the 7-bar pressure amplitude required for internally pumped hydrostatic bearings.

TABLE 8 — HYDRODYNAMIC VS. HYDROSTATIC BEARING LOSSES

(Losses (in watts) at 150-bar mean pressure and 20-mm stroke)

Loss Mechanism	Hydrostatic	Hydrodynamic
Seals	176	176 <sup>1</sup>
Gas Spring/Porting	1500	320 <sup>2</sup>
Rotation-Induced Losses (viscous, windage, and alternator eddy current)	0	69
Spin Motor Power	0	130 <sup>3</sup>
Bearing Flow Power	50	0
Total	1726	695

<sup>1</sup>Seal loss can be reduced further by designing for a longer seal length.

<sup>2</sup>Gas spring loss is reduced by designing the piston gas spring with 3-bar pressure amplitude versus the 7-bar pressure amplitude required for internally pumped hydrostatic bearings.

<sup>3</sup>Spin motor power can be reduced to 100 W by operating at 1-ampere draw at 600 rpm.

### 4.3 Recommendations

Although the hydrodynamic bearing operation on the SPRE power piston was successfully demonstrated in a running engine mode, hydrodynamic bearing development needs to be continued for the following reasons:

- The SPRE hydrodynamic bearing with Cylinder No. 2, although showing stable operation, has not been optimized for minimum loss. The optimum seal length must be both long enough to minimize seal leakage loss and short enough to provide an adequate stability margin during stroking. The effort required to determine the above optimized length needs to be continued.
- An unloaded plain cylindrical hydrodynamic bearing is inherently unstable. Unlike the power piston bearing, which is loaded by alternator side loads, the displacer does not have any inherent side-loading mechanism. The displacer bearing, as presently configured in the SPRE, can be unstable under micro-gravity space operating conditions. Therefore, displacer bearing technology development must be conducted.
- The spin motor currently used, a permanent-magnet synchronous motor, was selected on the basis of immediate availability. Based on overall system considerations, an induction motor will be superior because it requires potentially simpler controls and is less sensitive to system transients. A suitable induction motor has been identified and is available from Walco Industries.

215 \_\_\_\_\_ INTENTIONALLY BLANK

## 5.0 SPRE LINEAR ALTERNATOR DYNAMOMETER EVALUATION

The SPDE alternator performed with lower-than-expected efficiency during testing. The maximum electrical power achieved was 17 kW compared to the 25-kW design goal. Subsequent SPDE alternator bench tests and a detailed finite element analysis identified problems in two areas: high magnetic permeability of the engine structure adjacent to the alternator, and excessive flux density in the inner stator at high alternator current levels. The first item results in the generation of eddy currents and corresponding eddy current losses in the adjacent structure. The second item results in local flux saturation in the inner stator at high alternator current levels and a corresponding decrease in alternator force generation, power output, and efficiency.

Finite element analysis and alternator bench tests indicated that the structural eddy current losses were the primary cause of the alternator efficiency shortfall. To verify this preliminary conclusion, additional SPDE alternator tests were performed on MTI's linear alternator dynamometer. The complete test report is contained in Rauch (1990). The specific objectives of the tests were to:

- Evaluate alternator performance with a nonmagnetic adjacent structure
- Evaluate alternator performance in a simulated engine configuration (i.e., with a magnetic adjacent structure)
- Generate alternator performance maps to validate the alternator design and analysis methodology.

### 5.1 Test Results

The following alternator tests were performed on the linear alternator dynamometer:

- Locked plunger test
- Alternator open-circuit voltage test
- Alternator performance test with nonmagnetic adjacent structure
- Alternator performance test with magnetic adjacent structure.

The following subsections present the test results and compare the measured data to code predictions.

#### 5.1.1 Locked Plunger Test

Locked plunger tests were performed on the SPDE alternator with a nonmagnetic adjacent structure (aluminum joining ring and cylinder). These tests were performed by setting the plunger stroke to zero amplitude and passing ac current at 60 Hz through the coil. The input current and the alternator terminal voltage were measured. A comparison of measured versus predicted voltage at various coil current levels is shown in Figure 21.

The experimental and predicted values compare well over the range of current excitation, and both indicate the fall-off of terminal voltage at high current levels due to alternator inner stator saturation.

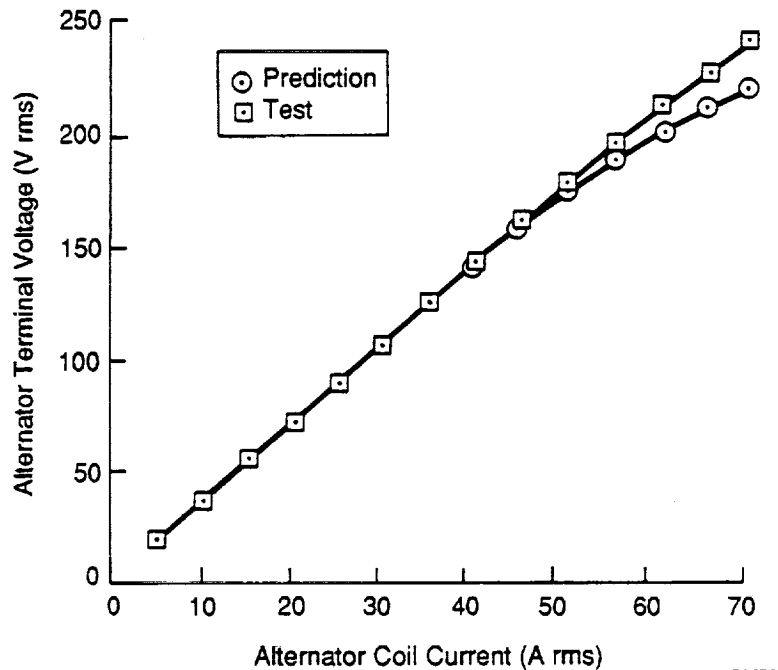


Figure 21. Locked-Plunger: Voltage vs. Current  
(Frequency = 60 Hz)

### 5.1.2 Open-Circuit Voltage Test

Open-circuit voltage tests were performed at 10.55-mm plunger amplitude, under no load (open circuit), and at various operating frequencies. Both the operating frequency and alternator terminal voltage were measured. Figure 22 shows the comparison of the predicted and measured alternator terminal voltage. As shown in the figure, the comparison is good.

### 5.1.3 Alternator Performance Test with a Nonmagnetic Adjacent Structure

To conduct the alternator performance test with a nonmagnetic adjacent structure, the SPDE alternator was tested on the dynamometer with the aluminum joining ring and aluminum cylinder. The alternator dynamometer tests were performed without the pressure vessel to allow for forced-air cooling. Alternator performance was measured with operating frequencies of 60 to 97 Hz, coil current of 0 to 70 A rms, and plunger amplitudes of 10.55 mm, 8.53 mm, and 6.28 mm. Most data were obtained at 10.55-mm amplitude. Due to resonance of the alternator support structure on the dynamometer, it was not possible to generate reliable test data above 90 Hz operating frequency. The choice of parameter range was based on SPDE operating conditions. The SPDE was designed with 10.16-mm plunger amplitude, 100-Hz operating frequency, and 66-A rms alternator terminal current.

Figure 23 shows the alternator efficiency versus coil current for 10.55-mm amplitude and for frequency varying from 50 to 70 Hz. The operating frequency was increased with coil current to maintain approximately zero relative phase angle between the plunger velocity and the coil current to simulate engine operating conditions with resistive load. Figure 24 shows the plot for operating frequency varying from 80 to 87 Hz.



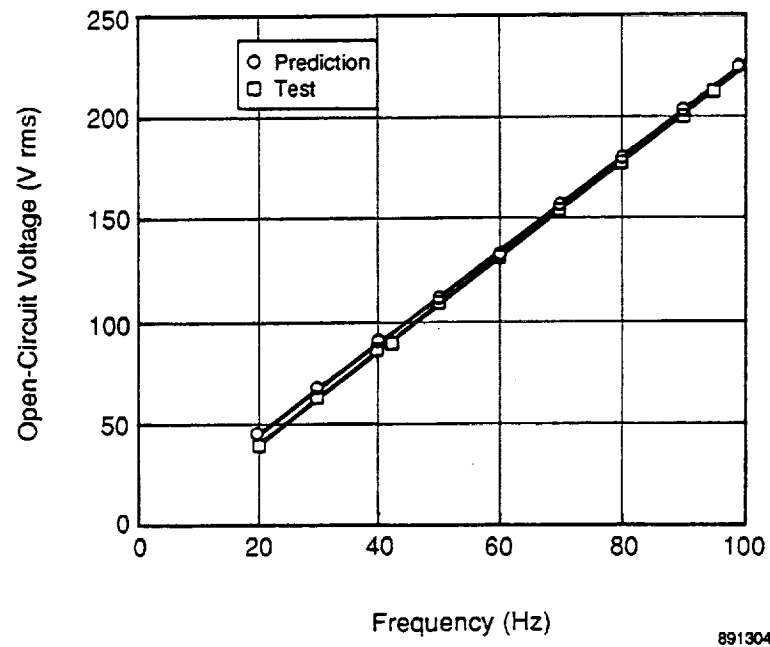


Figure 22. Alternator Open-Circuit Voltage at 21-mm Plunger Stroke

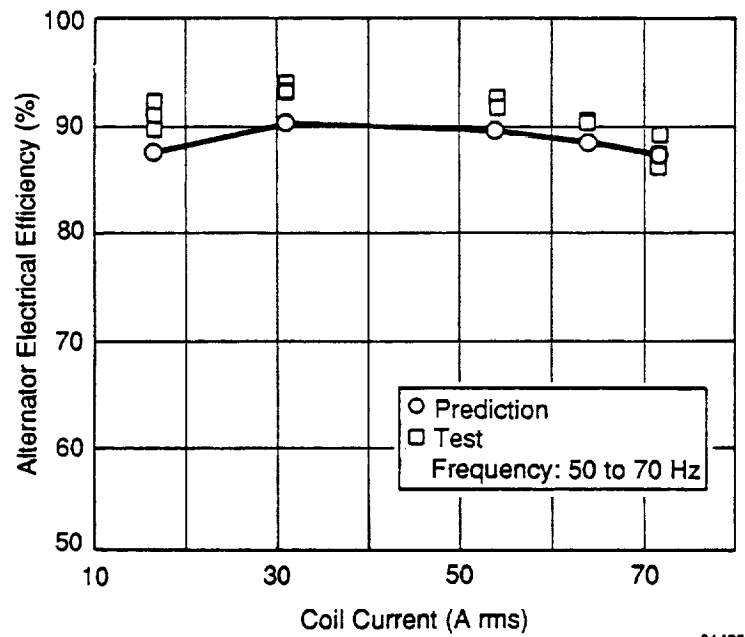


Figure 23. Predicted vs. Measured Alternator Efficiency with Nonmagnetic Adjacent Structure

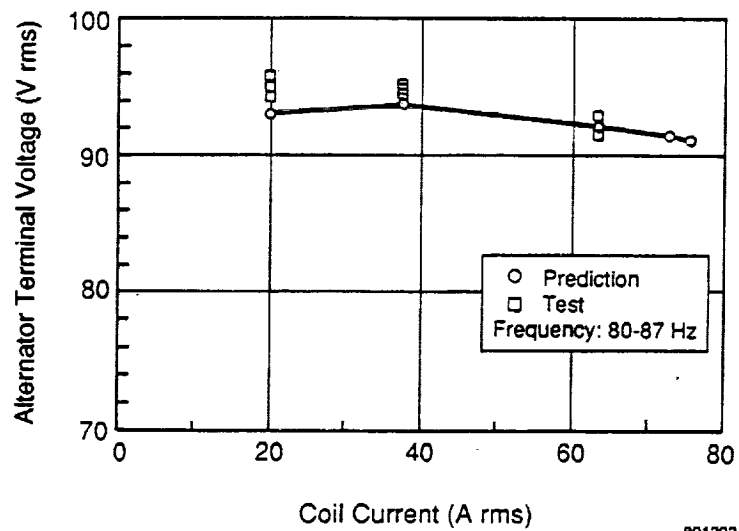


Figure 24. Predicted vs. Measured Alternator Performance with Nonmagnetic Adjacent Structure at Frequencies to 87 Hz

Figures 23 and 24 also compare the measured alternator efficiency to the code predicted efficiency. As anticipated, the measured efficiency for the SPDE alternator with a nonmagnetic adjacent structure is above 90%. As shown, the measured efficiency is close to predictions at high coil currents, and is higher than predictions at moderate currents. This behavior may be because structural eddy current losses were not calculated at all operating points. The structural eddy current losses were calculated using an axisymmetric finite element code, "FLUX," at 74 A rms coil current. At lower current levels, the eddy current losses were scaled down by the square of the value of the current.

#### 5.1.4 Alternator Performance Test with Magnetic Adjacent Structure

To perform the alternator performance test with a magnetic adjacent structure, the SPDE alternator was tested on the dynamometer with the steel joining ring (engine joining ring is Inco-718) and cylinder. Figure 25 compares the measured performance of the SPDE alternator with magnetic and nonmagnetic adjacent structures. This figure shows the large improvement in alternator performance by replacing the magnetic adjacent structure (steel) with nonmagnetic material (aluminum). This figure also shows the alternator efficiency measured during the engine test at operating conditions of frequency = 100 Hz, plunger amplitude = 10 mm, and coil current = 66 A rms.

The analytical predictions were made using an MTI-developed alternator code, Linear Permanent Magnet Motor and Alternator (LPMMA) design and analysis code, and FLUX, a commercial finite-element software package for electromagnetic analysis. LPMMA is a time-stepping code based on a two-dimensional magnetostatic field theory, which calculates magnetic flux density distribution, magnetic force on the plunger, inductance, terminal voltage, mechanical and electrical power, magnet and lamination eddy current losses, lamination hysteresis loss, alternator coil dc and ac losses, and alternator efficiency. The LPMMA does not model the leakage-flux-induced eddy current losses in the alternator adjacent structures. These losses were calculated using the FLUX code.

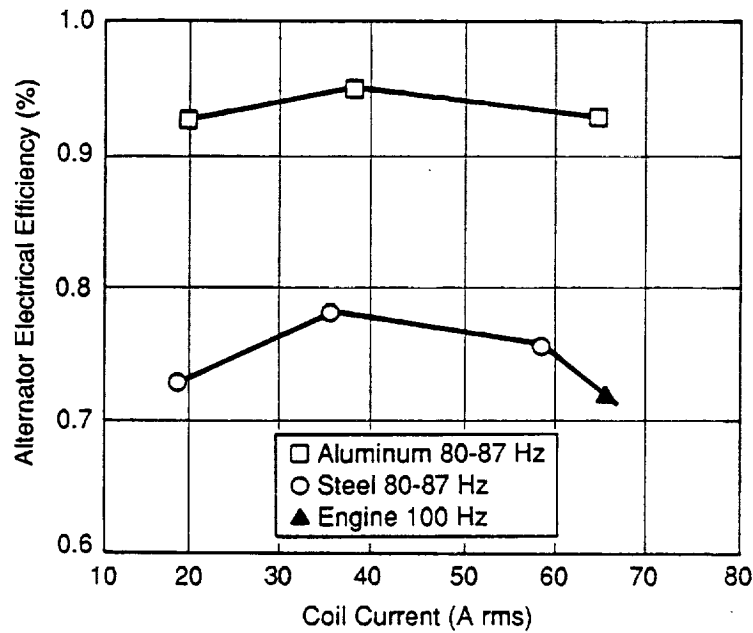


Figure 25. Alternator Performance Comparison with Magnetic and Nonmagnetic Adjacent Structure

## 5.2 Conclusions

The dynamometer test verified the alternator performance previously measured from the SPDE engine tests and alternator bench tests. The test results confirmed the following:

- The electrical output power shortfall in the SPDE is primarily due to eddy current losses in the magnetic structure adjacent to the alternator
- SPDE alternator efficiency of greater than 90% was demonstrated by replacing the magnetic adjacent structure with nonmagnetic material
- Code predictions compare well with the measured dynamometer test data.

The alternator was subsequently tested in the engine with a beryllium power piston cylinder and Inco-718 joining ring and pressure vessel (nonmagnetic structure). Engine test results confirm the significant improvement in alternator efficiency and, hence, electrical power output. The maximum electrical power generated was 11.4 kW<sub>e</sub>. Appendix D contains the high-efficiency alternator SPRE test results, including build sheets, data plots, and data summary tables.

216 INTENTIONALLY BLANK

## 6.0 SPRE HEAT PIPE HEATER HEAD

Integrating the FPSE into a total space power conversion system will require proper interface of the heat input to the engine and the system heat source. For a nuclear reactor system, a potential method to connect the FPSE with the primary reactor loop is via heat pipes. A heat pipe heater head was designed to assess the performance, fabrication, and geometric constraints of incorporating heat pipes into the FPSE. The heater head was designed to mate with the SPRE.

The proposed design of the SPRE heat exchangers (i.e., heater head, regenerator, and cooler) is shown in Figures 26 and 27. The design meets the following requirements:

- Incorporates heat pipes into the SPRE to assess the thermodynamic performance of a finned sodium heat pipe heater concept.
- Designed for a temperature of 1050 K in the hot, pressurized head and heater structure.
- Provides the capability to incorporate electric resistance heaters for initial testing. This will permit testing over a wide range of temperature ratios without raising the cold-side temperature.
- Minimizes hardware changes from the existing engine.
- Provides a design life of 10,000 hr for test purposes. Eventually, the head must be capable of >60,000 hr of life.

### 6.1 Heater Head Design

The pressure boundary comprises a flat closure plate with a cylindrical vessel at the plate OD. The cold end of the cylindrical section is a gusseted flange of the same geometry as the current design. This design permits the same post and flange and displacer assemblies to be used without modification. The regenerator has a frontal area of 116.8 cm<sup>2</sup> (versus 83.8 cm<sup>2</sup> on the current design), which will result in higher thermodynamic efficiency. The larger frontal area was obtained in the same diametral envelope by making more effective use of the space between the displacer OD and the pressure vessel.

The cooler is conceptually similar to the existing SPRE cooler design, but has been redesigned to accommodate the added frontal area. It will also provide the seal between the expansion and compression space at the displacer OD.

The primary difference between the new design and the existing SPRE design is in the heater. It is formed by a set of tubular wells attached to the head in the annular region on the hot side of the regenerator. The heater has 45 wells symmetrically spaced in three rows, as shown in Figure 26. The outer surfaces of the wells are finned in the longitudinal direction to form flow passages for the engine working gas (helium). A solid stuffer with cylindrical holes that match the OD of the fins is used to confine the working gas to the passages between the fins.

Heat is supplied to the engine by either electric resistance heaters or heat pipes inserted into the wells. By closely controlling diametral and straightness tolerances on the ID of the wells and the OD of the electric heaters or heat pipes, and by using a heat transfer agent supplied by the heater manufacturer, good thermal contact can be ensured and the temperature of the heater element or heat pipe fluid can be kept to acceptable levels.

PRECEDING PAGE BLANK NOT FILMED

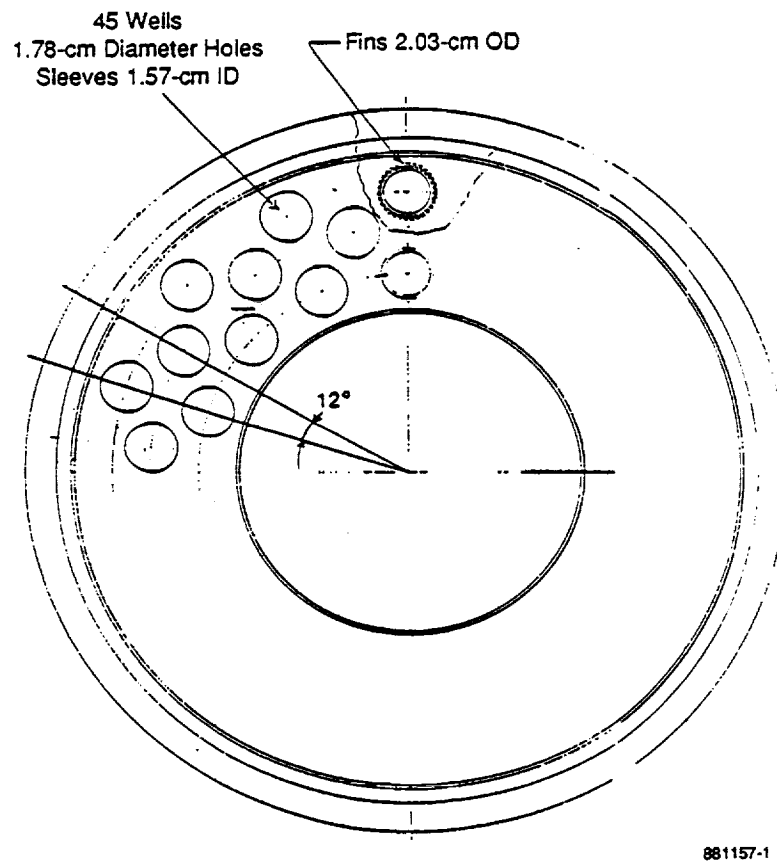
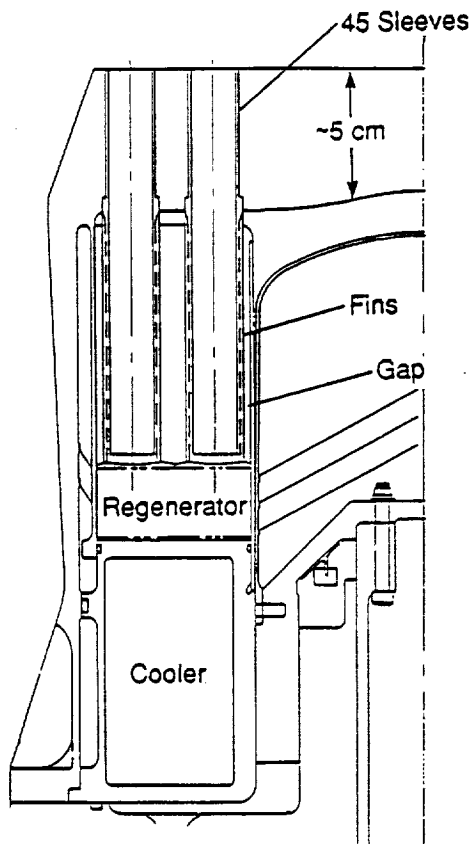


Figure 26. Top View — SPRE Head



881155-2

Figure 27. SPRE Heat Exchangers

Proper selection of material for the high temperature and high pressure is a critical issue. Material thicknesses and associated weights must be determined and the need (if any) to make any special provisions to control the temperature distribution of the heater head must be evaluated. Evaluations required to select the heater head material are:

- Thermal analysis to determine the temperature distribution along the vessel wall for use in determining thermal stresses and for evaluating the heat loss from the hot section
- Stress analyses to assess the structural integrity of the flat head, the vessel, and the heater wells
- Determination of assembly and fabrication procedures and associated reliability.

Listed in descending order of creep strength, the materials that have been considered for the SPRE heater head are Inco-713LC, HS-31, Inco-625, and Inco-718. Creep properties for the various materials are shown in Figure 28. The Inco-718 has higher yield and ultimate tensile strength and consequently higher fatigue strength than the other alloys.

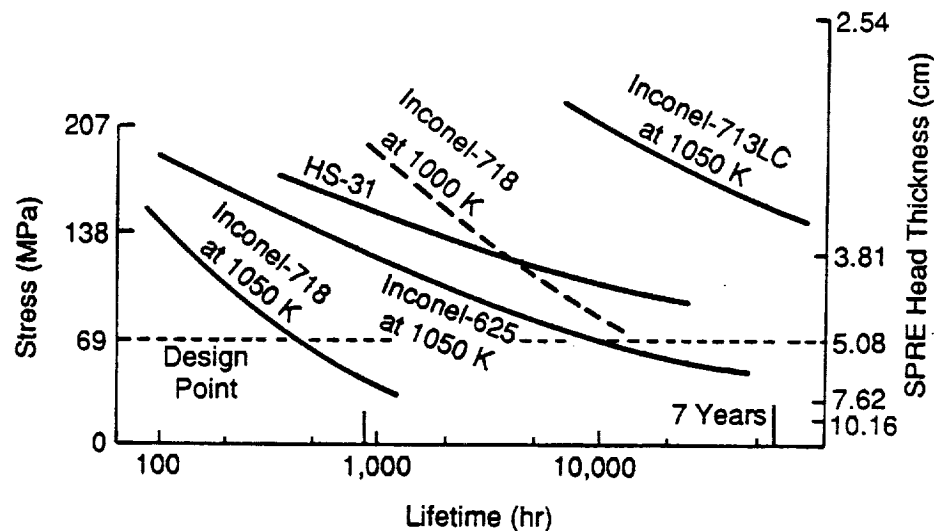


Figure 28. Material Creep Properties

## 6.2 Thermal Analysis

The objective of the thermal analysis was to determine the temperature distribution along the vessel wall outboard of the heater/regenerator/cooler. This distribution then was used to determine the thermal stresses in the wall. The regenerator is approximately 2.54 cm long. The operating temperature of the heater and cooler vary during testing. For design purposes, the maximum range was selected at 1050 K on the hot side and 300 K on the cold side. The gradient across the regenerator was thus 295 °C/cm. The vessel wall would be overstressed if it were located in contact with the regenerator such that it experienced the same gradient. The gap between the heater and vessel wall was incorporated into the design to help spread the thermal gradient along the wall.

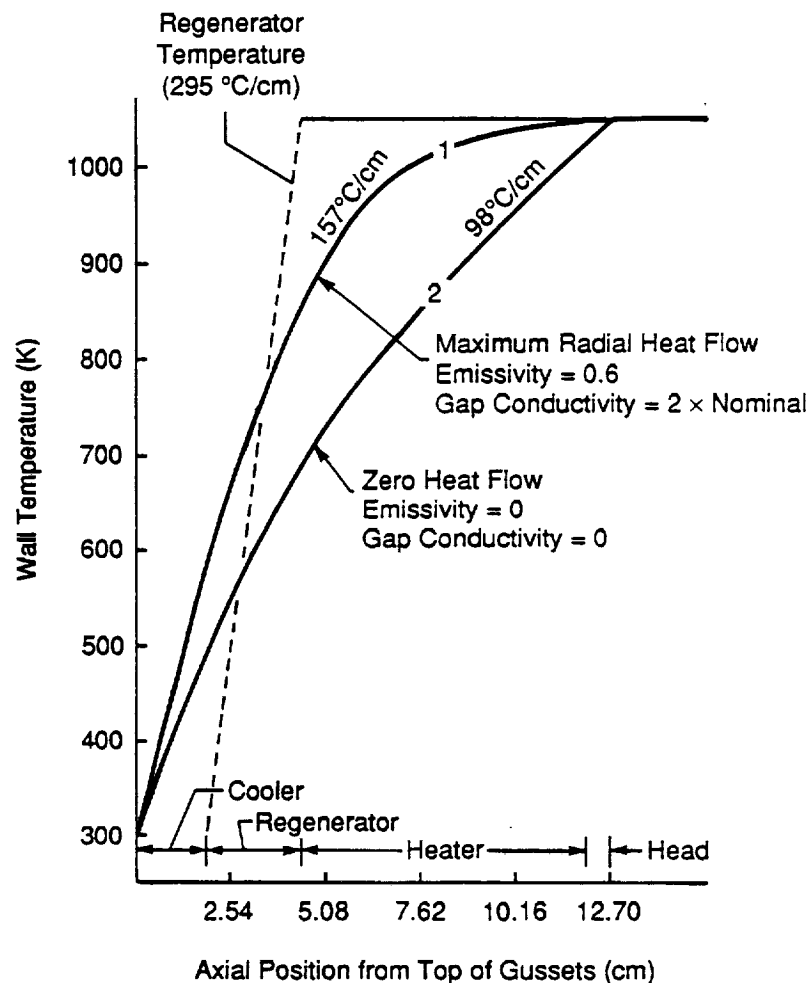
A thermal model was generated to represent the high temperature gradient in the regenerator wall. One-dimensional (1-D) radial heat flow was assumed across the gap at the inner surface of the vessel wall. Conduction across the gap is formulated from gap radial conductivity and gap radial dimension. Radiation was formulated assuming constant but adjustable emissivity of the two surfaces. Again, 1-D heat flow was assumed. The 1-D heat flow was also modeled at the outer surface. Natural convection and radiation were included. The effect of incomplete insulation of this surface on the gradient and heat loss was analyzed.

Axial heat flow along the wall results from conduction in the vessel material and was determined from material thermal conductivity and wall thickness. Heat balance equations were written for elements of the wall.



Analyses in which the outer wall was not fully insulated showed that a heat loss of 3 kW was too large a penalty to pay for the small reduction in the steepness of the gradient that could be achieved. A fully insulated outer wall was selected as reference. Analyses were conducted in which the emissivity and gap conductivity were varied between the extremes of zero and maximum radial heat flow. The results of these analyses are shown in Figure 29. If heat flow across the gap could be completely suppressed, which is not physically possible, the gradient at the cold end would be 98 °C/cm and would be approximately 39 °C/cm at the hot end. At the extreme of twice nominal conduction (to allow for high convective heat transfer and for radiation based on an emissivity of 0.6, i.e., no special surface treatment to minimize it), the gradient at the cold end is approximately 157 °C/cm and the gradient at the hot end is small. The 157 °C/cm gradient will be used as reference unless stress analysis dictates that a reduction of this is mandatory to meet stress limitations.

To ensure that natural convection, which was not modeled, does not introduce serious error in the estimated gradient, circumferential fins will be machined on the shell that forms the inner surface of the annular gap.



91429-1

Figure 29. SPRE Wall Temperature Analysis

### 6.3 Stress Analysis

The dominant structural requirements on the heater head are as follows:

- Material creep of the hot section of the heater head must not result in failure or gross deformation
- Pressure cycling coupled with the effects of the thermal gradient must not result in high cycle fatigue failure
- Thermal cycling due to startup and shutdown coupled with the pressure loading must not result in low cycle fatigue failure. (This condition is usually met automatically if there is no high cycle fatigue failure.)
- Stresses due to pressure on the cold end must not produce gross yielding or rupture. This sets the thickness of the cold section of the vessel.

The stress criteria defined by practice include a factor of safety of 1.5 against failure.

Loading conditions to be considered include:

- Mean pressure — 150 bar
- Thermal gradient — see Figure 29
- Alternating pressure — 20 bar maximum.

The vessel thickness is selected so that the membrane stresses in the wall due to pressure do not exceed  $S_m$ .<sup>\*</sup> The flat head thickness is selected so that the primary bending stresses due to pressure do not exceed  $1.5 \times S_m$ .

#### 6.3.1 Creep Analysis

Conservative hand calculations of the stresses in a flat plate and a cylindrical shell under a uniform pressure load were used to select the thickness of the top plate and the outer shell using HS-31 as the preliminary reference material.

For the 5-cm thick head shown in Figure 27, the strength required based on the primary bending stresses in the head being held to  $1.5 \times S_m$  dictates that  $S_m$  (i.e.,  $2/3 \times$  stress to rupture) (see Figure 28) be no less than 68 MPa at the design temperature of 1050 K and design mean pressure of 150 bar. The right ordinate on Figure 28 shows the thickness of the flat head to give the stress level on the left ordinate at a pressure level of 150 bar. If Inco-713LC were selected, the head thickness could be reduced to approximately 3.81 cm and meet the 7-yr life requirement of a space application. HS-31 could meet this requirement at a head thickness of approximately 5 cm. For Inco-625, the head would have to be even thicker (heavier) to meet the 7-yr life goal. Inco-718 has a few hundred hours of life at 1050 K and several thousand hours at 1000 K, but cannot meet the 7-yr goal.

---

<sup>\*</sup>  $S_m = 2/3$  yield or  $1/2$  ultimate strength at cold end and  $2/3$  stress to rupture or 1% creep in design life at hot end.

### 6.3.2 Outer Shell Fatigue Evaluation (2-D Analysis)

Figures 30 and 31 show low-temperature and high-temperature, high-cycle fatigue diagrams generated by assuming a straight failure line between the endurance limit on the alternating stress axis and the ultimate tensile strength on the mean stress axis. These diagrams were used to design the SPRE heat pipe heater head.

The ISOPDQ 2-D, axisymmetric, finite-element code and the heater head finite-element model were used to analyze the stresses in the vessel and head. This analysis ignores the heat pipe penetrations, which were analyzed separately. This code was used for the stress analysis because it is economical and the array of gussets at the flange can be easily modeled.

Regions where stress conditions are of primary concern are:

- The point where the cylindrical section and the gusseted flange section meet (since this is where the sharp change in thermal gradient, as shown in Figure 29, occurs).
- The intersection of the vessel and flat head, where discontinuity stresses are induced by the pressure loading. The thermal stresses at this location reduce the maximum stress. However, since the gradient is small, as shown on Figure 29, this reduction is neglected.

At the cold end, thermal stress adds to the pressure stress. At the hot end, thermal stress subtracts from the pressure stress. Distribution No. 1, as shown in Figure 29, was selected as the reference for the cold end. This distribution is believed to be more severe than would be expected. The actual temperature distribution could be reduced (closer to Distribution No. 2) by controlling the emissivity with appropriate plating. It is predicted that any of the four materials could meet the fatigue limits at the cold end of the gradient. Sufficient data exists on Inco-718 to confirm that the design would be satisfactory. Additional data needs to be obtained on the other materials to verify the design. Since the thermal stresses are fairly small for Distribution No. 1, and since they subtract from the pressure stresses, they are conservatively neglected.

### 6.3.3 Heat Pipe Penetration Fatigue Evaluation (Three-Dimensional Analysis)

In order to evaluate the stresses around the holes in the top plate where the heat pipes (or electric heaters) penetrate the pressure boundary, a three-dimensional (3-D) finite-element analysis was performed using the ANSYS code.

Pressure loading was applied to the underside of the head and at the cylinder ID. The maximum stress in the head was in the ligament at the inner row of holes, which is what would be expected. As shown in Figure 32, the margin against fatigue is ample.

### 6.3.4 Heat Well Stress Analysis

The heater well is subjected to an external pressure load on the finned section below the head. The design pressure load is 150 bar mean pressure and 22.5 bar alternating pressure.

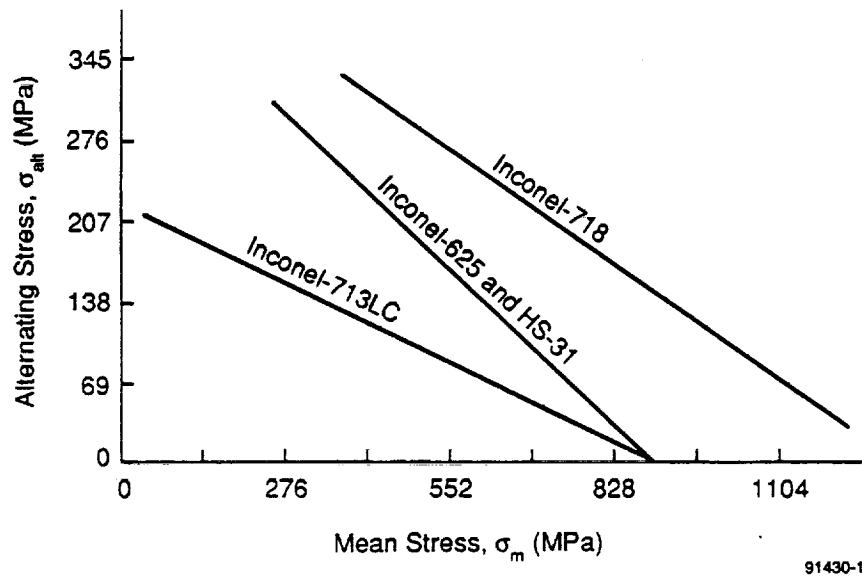


Figure 30. High-Cycle Fatigue at Low Temperature (273 to 523 K)

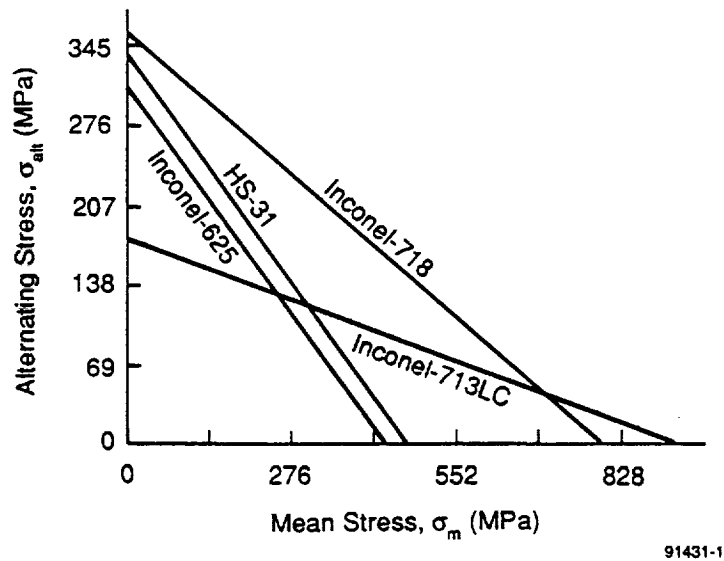


Figure 31. High-Cycle Fatigue at High Temperature (1050 K)

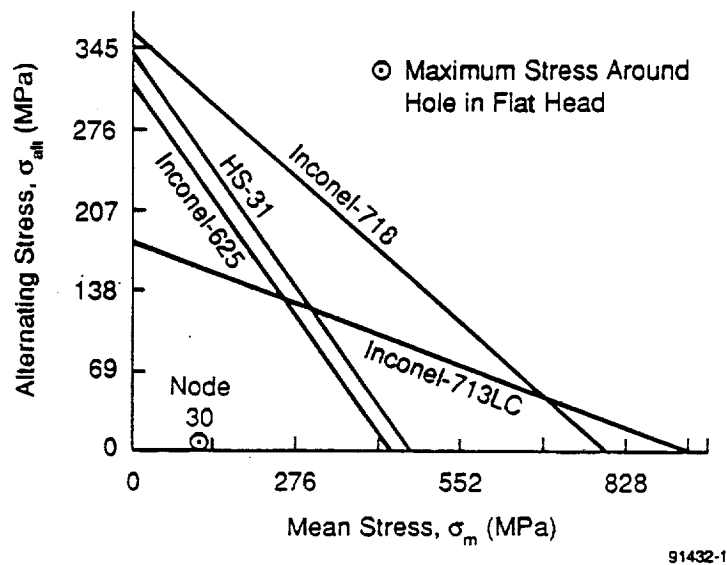


Figure 32. Predicted vs. High-Cycle Fatigue at High Temperature (1050 K)

The ID of the well is 1.57 cm, which has an interference fit with a nominal 1.58-cm diameter heater or heat pipe. The OD in the head section is selected at 1.78 cm (i.e., 0.1-cm wall) to minimize the diameter of the penetrations in the head. In the finned section, the wall thickness, and consequently the wall OD at the base of the fins, can be larger, if necessary.

At a thickness of 0.1 cm, the hoop stress in the well at a mean pressure of 150 bar is 129 MPa. At the maximum pressure of 172.5 bar, the stress is 148 MPa. These calculations neglect any load-carrying capability of the heater or heat pipe inside the well. They are compressive membrane stresses that are limited by creep and buckling, respectively. For a 0.1-cm wall, the critical buckling pressure is 565 bar. Hence, the factor of safety is 3.3, which is above the required value of 2.5.

It is conventional to assume that creep in compression has the same magnitude as in tension. This is probably a highly conservative assumption and tests are being recommended to evaluate this further, since it can have significant impact on the temperature drop across the wall of the engine heater and can affect the overall efficiency of space engine power systems.

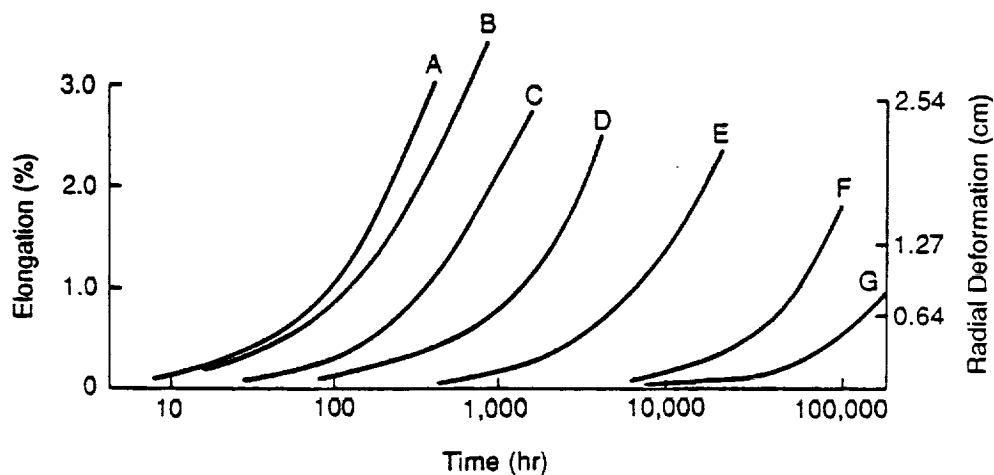
For the SPRE, this assumption is not a critical issue since the performance tests will be conducted over a wide range of temperature levels and temperature ratios, and the temperature ratio will be referenced to the base of the fins. At 1050 K, the maximum temperature drop across the well wall adjacent to the regenerator is approximately 270 °C/cm.

Since compressive creep of the well could deform the electric heater or heat pipe, a conservative approach is to assume that compressive creep is the same as tensile creep and limit the radial deformation due to this mechanism. It is uncertain whether removal

of electric heaters following operation can be done without a machining operation. Limiting compressive creep deformation increases the chance that such removal will be possible. Replacement of heat pipes is less likely, but the same argument applies.

Figure 33 shows the calculated percent reduction in well diameter and the approximate radial deformation in mils. The high-strength casting alloys, HS-31 and Inco-713LC, show very small deformation (less than 0.00025 cm for operation of over 10,000 hr). The lower creep strength of Inco-718 and -625 results in 1% deformation (about 0.00075 cm) for a 0.1-cm thick wall at 1000 K at about 100 hr. As shown on the figure, a thicker wall (0.2 cm) can operate at 1000 K for about 1,000 hr. This is a viable option for a performance test engine, where operating hours at the peak temperature will be limited. For an endurance demonstration at 1050 K, the high-strength alloys should be selected pending further data on compressive creep.

Line	Material	Temperature (K)	Well Wall Thickness (cm)
A	Inconel-718	1050	0.10
B	Inconel-625	1050	0.10
C	Inconel-718	1050	0.20
D	Inconel-718	1000	0.10
E	Inconel-718	1000	0.20
F	HS-31	1050	0.10
G	Inconel-713LC	1050	0.10



91433-1

Figure 33. Creep SPRE Heater Wells Assuming Compressive Creep is the Same as Tensile Creep (Mean Pressure = 150 bar; ID = 1.57 cm)

#### 6.4 Recommendations

Based on the analyses presented in this section, the following recommendations are made.

For the near term, an Inco-718 head should be considered since:

- A comfortable margin against fatigue failure is predicted.
- The cost should be modest since the gusset section from an existing head could be used and the plate and cylinder sections are straightforward.
- Fabrication should be straightforward since the joining to the head of the wells and shell can be done reliably with electron-beam welds.
- The time required to procure material and fabricate the heater head will be much less than for a cast material (Inco-713LC or HS-31).
- The life at 1050 K is conservatively estimated to be 500 hr. This is less than the specified requirement. However, since the time at temperature does not need to be very long during typical performance tests, this life span should be acceptable for the first head.

A second head made of cast Inco-713LC should be considered since:

- Inco-713LC would be the material of choice for a long-life, minimum-weight design.
- This head has a 7-yr life and would permit endurance testing at a hot-side temperature of 1050 K to be performed after other performance and development tests have been completed.
- A long-life head operating at 1100 K or slightly higher is possible.
- The joining processes are more difficult than with Inco-718 but are not expected to be extremely difficult since they are primarily for sealing.
- The Inco-713LC head and heat pipe heater arrangement, with relatively minor modifications, could be a viable candidate for a system that meets space application goals of efficiency and specific weight.

415 INTENTIONALLY BLANK



**APPENDIX A**  
**SPDE INSPECTION AND BUILD SUMMARY**

**PRECEDING PAGE BLANK NOT FILMED**

176 INTENTIONALLY BLANK

Engine No: <u>11 left</u>		Build Start: <u>6/19/86</u>		Engineer <u>JSR</u>	
Build No: <u>20</u>		Build Complete: <u>7/11/86</u>		Technician <u>JVH/PU</u>	
Component	P/N: 1015-	S/N	Design Actual	Weight	Date Tech
1 Heater (1632 tubes) E 0060		1	(1632 tubes)	18.035 Kg	5/20/86 GDA
2 Displ Cyl Seal		1 ID	4.5040 4.504		5/23/86 GDA
3 Regenerator C-0119		N/A	(54 scrns)	1.005 Kg	2/25/86 JVH
4 Cooler (1584 tubes) D-0068		3-Brunswick 2-Dutch weave		9.290 Kg	4/25/85 JSR
5 Outer vent orifice H-0147		1 ID	0.006		
6 Inner vent orifice H-0174		1 ID	0.006		
7 Nuts (24)				.300 Kg	4/28/85 JSR
8 Cooler I/O Flanges(2) -0130		1&2		.694 Kg	5/24/85 JSR
9 Bolts (8)				.024 Kg	5/24/85 JSR
10 Pressure Vessel w/s D-0122		1 with outstops		19.245 Kg	4/14/86 JVH
11 Nuts (30)				.535 Kg	4/25/85 JSR
12 Alt Cooling Jacket -0123		1		3.153 Kg	4/25/85 JSR
13 Bolts (4)				.064 Kg	2/1/86 JSR
14 Disp Dome Assem D-0037		2		1.1457 Kg	4/24/86 PU
15 Fwd G.S. Seal		1 ID	3.3514 3.3514		5/1/86 PU
16 Disp Exp/Cmp Seal		1 OD	4.5000 4.5000		5/1/86 PU
17 Disp Rod D-0070		3		.2775 Kg	4/29/86 PU
18 Bolts & Washers(4)				.0282 Kg	4/29/86 PU
19 Disp Rod Krng/Seal		1 OD	1.8000 1.7996 avg.		4/29/86 PU
20 Gas Spring Piston D-0075		P3-2		.2445 Kg	4/29/86 PU
21 Bolts & Washers(4)				.055 Kg	4/29/86 PU
22 Gas Spr Piston Seal		1 OD	3.2640 3.2651 avg		5/1/86 PU
23 Flange & Post w/inst D-0113		3		12.5002 Kg	4/29/86 PU
24 Bore Krng/Seal		1 ID	1.8010 1.8017		4/29/86 PU
25 Fwd G.S. Seal		1 OD	3.3500 3.3499		5/1/86 PU
26 Fixture Bolts (4)				.029 Kg	2/11/86 JSR
26 Damper Valve Assy		Not installed			
27 Gas Spring Cylinder D-0106		P3-2		3.7045 Kg	4/29/86 PU
28 Bolts (8)				.0508 Kg	4/29/86 PU
29 Aft G.S. Seal		1 ID	3.2659 3.2667		4/29/86 PU
30 Stuffer Volume		(5.38 in <sup>3</sup> )			2/2/86 JSR
30 Joining Ring D-0112		1		25.170 Kg	5/22/85 JVH
31 w/ inst & studs					
31 Piston Cyl w/ plugs D-0089		2		18.350 Kg	4/19/85 JSR
32 Bolts (8)				.022 Kg	4/25/85 JSR
33 G.S. Krng Supply Port Plug		Open X Clsd			4/19/85 JSR
34 Krng Ket Orifice		1 ID	0.0200		
35 Cyl Bore		1 ID	5.7010 5.7018		1/8/86 MM
36 Power Piston w/studs D-0088		2		3.025 Kg	4/19/85 JSR
37 Pist Krng/Seal		1 OD	5.7000 5.7003		1/8/86 MM
38 Plenum Cap Assy w/stiffners-0100		5		.378 Kg	5/30/86 PU
39 Bolts (9)				.025 Kg	4/14/86 JVH
40 Alternator Plunger D-0036		2		5.580 Kg	4/14/86 JVH
41 Nuts (18)				.025 Kg	4/24/85 JSR
42 Magnet Diameter		1 ID	8.360 ~ 8.330		4/14/86 PU
43 Magnet Diameter		1 OD	8.940 ~ 8.920		4/14/86 PU
44 Additional Plunger Mass				10.040 Kg	4/15/86 JVH
44 Inner Alt Stator w/s D-0020		2		6.612 Kg	4/18/85 JSR
45 Nuts & Washers Plenum plugs in				.010 Kg	4/19/85 JSR
46 Inner Stator		1 OD	8.300 8.298		4/19/85 JSR
47 Outer Alt Stator w/s D-0015		1		26.00 Kg	3/14/85 JVH
48 Nuts & Washers				.013 Kg	4/19/85 JSR
49 Stator Bore		1 ID	9.000 8.990		2/6/85 JSR

Note: All length dimensions are in inches.

Engine No:	<u>1144</u>	Build Start:	<u>6/19/86</u>	Engineer	<u>JSR</u>
Build No:	<u>20</u>	Build Complete:	<u>7/11/86</u>	Technician	<u>JVH/AU</u>
Component	P/N: 1015-	S/N	Design	Actual	Weight Date Tech

Bearing Clearances:				
50	Displacer Rod	0.0010	<u>.0020</u>	
51	Power Piston	0.0010	<u>.0015</u>	
Seal Clearances:				
53	Disp Exp/Cmp	0.0040	<u>.0042</u>	
54	Fwd Disp G.S. Disp	0.0014	<u>.00146</u>	
55	Fwd Disp G.S. Rod	0.0010	<u>.0020</u>	
56	Aft Disp G.S. Piston	0.0014	<u>.0016</u>	
57	Aft Disp G.S. Rod	0.0010	<u>.0020</u>	
58	Piston Cmp Space	0.0010	<u>.0009</u>	
	Piston Gas Spring	0.0010	<u>.0007</u>	
Alternator Plunger Clearances:				
59	Inner Gap	0.060	<u>~.030</u>	
60	Outer Gap	0.050	<u>~.030</u>	
Total Dynamic Mass:				
61	Piston Assem Dynamic Mass		<u>10.04</u> Kg	<u>1/20/86</u> <u>AU</u>
62	Displacer Assem Dynamic Mass		<u>1.6832</u> Kg	<u>4/20/86</u> <u>AU</u>
63	Casing Assem Dynamic Mass		<u>145.05</u> Kg	<u>      </u> <u>      </u>
64	Total Engine Mass		<u>      </u> Kg	<u>      </u> <u>      </u>

Note: All length dimensions are in inches.

Engine No:	<u>2Right</u>	Build Start:	<u>6/19/86</u>	Engineer	<u>JSR</u>		
Build No:	<u>20</u>	Build Complete:	<u>   </u> / <u>   </u> / <u>   </u>	Technician	<u>JVH/OU</u>		
Component	P/N: 1015-	S/N	Design	Actual	Weight	Date	Tech
1	Heater (1632 tubes)	E 0060	<u>2</u>	( <u>1477</u> tubes)	<u>18.035</u> Kg	<u>5/25/85</u>	<u>GDA</u>
2	Displ Cyl Seal		<u>ID</u>	<u>4.5040</u> <u>4.504</u>		<u>9/10/85</u>	<u>MM</u>
3	Regenerator	C-0119	<u>N/A</u>	( <u>54</u> scrns)	<u>9.40</u> Kg	<u>2/25/86</u>	<u>JVH</u>
	( 1.6 mil x 200 mesh )						
4	Cooler (1584 tubes )	D-0068	<u>36</u>	<u>Brunswick 2 Dutch weave</u>	<u>9.327</u> Kg	<u>5/20/85</u>	<u>GDA</u>
5	Outer vent orifice	E-0147	<u>ID</u>	<u>0.006</u>			
6	Inner vent orifice	E-0174	<u>ID</u>	<u>0.006</u>			
7	Nuts ( 24 )				<u>.300</u> Kg	<u>5/24/85</u>	<u>JSR</u>
8	Cooler I/O Flanges(2)	-0130	<u>3&amp;4</u>		<u>.693</u> Kg	<u>5/24/85</u>	<u>JSR</u>
9	Bolts ( 8 )				<u>.024</u> Kg	<u>5/24/85</u>	<u>JSR</u>
10	Pressure Vessel w/s	D-0122	<u>2</u>	<u>with outstps</u>	<u>19.42</u> Kg	<u>4/14/86</u>	<u>JVH</u>
11	Nuts ( 30 )				<u>.365</u> Kg	<u>4/14/86</u>	<u>JVH</u>
12	Alt Cooling Jacket	-0123	<u>2</u>		<u>3.105</u> Kg	<u>4/25/85</u>	<u>JSR</u>
13	Bolts ( 4 )				<u>.064</u> Kg	<u>7/11/85</u>	<u>JSR</u>
14	Disp Dome Assem	D-0037	<u>1</u>		<u>1.168</u> Kg	<u>5/22/85</u>	<u>JVH</u>
15	Fwd G.S. Seal		<u>ID</u>	<u>3.3514</u> <u>3.3514</u>		<u>3/30/85</u>	<u>JT</u>
16	Disp Exp/Cmp Seal		<u>OD</u>	<u>4.5000</u> <u>4.4997</u>		<u>2/20/86</u>	<u>MM</u>
17	Disp Rod	D-0070	<u>1</u>		<u>.220</u> Kg	<u>4/1/85</u>	<u>JSR</u>
18	Bolts & Washers(4)				<u>.028</u> Kg	<u>4/1/85</u>	<u>JSR</u>
19	Disp Rod Brng/Seal		<u>OD</u>	<u>1.8000</u> <u>1.8000</u>		<u>7/3/86</u>	<u>JS</u>
20	Gas Spring Piston	D-0075	<u>P2-1</u>		<u>.245</u> Kg	<u>3/20/85</u>	<u>JSR</u>
21	Bolts & Washers(4)				<u>.015</u> Kg	<u>4/23/85</u>	<u>JSR</u>
22	Gas Spr Piston Seal		<u>OD</u>	<u>3.2640</u> <u>3.2653 avg</u>		<u>1/30/85</u>	<u>JT</u>
23	Flange & Post w/inst	D-0113	<u>1</u>		<u>15.557</u> Kg	<u>2/22/85</u>	<u>JVH</u>
24	Bore Brng/Seal		<u>ID</u>	<u>1.8010</u> <u>1.8013</u>		<u>7/3/86</u>	<u>JVH</u>
25	Fwd G.S. Seal		<u>OD</u>	<u>3.3500</u> <u>3.3500</u>		<u>2/20/86</u>	<u>JT</u>
	Fixture Bolts (4)				<u>.029</u> Kg	<u>7/11/85</u>	<u>JSR</u>
26	Damper Valve Assy		<u>Not installed</u>				
27	Gas Spring Cylinder	D-0106	<u>P2-1</u>		<u>3.434</u> Kg	<u>4/13/85</u>	<u>JSR</u>
28	Bolts ( 8 )				<u>.052</u> Kg	<u>4/13/85</u>	<u>JSR</u>
29	Aft G.S. Seal		<u>ID</u>	<u>3.2659</u> <u>3.2668</u>		<u>2/8/85</u>	<u>JT</u>
	Stuffer Volume			( <u>5.38</u> in**3 )		<u>7/2/85</u>	<u>JSR</u>
30	Joining Ring	D-0112	<u>2</u>		<u>25.14</u> Kg	<u>4/25/85</u>	<u>JSR</u>
	w/ inst & studs						
31	Piston Cyl w/ plugs	D-0089	<u>1</u>		<u>18.37</u> Kg	<u>5/2/85</u>	<u>JSR</u>
32	Bolts (8)				<u>.072</u> Kg	<u>4/25/85</u>	<u>JSR</u>
33	G.S. Brng Supply Port Plug			<u>Open</u> <u>X Clsd</u>			
34	Brng Ret Orifice		<u>ID</u>	<u>5.7000</u> <u>5.7010</u>			
35	Cyl Bore		<u>ID</u>	<u>5.7010</u> <u>5.7014 avg</u>		<u>1/8/86</u>	<u>MM</u>
36	Power Piston w/studs	D-0088	<u>1</u>		<u>3.025</u> Kg	<u>4/18/85</u>	<u>JSR</u>
37	Pist Brng/Seal		<u>UD</u>	<u>5.7000</u> <u>5.7001</u>		<u>1/8/86</u>	<u>MM</u>
38	Plenum Cap Assy with stiffener	D-0100	<u>4</u>		<u>.375</u> Kg	<u>4/16/86</u>	<u>JVH</u>
39	Bolts ( 9 )				<u>.025</u> Kg	<u>4/24/85</u>	<u>JSR</u>
40	Alternator Plunger	D-0036	<u>1</u>		<u>5.553</u> Kg	<u>4/16/86</u>	<u>JVH</u>
41	Nuts ( 18 )				<u>.025</u> Kg	<u>4/24/85</u>	<u>JSR</u>
42	Magnet Diameter		<u>ID</u>	<u>8.3602</u> <u>8.330</u>		<u>2/23/86</u>	<u>MM</u>
43	Magnet Diameter		<u>OD</u>	<u>8.9402</u> <u>8.920</u>		<u>2/23/86</u>	<u>MM</u>
44	Additional Plunger mass				<u>10.04</u> Kg	<u>4/18/85</u>	<u>JVH</u>
45	Inner Alt Stator w/s	D-0020	<u>1</u>		<u>6.655</u> Kg	<u>3/18/85</u>	<u>JSR</u>
46	Nuts & Washers				<u>.010</u> Kg	<u>4/19/85</u>	<u>JSR</u>
	Inner Stator		<u>OD</u>	<u>8.300</u> <u>8.297</u>		<u>2/6/85</u>	<u>JT</u>
47	Outer Alt Stator w/s	D-0015	<u>2</u>		<u>26.61</u> Kg	<u>4/10/85</u>	<u>JSR</u>
48	Nuts & Washers				<u>.015</u> Kg	<u>4/10/85</u>	<u>JSR</u>
49	Stator Bore		<u>ID</u>	<u>9.000</u> <u>8.9983</u>		<u>2/6/85</u>	<u>JT</u>

Note: All length dimensions are in inches.

Engine No:	<u>2Right</u>	Build Start:	<u>6/19/86</u>	Engineer	<u>JR</u>
Build No:	<u>20</u>	Build Complete:	<u>7/11/86</u>	Technician	<u>JWH/AU</u>
Component	P/N: 1015-	S/N	Design	Actual	Weight Date Techn

Bearing Clearances:					
50	Displacer Rod	0.0010	<u>.0013</u>		
51	Power Piston	0.0010	<u>.0015</u>		
Seal Clearances:					
52	Disp Exp/Cmp	0.0040	<u>.0043</u>		
53	Fwd Disp G.S. Disp	0.0014	<u>.0015</u>		
54	Fwd Disp G.S. Rod	0.0010	<u>.0009</u>		
55	Aft Disp G.S. Piston	0.0014	<u>.0014</u>		
56	Aft Disp G.S. Rod	0.0010	<u>.0009</u>		
57	Piston Cmp Space	0.0010	<u>.0009</u>		
58	Piston Gas Spring	0.0010	<u>.0009</u>		
Alternator Plunger Clearances:					
59	Inner Gap	0.0600	<u>.330</u>		
60	Outer Gap	0.0500	<u>.283</u>		
Total Dynamic Mass:					
61	Piston Assem Dynamic Mass		<u>10.04</u>	Kg	<u>4/29/86 AU</u>
62	Displacer Assem Dynamic Mass		<u>1.33</u>	Kg	<u>4/29/86 AU</u>
63	Casing Assem Dynamic Mass			Kg	
64	Total Engine Mass			Kg	

Note: All length dimensions are in inches.

**APPENDIX B**  
**SPDE DATA SUMMARY REPORTS**

~~THE~~ INTENTIONALLY BLANK



## NOMENCLATURE

$P_{\text{mean}}$	Mean Pressure (Pa)
FRQ	Frequency (Hz)
TRTOA	Temperature Ratio
XPA	Piston Amplitude (m)
XDA	Displacer Amplitude (m)
XDPA	Displacer Phase Angle (deg)
PVPSTS	Piston PV Power (W)
KW(ALT)	Electrical Power Output (W)

PRECEDING PAGE BLANK NOT FILMED

216 INTENTIONALLY BLANK









Data Summary Report from: SP106B:45 at 8:37 AM FRI., 17 OCT., 1986 Plot file: SPL1E:45										
No	Date	Time	PHEQN	FRQ(XPL)	TRTQA	XPA <sub>6</sub>	XDA <sub>7</sub>	XDPA <sub>8</sub>	PUPSTS <sub>9</sub>	KW(ALT) <sub>10</sub>
1	1010	1407	7.2262E+06	7.0381E+01	1.6479E+00	5.1250E-03	4.0534E-03	9.8058E+01	-1.1692E-01	8.1554E+02
2	1010	1412	7.4823E+06	7.1577E+01	1.6385E+00	5.0702E-03	4.0300E-03	9.8157E+01	1.0165E+03	8.1343E+02
3	1010	1415	7.4459E+06	7.1412E+01	1.6383E+00	5.0461E-03	4.0224E-03	9.8248E+01	9.9796E+02	8.0182E+02
4	1010	1418	7.4136E+06	7.1255E+01	1.6432E+00	5.0821E-03	4.0515E-03	9.8045E+01	1.0345E+03	8.2002E+02
5	1010	1436	7.4909E+06	7.1742E+01	1.7221E+00	6.0438E-03	4.8737E-03	9.5135E+01	1.8058E+03	1.5266E+03
6	1014	1008	7.5340E+06	7.1732E+01	1.6271E+00	4.9768E-03	3.9325E-03	9.8811E+01	9.2110E+02	7.5420E+02
7	1014	1018	7.5140E+06	7.1590E+01	1.6131E+00	4.9340E-03	3.8731E-03	9.9120E+01	8.6878E+02	6.8271E+02
8	1014	1038	7.5159E+06	7.1461E+01	1.5954E+00	4.9734E-03	3.8671E-03	9.9607E+01	8.7774E+02	6.6381E+02
9	1014	1046	7.5340E+06	7.1662E+01	1.6113E+00	4.9730E-03	3.9091E-03	9.9158E+01	8.8454E+02	6.9907E+02
10	1014	1106	7.4338E+06	6.8429E+01	1.6424E+00	4.8850E-03	2.7363E-03	1.1315E+02	-4.6622E+02	-7.5262E+02
11	1014	1110	7.5683E+06	7.1791E+01	1.7111E+00	4.9135E-03	3.9232E-03	9.9719E+01	1.2077E+03	1.0282E+03
12	1014	1112	7.5395E+06	7.2029E+01	1.7070E+00	4.8380E-03	3.9984E-03	9.6553E+01	1.2257E+03	1.0018E+03
13	1014	1117	7.5019E+06	7.1785E+01	1.7026E+00	5.0144E-03	4.1087E-03	9.6742E+01	1.2508E+03	1.0299E+03
14	1014	1139	7.5046E+06	7.2101E+01	1.8049E+00	5.0631E-03	4.3959E-03	9.3958E+01	1.6402E+03	1.3942E+03
15	1014	1141	7.4912E+06	7.2040E+01	1.8041E+00	4.9768E-03	4.2291E-03	9.4093E+01	1.6098E+03	1.3392E+03
16	1014	1156	7.5020E+06	7.2326E+01	1.9021E+00	4.9582E-03	4.3344E-03	9.1994E+01	1.9252E+03	1.6133E+03
17	1014	1216	7.4947E+06	7.2492E+01	2.0030E+00	4.9739E-03	4.4547E-03	8.9941E+01	2.3166E+03	1.8657E+03
18	1014	1245	7.5067E+06	7.2466E+01	2.0067E+00	4.9282E-03	4.4155E-03	9.0042E+01	2.2614E+03	1.8403E+03
19	1014	1253	7.5116E+06	7.2497E+01	2.0011E+00	6.0868E-03	5.2579E-03	8.9000E+01	2.2437E+03	1.6313E+03
20	1014	1255	7.5035E+06	7.2394E+01	2.0020E+00	5.9740E-03	5.2345E-03	8.9079E+01	1.598E+03	2.6123E+03
21	1014	1257	7.5173E+06	7.2520E+01	2.0039E+00	5.9821E-03	5.2444E-03	8.8913E+01	3.2450E+03	2.6284E+03
22	1014	1303	7.5127E+06	7.2354E+01	2.0032E+00	6.0388E-03	5.9357E-03	8.7962E+01	4.1286E+03	3.3822E+03
23	1014	1304	7.5056E+06	7.2379E+01	2.0033E+00	6.0589E-03	5.9507E-03	8.7961E+01	4.1756E+03	3.4082E+03
24	1014	1309	7.5058E+06	7.2379E+01	2.0033E+00	6.0589E-03	5.9507E-03	8.8370E+01	4.9955E+03	3.4256E+03
25	1014	1323	7.5371E+06	7.2397E+01	2.0063E+00	7.0112E-03	5.8737E-03	8.8326E+01	4.0102E+03	3.3103E+03
26	1014	1342	7.5091E+06	7.2231E+01	2.0076E+00	7.9584E-03	6.5411E-03	8.7377E+01	5.0487E+03	4.1323E+03
27	1014	1346	7.5037E+06	7.2235E+01	2.0068E+00	7.9589E-03	6.5433E-03	8.7297E+01	5.0249E+03	4.1369E+03
28	1014	1347	7.5085E+06	7.2235E+01	2.0073E+00	7.9589E-03	6.5433E-03	8.7297E+01	5.0249E+03	4.1369E+03
29	1014	1402	1.8058E+07	8.3120E+01	2.0080E+00	5.9888E-03	4.7861E-03	9.1380E+01	4.9897E+03	3.7441E+03
30	1014	1431	1.2530E+07	9.2048E+01	1.9998E+00	5.9432E-03	5.6612E-03	9.2481E+01	6.7994E+03	4.7881E+03
31	1014	1457	1.5000E+07	9.9878E+01	1.9931E+00	6.0749E-03	5.9613E-03	9.2843E+01	9.3314E+03	6.1692E+03
32	1014	1500	1.4962E+07	9.9833E+01	1.9935E+00	5.9738E-03	5.9369E-03	9.3116E+01	8.9030E+03	5.7355E+03
33	1014	1517	1.5018E+07	9.9775E+01	2.0027E+00	6.0452E-03	6.0247E-03	9.1766E+01	1.1737E+04	7.6801E+03
34	1014	1519	1.5027E+07	9.9790E+01	2.0087E+00	6.0393E-03	6.0335E-03	9.1609E+01	1.1936E+04	7.6593E+03
35	1014	1558	1.5045E+07	9.9902E+01	2.0077E+00	6.0591E-03	6.0206E-03	9.1809E+01	1.1595E+04	7.4181E+03
36	1014	1606	1.5013E+07	9.9769E+01	2.0066E+00	6.9181E-03	6.5491E-03	9.1761E+01	1.1734E+04	7.5451E+03
37	1014	1608	1.5011E+07	9.9774E+01	2.0070E+00	6.9261E-03	6.5425E-03	9.1847E+01	1.1757E+04	7.5475E+03
38	1014	1609	1.5010E+07	9.9762E+01	2.0071E+00	6.9437E-03	6.5751E-03	9.1578E+01	1.1876E+04	7.5554E+03
39	1014	1618	1.5000E+07	9.9740E+01	2.0083E+00	6.9528E-03	6.5631E-03	9.1763E+01	1.1755E+04	7.5740E+03
40	1014	1624	1.5003E+07	9.9643E+01	1.9852E+00	6.9247E-03	6.5161E-03	9.1988E+01	1.1309E+04	7.3340E+03
41	1014	1629	1.4999E+07	9.9556E+01	1.9566E+00	6.9475E-03	6.5313E-03	9.1919E+01	1.0835E+04	7.0729E+03
42	1014	1636	1.5015E+07	9.9522E+01	1.9216E+00	6.9912E-03	6.4751E-03	9.2574E+01	1.0367E+04	6.8839E+03
43	1014	1642	1.5017E+07	9.9472E+01	1.8904E+00	6.9921E-03	6.3931E-03	9.2994E+01	9.4185E+03	6.4152E+03
44	1014	1650	1.4979E+07	9.9259E+01	1.8585E+00	6.9563E-03	6.3360E-03	9.3459E+01	8.7910E+03	6.0421E+03
45	1014	1659	1.4994E+07	9.9180E+01	1.8221E+00	6.9532E-03	6.2827E-03	9.3851E+01	7.9729E+03	5.5609E+03
46	1014	1706	1.4999E+07	9.8747E+01	1.7687E+00	7.7646E-03	6.7055E-03	9.3574E+01	8.3827E+03	5.7965E+03
47	1014	1710	1.5024E+07	9.8937E+01	1.7674E+00	7.3693E-03	6.4424E-03	9.4165E+01	7.5712E+03	5.3765E+03
48	1014	1713	1.4988E+07	9.8496E+01	1.7292E+00	8.6688E-03	7.2859E-03	9.2130E+01	8.7674E+03	6.1071E+03
49	1014	1723	1.4995E+07	9.8755E+01	1.7128E+00	6.8803E-03	6.0520E-03	9.5611E+01	5.7362E+03	4.0427E+03
50	1014	1749	1.5004E+07	9.8144E+01	1.6214E+00	7.9089E-03	6.5131E-03	9.5304E+01	4.6837E+03	2.9949E+03
51	1014	1800	1.4977E+07	9.8183E+01	1.5904E+00	6.4138E-03	5.5998E-03	9.8054E+01	3.1017E+03	2.0412E+03
52	1014	1802	1.5003E+07	9.8337E+01	1.5859E+00	6.4777E-03	5.3611E-03	9.9071E+01	3.6654E+03	1.7729E+03
53	1014	1805	1.4987E+07	9.8389E+01	1.5798E+00	4.2057E-03	4.8396E-03	1.0031E+02	2.280E+03	1.4742E+03
54	1014	1808	1.5004E+07	9.8434E+01	1.5701E+00	4.0557E-03	4.8474E-03	9.9911E+01	2.1049E+03	1.4314E+03
55	1014	1811	1.5009E+07	9.8533E+01	1.5662E+00	4.9346E-03	4.5484E-03	1.0069E+02	2.036E+03	1.2217E+03
56	1014	1814	1.4997E+07	9.8553E+01	1.5636E+00	4.4765E-03	4.1349E-03	1.0187E+02	1.6012E+03	1.0126E+03
57	1014	1817	1.5023E+07	9.8722E+01	1.5610E+00	3.9473E-03	3.9513E-03	1.0281E+02	1.3209E+03	7.8784E+02





Data Summary Report from: SP106D:45 at 2:47 PM TUE., 21 OCT., 1986 Plot file: SPL01D:45										
N <sub>1</sub>	Date	Time	PMEAN <sub>3</sub>	FRQ(XPL) <sub>4</sub>	TRTQA <sub>5</sub>	XPA <sub>6</sub>	XDA <sub>7</sub>	XDPA <sub>8</sub>	PUPSTS <sub>9</sub>	KW(ALT) <sub>10</sub>
1	1020	1022	7.5244E+06	7.1815E+01	1.6433E+00	5.4472E-03	4.1338E-03	9.7701E+01	1.1736E+03	8.8373E+03
2	1020	1040	7.4803E+06	7.1739E+01	1.6411E+00	5.2429E-03	3.9683E-03	9.8208E+01	1.0624E+03	8.1923E+03
3	1020	1117	7.4865E+06	7.1846E+01	1.6987E+00	5.4529E-03	4.2504E-03	9.6219E+01	1.4249E+03	1.1114E+03
4	1020	1139	7.5023E+06	7.2021E+01	1.7557E+00	5.3828E-03	4.2835E-03	9.4859E+01	1.5999E+03	1.2818E+03
5	1020	1159	7.4833E+06	7.2113E+01	1.8137E+00	5.4130E-03	4.3764E-03	9.3799E+01	1.8832E+03	1.4708E+03
6	1020	1232	7.4866E+06	7.2478E+01	1.9445E+00	5.3794E-03	4.5536E-03	9.0829E+01	2.3486E+03	2.1840E+03
7	1020	1244	7.5187E+06	7.2651E+01	2.0066E+00	5.4103E-03	4.5972E-03	9.9900E+01	2.6012E+03	2.0220E+03
8	1020	1304	7.5000E+06	7.2506E+01	2.0066E+00	5.4299E-03	4.5973E-03	9.9707E+01	2.6009E+03	2.0220E+03
9	1020	1306	7.5000E+06	7.2506E+01	2.0066E+00	5.4299E-03	4.5973E-03	9.9707E+01	2.6009E+03	2.0220E+03
10	1020	1341	1.0000E+07	8.3188E+01	2.0081E+00	5.3738E-03	4.6705E-03	9.0032E+01	4.2801E+03	2.9448E+03
11	1020	1343	1.0001E+07	8.3188E+01	2.0060E+00	5.3718E-03	4.6552E-03	9.1672E+01	4.1888E+03	2.9440E+03
12	1020	1345	1.0000E+07	8.3188E+01	2.0061E+00	5.3624E-03	4.6461E-03	9.1821E+01	4.2009E+03	2.9240E+03
13	1020	1347	1.0000E+07	8.3188E+01	2.0061E+00	5.3624E-03	4.6461E-03	9.1821E+01	4.2009E+03	2.9240E+03
14	1020	1355	1.0000E+07	8.3188E+01	2.0061E+00	5.3624E-03	4.6461E-03	9.1821E+01	4.2009E+03	2.9240E+03
15	1020	1357	1.0002E+07	8.3188E+01	2.0058E+00	5.3607E-03	4.6443E-03	9.1000E+01	4.4488E+03	2.9133E+03
16	1020	1430	1.2554E+07	9.2314E+01	2.0018E+00	5.3351E-03	5.0246E-03	9.3129E+01	5.9633E+03	7.2324E+03
17	1020	1432	1.2553E+07	9.2333E+01	2.0004E+00	5.3351E-03	5.0246E-03	9.3040E+01	6.0849E+03	7.3087E+03
18	1020	1434	1.2553E+07	9.2333E+01	2.0004E+00	5.3414E-03	5.0246E-03	9.3110E+01	6.0849E+03	7.3087E+03
19	1020	1450	1.2553E+07	9.2333E+01	2.0004E+00	5.3368E-03	5.0246E-03	9.3339E+01	6.0849E+03	7.3087E+03
20	1020	1452	1.2553E+07	9.2333E+01	2.0004E+00	5.3368E-03	5.0246E-03	9.3339E+01	6.0849E+03	7.3087E+03
21	1020	1453	1.2552E+07	9.2333E+01	2.0004E+00	5.3368E-03	5.0246E-03	9.3339E+01	6.0849E+03	7.3087E+03
22	1020	1500	1.2552E+07	9.2333E+01	2.0004E+00	5.3368E-03	5.0246E-03	9.3339E+01	6.0849E+03	7.3087E+03
23	1020	1503	1.2552E+07	9.2333E+01	2.0004E+00	5.3368E-03	5.0246E-03	9.3339E+01	6.0849E+03	7.3087E+03
24	1020	1504	1.2552E+07	9.2333E+01	2.0004E+00	5.3368E-03	5.0246E-03	9.3339E+01	6.0849E+03	7.3087E+03
25	1020	1504	1.2552E+07	9.2333E+01	2.0004E+00	5.3368E-03	5.0246E-03	9.3339E+01	6.0849E+03	7.3087E+03
26	1020	1546	1.5029E+07	9.9959E+01	2.0057E+00	6.3331E-03	5.9463E-03	9.3014E+01	9.8808E+03	6.0926E+03
27	1020	1559	1.5000E+07	9.9795E+01	2.0000E+00	6.3331E-03	5.9463E-03	9.2039E+01	1.2337E+04	7.7018E+03
28	1020	1601	1.5000E+07	9.9795E+01	2.0000E+00	6.3331E-03	5.9463E-03	9.2039E+01	1.2337E+04	7.7018E+03
29	1020	1613	1.5000E+07	9.9795E+01	2.0000E+00	6.3331E-03	5.9463E-03	9.2039E+01	1.2337E+04	7.7018E+03
30	1020	1730	1.5000E+07	9.9795E+01	2.0000E+00	6.3331E-03	5.9463E-03	9.2039E+01	1.2337E+04	7.7018E+03
31	1020	1747	7.5428E+06	7.2467E+01	1.9433E+00	7.4217E-03	6.0087E-03	8.8570E+01	4.2403E+03	3.3218E+03
32	1020	1800	7.5428E+06	7.2467E+01	1.9433E+00	7.4217E-03	6.0087E-03	8.8570E+01	4.2403E+03	3.3218E+03
33	1020	1801	7.5428E+06	7.2467E+01	1.9433E+00	7.4217E-03	6.0087E-03	8.8570E+01	4.2403E+03	3.3218E+03
34	1020	1802	7.5428E+06	7.2467E+01	1.9433E+00	7.4217E-03	6.0087E-03	8.8570E+01	4.2403E+03	3.3218E+03
35	1020	1900	7.5152E+06	7.1438E+01	1.7143E+00	1.0714E-03	7.4888E-03	8.9533E+01	4.4320E+03	4.4647E+03
36	1020	1917	7.5210E+06	7.1266E+01	1.6223E+00	1.0661E-03	7.2928E-03	9.1002E+01	2.9990E+03	2.2937E+03
37	1020	1951	7.5140E+06	7.0950E+01	1.4644E+00	1.0000E-03	7.0000E-03	9.0000E+01	6.4733E+03	5.3711E+03
38	1020	2000	7.5111E+06	7.0600E+01	1.4450E+00	1.0000E-03	7.0000E-03	9.0000E+01	6.4733E+03	5.3711E+03
39	1020	2006	7.5054E+06	7.0451E+01	1.4514E+00	1.0000E-03	7.0000E-03	9.0000E+01	6.4733E+03	5.3711E+03

Data Summary Report from:

SP106E:45

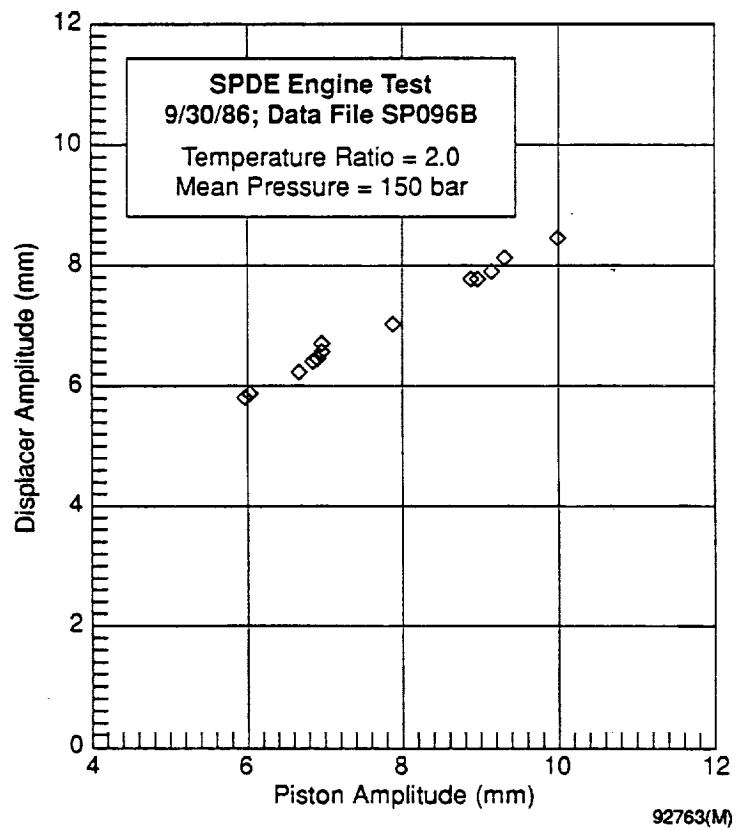
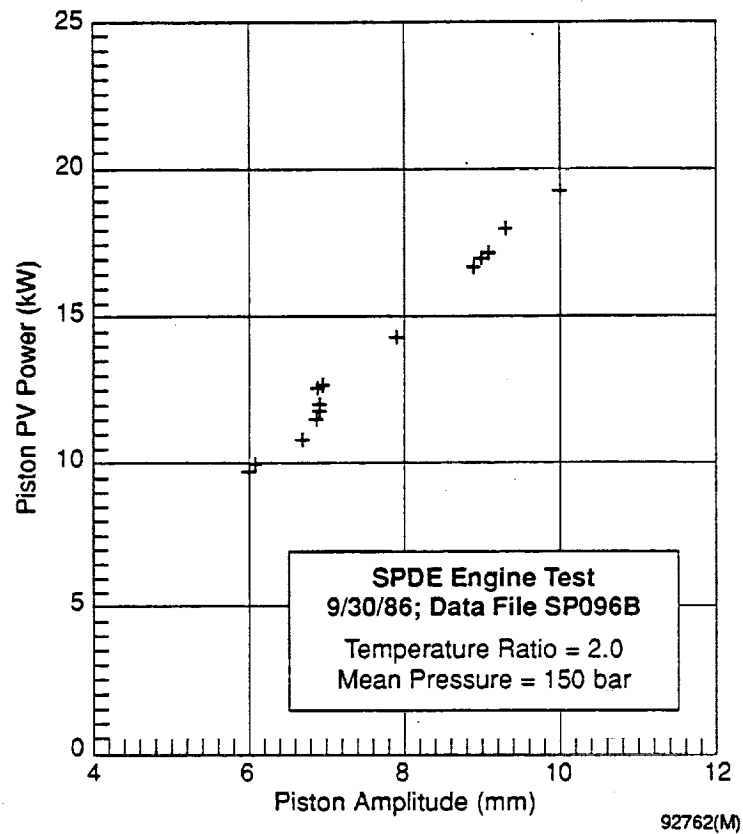
at 4:36 PM FRI., 24 OCT., 1986

Plot file: SPL1E:45

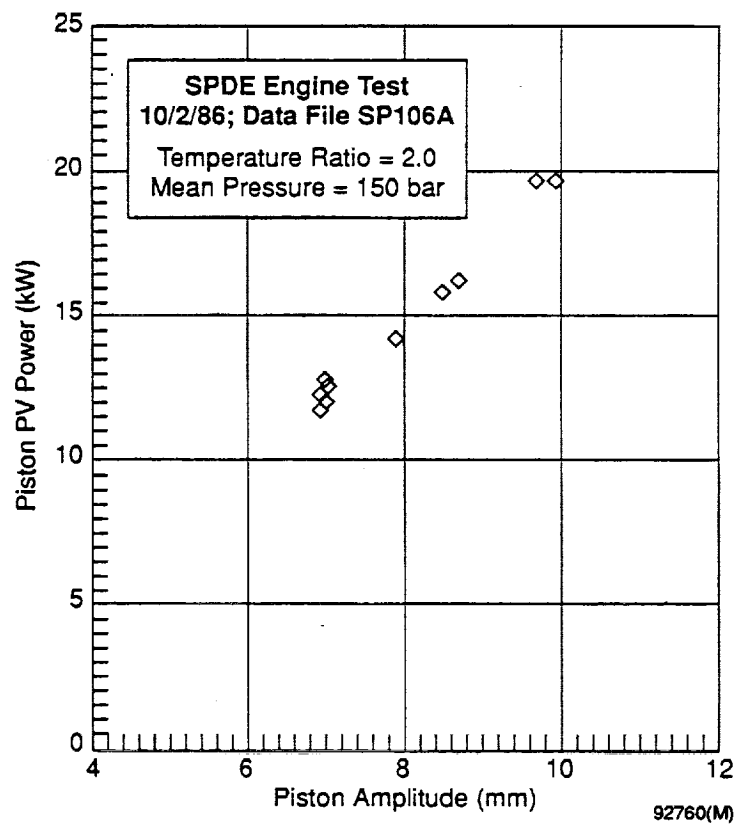
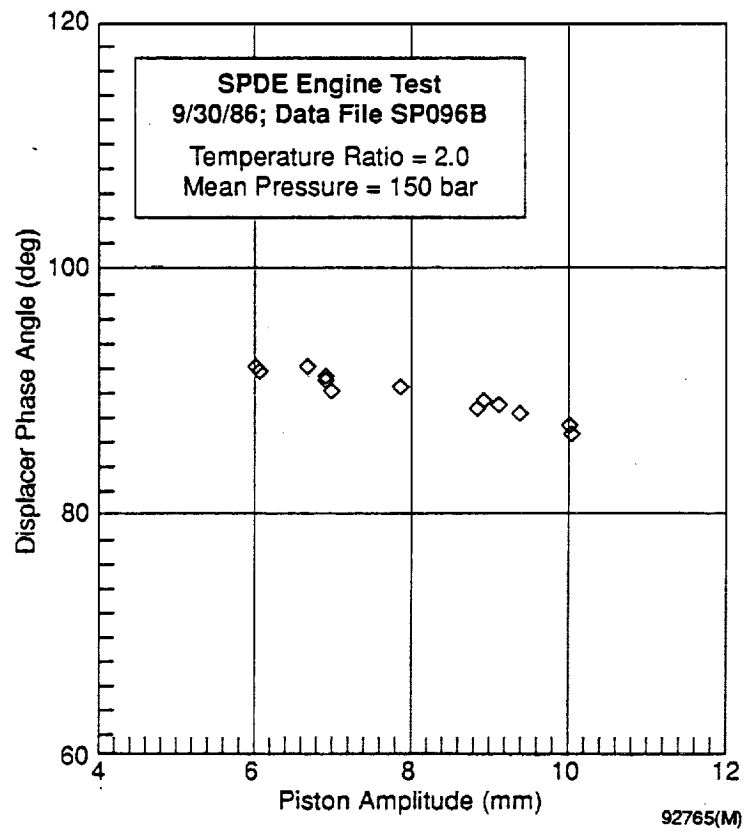
No 1	Date 2	Time 3	PMEAN 4	FRQ(XPL) 5	TRTOA 6	XPA 7	XDA 8	XDPA 9	PUPSTS 10	KW(ALT) 11
1	1024	0957	7.5577E+06	7.2006E+01	1.5921E+00	5.0658E-03	4.0431E-03	9.7790E+01	8.7719E+02	6.7084E+02
2	1024	1012	7.5530E+06	7.1939E+01	1.6155E+00	5.0640E-03	4.1060E-03	9.6716E+01	1.0017E+03	7.3468E+02
3	1024	1049	7.5540E+06	7.2289E+01	1.7114E+00	5.0658E-03	4.0363E-03	9.5218E+01	9.9818E+02	7.0104E+02
4	1024	1110	7.5508E+06	7.2327E+01	1.8133E+00	5.0658E-03	4.1388E-03	9.4268E+01	9.4598E+02	7.9567E+02
5	1024	1139	7.5192E+06	7.2785E+01	1.9125E+00	5.0633E-03	4.2934E-03	8.7541E+01	9.9670E+02	7.3179E+02
6	1024	1157	7.5063E+06	7.2903E+01	2.0226E+00	5.9638E-03	5.4325E-03	8.5710E+01	3.5061E+03	2.7152E+03
7	1024	1200	7.4615E+06	7.2699E+01	2.0241E+00	5.9519E-03	5.4258E-03	8.5732E+01	3.4770E+03	2.7028E+03
8	1024	1215	1.0002E+07	8.3297E+01	1.9990E+00	5.9875E-03	6.9123E-03	8.9160E+01	3.3944E+03	2.9082E+03
9	1024	1217	1.0000E+07	8.3272E+01	1.9996E+00	5.9953E-03	6.8874E-03	8.9133E+01	3.3223E+03	2.9267E+03
10	1024	1244	1.2497E+07	9.2222E+01	2.0200E+00	6.0041E-03	6.9944E-03	8.9971E+01	3.8206E+03	5.2992E+03
11	1024	1246	1.2496E+07	9.2229E+01	2.0197E+00	6.0366E-03	6.0101E-03	9.0049E+01	7.9079E+03	5.3467E+03
12	1024	1349	1.3351E+07	9.2330E+01	2.0237E+00	5.9778E-03	6.8506E-03	9.0641E+01	2.3784E+03	5.0532E+03
13	1024	1351	1.3349E+07	9.2324E+01	2.0261E+00	6.0094E-03	6.8665E-03	9.0662E+01	2.5624E+03	5.1095E+03
14	1024	1355	1.5005E+07	1.0022E+02	2.0183E+00	5.9724E-03	6.0648E-03	9.1473E+01	9.9824E+03	6.2646E+03
15	1024	1358	1.5005E+07	1.0030E+02	2.0129E+00	6.0300E-03	6.1023E-03	9.1433E+01	9.8763E+03	6.2525E+03
16	1024	1331	1.5005E+07	1.0031E+02	2.0118E+00	5.9662E-03	6.0109E-03	9.1706E+01	9.4742E+03	6.1440E+03
17	1024	1334	1.5006E+07	1.0033E+02	2.0093E+00	5.9896E-03	6.0179E-03	9.1688E+01	9.4564E+03	6.1505E+03
18	1024	1350	1.5003E+07	1.0023E+02	2.0078E+00	5.9807E-03	6.0953E-03	9.1011E+01	9.5800E+03	6.0464E+03
19	1024	1356	1.5005E+07	1.0023E+02	2.0067E+00	5.9915E-03	6.0178E-03	9.1730E+01	9.5324E+03	6.0385E+03
20	1024	1408	1.5000E+07	1.0011E+02	2.0050E+00	6.0058E-03	6.0341E-03	9.1680E+01	9.4213E+03	6.0504E+03
21	1024	1417	1.5004E+07	1.0020E+02	2.0050E+00	6.0693E-03	6.0717E-03	9.1538E+01	9.7337E+03	6.2216E+03
22	1024	1426	1.5005E+07	1.0020E+02	2.0064E+00	6.0073E-03	6.0259E+01	9.1692E+01	9.6442E+03	6.1295E+03
23	1024	1436	1.5003E+07	1.0020E+02	2.0066E+00	6.0031E-03	6.0084E-03	9.1855E+01	9.6161E+03	6.0260E+03
24	1024	1448	1.5003E+07	1.0020E+02	2.0068E+00	6.0058E-03	6.0169E-03	9.1792E+01	9.5580E+03	6.1481E+03
25	1024	1455	1.5005E+07	9.9953E+01	1.9838E+00	6.0331E-03	6.7839E-03	9.0361E+01	1.2064E+04	7.8847E+03
26	1024	1528	1.5010E+07	9.9462E+01	2.0174E+00	9.6437E-03	8.4714E-03	8.7056E+01	2.0531E+04	1.2976E+04
27	1024	1529	1.5007E+07	9.9543E+01	2.0148E+00	9.6248E-03	8.4208E-03	8.7643E+01	1.9104E+04	1.2221E+04
28	1024	1532	1.5004E+07	9.9804E+01	2.0441E+00	7.9139E-03	8.4002E-03	8.9668E+01	2.0037E+04	1.8551E+04
29	1024	1534	1.5002E+07	9.9276E+01	1.9870E+00	1.0275E-03	9.9554E-03	8.9597E+01	2.0023E+04	1.4414E+04
30	1024	1536	1.5009E+07	9.9322E+01	1.9823E+00	1.0264E-03	9.9154E-03	8.9597E+01	2.0023E+04	1.4260E+04
31	1024	1550	1.5001E+07	9.9592E+01	2.0650E+00	8.3114E-03	7.6140E-03	8.9464E+01	1.6830E+04	1.0796E+04
32	1024	1552	1.5004E+07	9.9568E+01	2.0643E+00	8.5599E-03	7.7577E-03	8.9223E+01	1.7607E+04	1.1385E+04
33	1024	1557	1.5002E+07	9.8947E+01	2.0295E+00	9.9037E-03	7.8710E-03	8.9994E+01	1.8223E+04	1.3007E+04
34	1024	1600	1.5005E+07	9.9220E+01	2.0210E+00	8.8427E-03	6.6203E-03	8.7160E+01	2.0726E+04	1.3843E+04
35	1024	1602	1.5002E+07	9.9187E+01	2.0084E+00	9.9199E-03	6.6854E-03	8.6817E+01	2.0480E+04	1.3851E+04
36	1024	1613	1.5005E+07	9.9150E+01	1.9934E+00	1.0622E-03	9.1529E-03	8.5266E+01	2.2455E+04	1.5377E+04
37	1024	1616	1.5008E+07	9.9100E+01	1.9902E+00	1.1059E-03	9.5165E-03	8.4476E+01	4.0000E+04	1.6035E+04
38	1024	1621	1.5013E+07	9.9154E+01	1.9830E+00	1.1277E-03	9.5753E-03	8.4150E+01	4.8956E+04	1.6783E+04
39	1024	1628	1.5009E+07	9.9137E+01	1.9674E+00	1.1631E-03	9.7596E-03	8.4080E+01	4.5146E+04	1.6803E+04
40	1024	1631	1.5002E+07	9.9372E+01	2.0470E+00	9.4902E-03	8.3266E-03	8.7370E+01	1.8703E+04	1.3408E+04

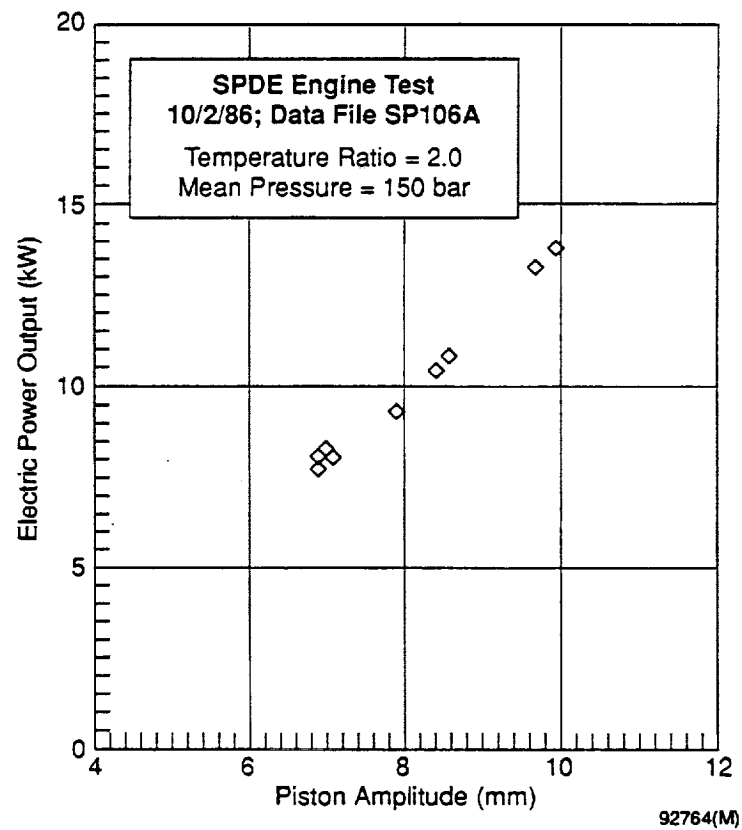
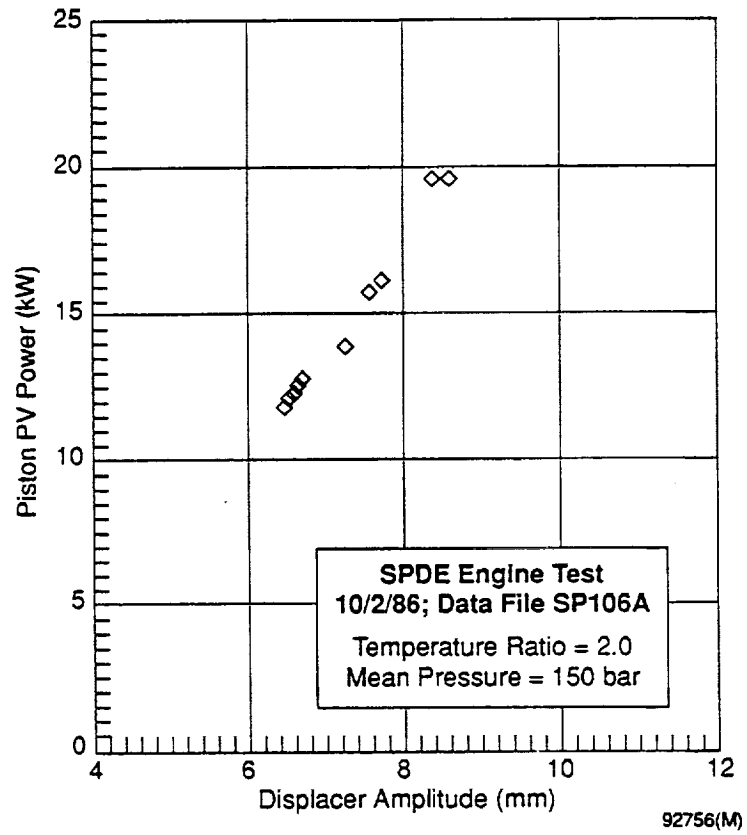
**APPENDIX C**  
**SELECTED SPDE PLOTS PRODUCED FROM**  
**APPENDIX B DATA**

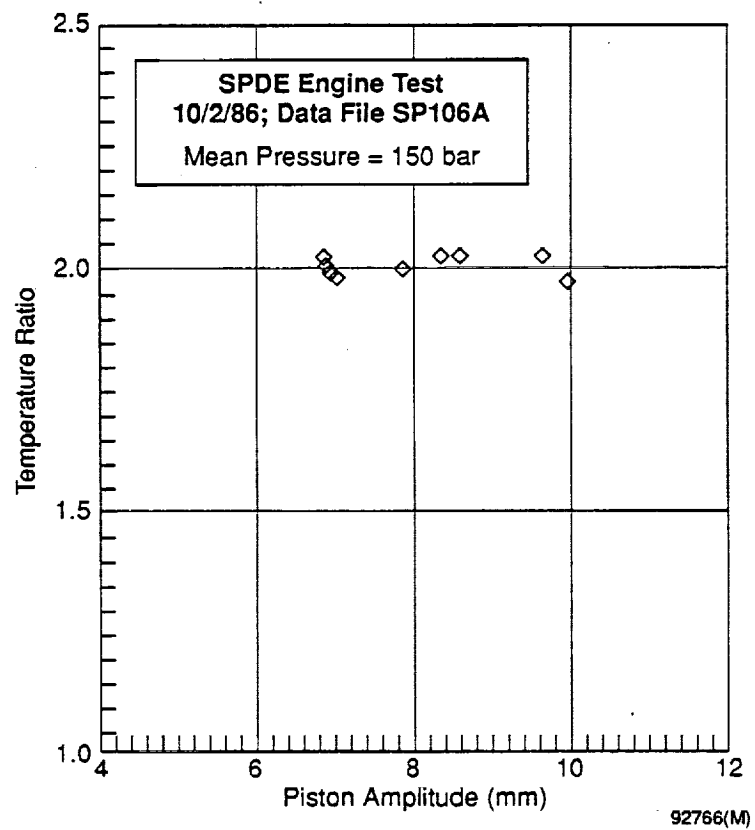




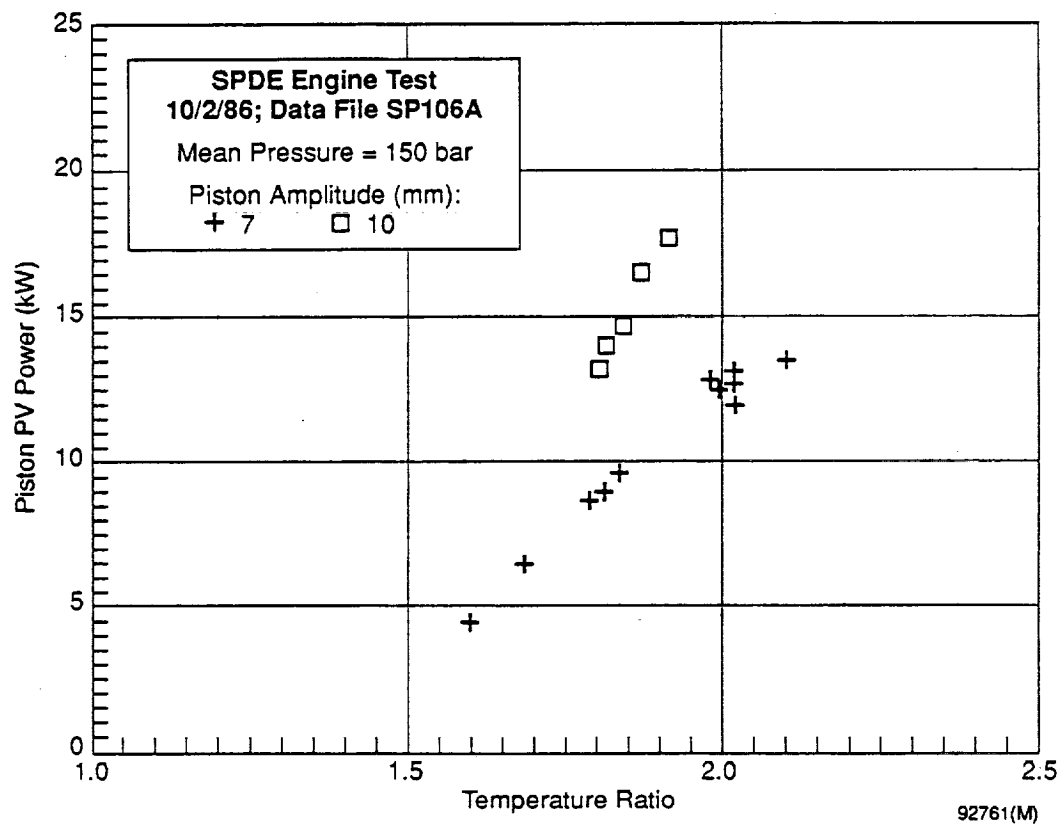
PRECEDING PAGE BLANK NOT FILMED

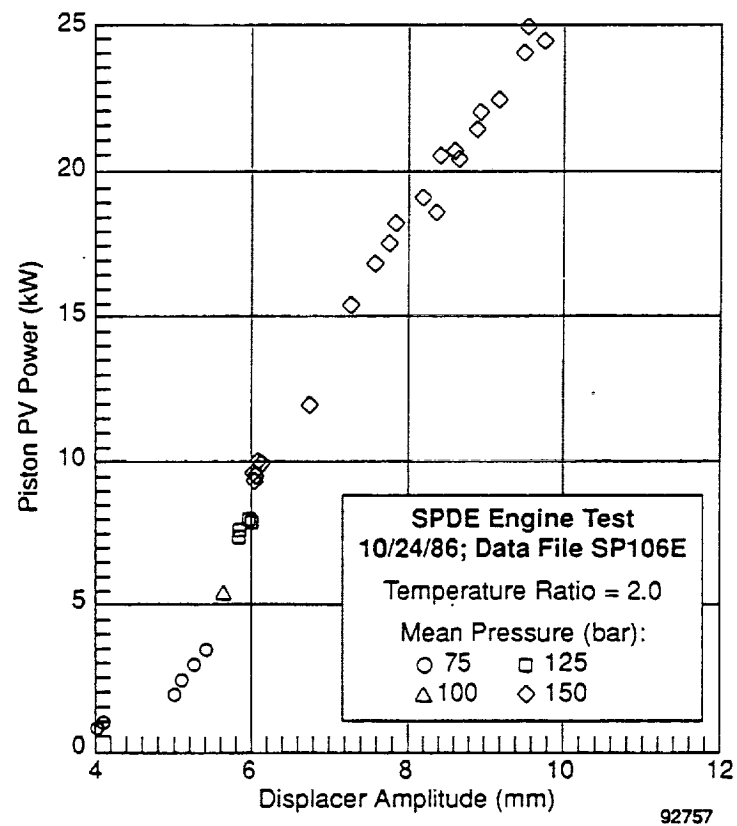
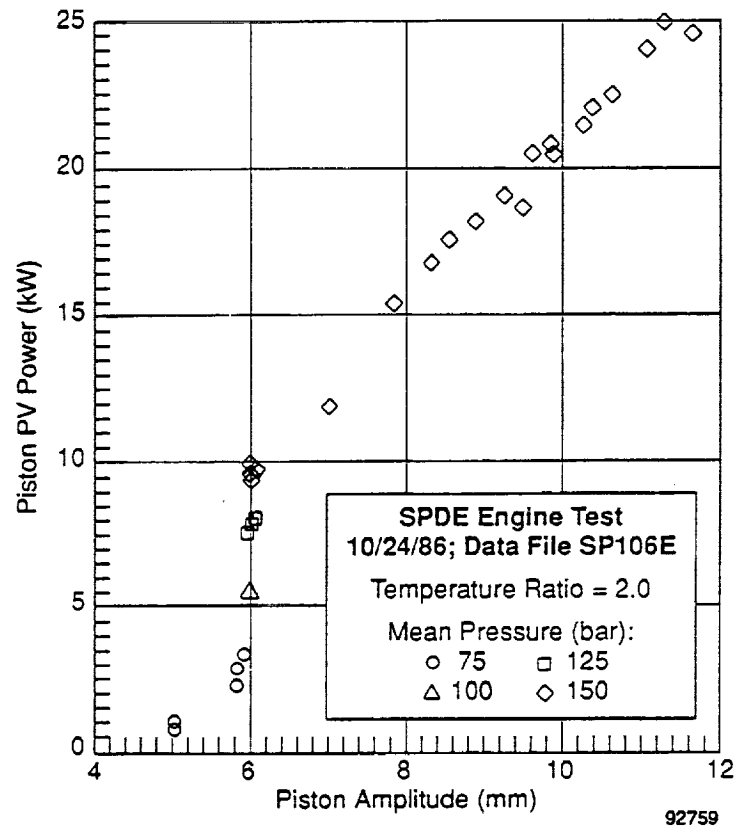


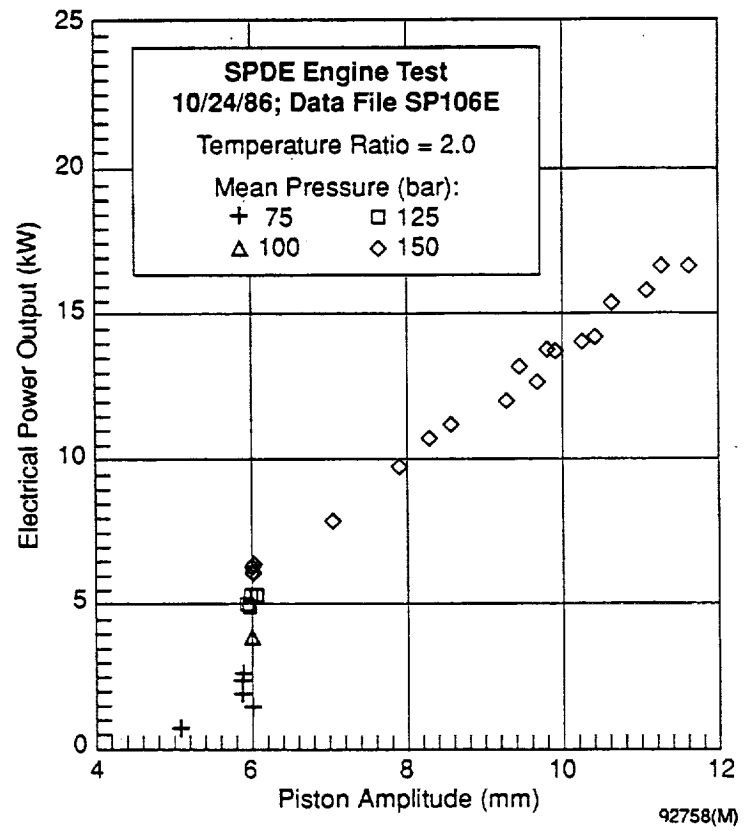














## **APPENDIX D**

### **SPRE HIGH-EFFICIENCY ALTERNATOR TEST**

- Run Sheet
- Inspection and Build Summary
- High-Efficiency Alternator Test Data Plots
- Data Summary Reports for High-Efficiency Alternator Tests

26

INTENTIONALLY BLANK

## NOMENCLATURE

ACASE	Case acceleration ( $\text{m/sec}^2$ )
ACCXC(A)	Case acceleration amplitude ( $\text{m/sec}^2$ )
AKADS	Aft displacer spring stiffness ( $\text{N/m}$ )
AKAPS	Piston spring stiffness ( $\text{N/m}$ )
AKFDS	Forward displacer spring stiffness ( $\text{N/m}$ )
AMP	First harmonic amplitude
CADS	Aft displacer spring damping coefficient ( $\text{N-s/m}$ )
CAPS	Piston spring damping coefficient ( $\text{N-s/m}$ )
CFDS	Forward displacer spring damping coefficient ( $\text{N-s/m}$ )
DPA	Calculated heat exchanger $\Delta P$ amplitude (Pa)
DPBNGD	Displacer bearing $\Delta P$ (Pa)
DPBNGP	Piston bearing $\Delta P$ (Pa)
DPPH	Calculated heat exchanger $\Delta P$ phase (deg)
DSFRG	Design frequency at operating pressure (Hz)
DTAFFH	Average heater fluid film $\Delta T$ ( $^{\circ}\text{C}$ )
DTBABS	Cooler thermocouple $\Delta T$ (backup)
DTBAC	Alternator cooler thermocouple $\Delta T$ (backup) ( $^{\circ}\text{C}$ )
DTBEC	Engine cooler thermocouple $\Delta T$ (backup)
DTBEH	Engine heater thermocouple $\Delta T$ (backup) ( $^{\circ}\text{C}$ )
DTPABC	Engine cooler delta temperature ( $^{\circ}\text{C}$ )
DTPAC	Alternator cooler $\Delta T$ ( $^{\circ}\text{C}$ )
DTPECn	Engine cooler $\Delta T$ ( $^{\circ}\text{C}$ )
DTPEHn	Engine heater $\Delta T$ ( $^{\circ}\text{C}$ )
DTPLD	Load thermocouple $\Delta T$ (backup) ( $^{\circ}\text{C}$ )
DTSLT	Salt heater temperature rise ( $^{\circ}\text{C}$ )
ETALT	Alternator efficiency
ETCRNO	Carnot efficiency (average wall temperature)
ETPVC	PV efficiency (based on heat reject)
ETPVP	PV efficiency (based on heat input)
ETSYS	System efficiency (power output/heat input)

## NOMENCLATURE (continued)

FBNGD	Displacer bearing flow $\Delta P$ (in. H <sub>2</sub> O)
FBNGR	Piston bearing flow $\Delta P$ (in. H <sub>2</sub> O)
FLAC	Alternator coolant flow (l/sec)
FLEC	Engine coolant flow (l/sec)
FLEH	Engine heater flow (l/sec)
FRQDVM	Not used
FRQ(SVM)	Engine frequency (Hz)
IALT	Alternator current (A rms)
IALTD	Alternator current (A)
IDC	dc load current (A)
KWALT	Alternator output power (W)
KWALTM	Alternator power output (W)
KW(HTRS)	Power to salt heaters (W)
Mean	Time averaged value
PADSD	Displacer aft gas spring pressure (Pa)
PALTS	Alternator shaft power (W)
PAPSP	Piston aft gas spring pressure (Pa)
PBRNGD	Displacer bearing supply pressure (Pa)
PBRNGP	Piston bearing supply pressure (Pa)
PCA	Compression space pressure amplitude (Pa)
PCL	Compression space pressure (Pa)
PCPH	Compression space pressure phase with respect to XP (deg)
PCPHI	Ideal pressure phase (deg)
PCPM	Compression space/mean pressure amplitude ratio
PEA	Calculated expansion space pressure amplitude (Pa)
PEPH	Calculated expansion space pressure phase (deg)
PES	Expansion space pressure (Pa)
PFDS	Displacer forward gas spring pressure (Pa)
PHADS	Aft displacer spring phase (deg)



## NOMENCLATURE (continued)

PHAPS	Piston spring pressure phase (deg)
Phase 1	Phase with respect to piston amplitude
Phase 2	Phase with respect to displacer
PHFDS	Forward displacer spring pressure phase (deg)
PMEAN	Mean pressure (Pa)
PNADS	Normalized aft displacer spring power (W)
PNAPS	Normalized spring power (W)
PNFDS	Normalized forward displacer spring power (W)
PRATIO	Maximum-minimum pressure ratio
Pturbine	Turbine pressure (bar)
PVPSN	Normalized piston PV power (W)
PVPST	Piston PV power (W)
PWADS	Aft displacer spring power (W)
PWAPS	Piston spring power (W)
PWDCS	Power transfer to casing (W)
PWFDS	Forward displacer spring power (W)
QALCA	Average alternator cooler heat reject (W)
QALCB	Alternator heat reject (backup) (W)
QALCP	Alternator heat reject (prime) (W)
QECA	Average engine cooler heat reject (W)
QECE	Engine heat reject (backup) (W)
QECF	Engine heat reject (prime) (W)
QEHA	Average engine heater heat input (W)
QEHB	Engine heat input (backup) (W)
QEHP	Engine heat input (prime) (W)
SPIN-RPM	Displacer (rpm)

## NOMENCLATURE (continued)

TAECW	Cooler wall temperature average (°C)
TAEHW	Average heater wall temperature (°C)
TALTL	Left alternator stator temperature (°C)
TAMBI	Inside ambient temperature (°C)
TAMBO	Outside ambient temperature (°C)
TBABSI	Cooler inlet temperature (backup) (°C)
TBACI	Alternator inlet temperature (backup) (°C)
TBECI	Engine cooler inlet temperature (backup) (°C)
TBECW	Cooler wall temperature (backup) (°C)
TBEHI	Engine heater inlet temperature (backup) (°C)
TBEHW	Heater wall temperature (backup) (°C)
TBRGR	Piston bearing return thermocouple temperature (°C)
TBRGSD	Displacer bearing supply thermocouple temperature (°C)
TBRGSP	Piston bearing supply thermocouple temperature (°C)
TCCR3	Cold regenerator 3:00 o'clock temperature (°C)
TCCR9	Cold regenerator 9:00 o'clock temperature (°C)
TCCRL6	Cold regenerator 6:00 o'clock temperature (°C)
TCCRL12	Cold regenerator 12:00 o'clock temperature (°C)
TCEXP1	Expansion space thermocouple temperature (°C)
TCHRL1	Hot regenerator thermocouple temperature (°C)
TCHRL2	Hot regenerator thermocouple temperature (°C)
TCSL1	Left compression space thermocouple temperature (°C)
TCSR1	Expansion space thermocouple temperature (°C)
TCSR2	Expansion space thermocouple temperature (°C)
TFDGSL	Forward displacer gas spring left thermocouple temperature (°C)
thtrent1	Salt heater control temperature (°C)
THTRI	Salt heater inlet temperature (°C)
THTRO	Salt heater outlet temperature (°C)
TPABCI	Engine cooler inlet temperature (°C)
TPACI	Alternator cooler inlet temperature (prime) (°C)
TPCYLL	Left piston cylinder temperature (°C)
TPECIn	Engine cooler inlet temperature (prime) (°C)
TPECW	Cooler wall temperature (prime)

## NOMENCLATURE (continued)

TPEHIn	Engine heater inlet temperature (prime) (°C)
TPEHW	Heater wall temperature (prime) (°C)
TPLDI	Load inlet temperature (prime) (°C)
TPPD1	Displacer position probe temperature (°C)
TREF-1	Thermocouple reference temperature (°C)
TREF-2	Thermocouple reference temperature (°C)
TREF-3	Thermocouple reference temperature (°C)
TREF-8	Reference suction temperature (°C)
TRTEC	Expansion/compression temperature ratio
TRTOA	Heater/cooler wall temperature ratio (average)
TRTOB	Heater/cooler wall temperature ratio (backup)
TRTOFB	Heater/cooler fluid temperature ratio (backup)
TRTOFP	Heater/cooler fluid temperature ratio (prime)
TRTOP	Heater/cooler wall temperature ratio (prime)
TRTRG	Regenerator temperature ratio
TSPOL1	Spool temperature engine end (°C)
TSPOL2	Spool temperature mass end (°C)
VACLD	Alternator load voltage (V rms)
VALT	Alternator terminal voltage (V)
VALTL	Alternator terminal voltage (V rms)
VCAP	Series capacitor voltage (V rms)
VCAPD	Tuning capacitor voltage (V)
VDC	dc load voltage (V)
VLD	Alternator load voltage (V)
VPA	Piston velocity amplitude (m/sec)
VSERLD	Series load voltage (V rms)
XCA	Calculated casing amplitude (m)
XCPH	Calculated casing phase with respect to XP (deg)
XDA	Displacer amplitude (m)
XDL	Displacer displacement (m)
XDL1	Mean displacer position (m)

## NOMENCLATURE (continued)

XDL2	Displacer amplitude (m)
XDL(A)	Displacer amplitude (m)
XDLCK	Displacer displacement check (m)
XDL(M)	Mean displacer position (m)
XDMA	Mean displacer position (m)
XDPH	Displacer phase with respect to piston (deg)
XDRP	Displacer/piston amplitude ratio
XDSPET	$XDA \times \sin(XDPH) \times ETCRNO$ (m)
XPA	Piston amplitude (m)
XPL	Piston displacement (m)
XPL1	Mean piston position
XPL2	Piston amplitude (m)
XPL(A)	Piston amplitude (m)
XPL(M)	Mean piston position (m)
XPMA	Mean piston position (m)

#### Test Configuration Summary

This test is the second test for the Hi-Efficiency Alternator evaluation. The engine configuration used standard hydrostatic bearings, 1.0 mil Brunswick regenerator material, spacer ring removed from pressure vessel.

This test was conducted after the flange/post to cylinder pins were redrilled to correct a misalignment problem discovered on the last test.

The Alternator efficiency was very close to code predictions, a major improvement from the magnetic material tested for the baseline test. Also the PV power and subsequently Alternator Power were higher than previously attained.

RJB 1-5-90

Test Engineer      Date

S P R E ENGINE RUN SHEET

OPERATOR: PWLF

DATE: 01/03/90

RUN NO.: 50 BUILD NO: 28

SALT PUMP START: 08 : 00 01/03/90;

ENGINE START: 09 : 54 01/03/90

STOP: 17 : 18 01/03/90;

STOP: 17 : 12 01/03/90

DAY TOTAL HRS: 9.3

DAY TOTAL HRS: 7.3

ACCUM. TOTAL HOURS: 1680.5

ACCUM. TOTAL HOURS: 244.3

BOOST PUMP START: 09 : 58 01/03/90

STOP: 17 : 12 01/03/90

DAY TOTAL HRS: 7.3

ACCUM. TOTAL HOURS: 167.0 Displacer

166.0 Piston

TEST OBJECTIVES:

*Base line map - high eff. alt. test.*

COMMENTS/PROBLEMS:

*Completed test*

## SPRE INSPECTION AND BUILD SUMMARY

PAGE 1

ENGINE #1: 2		BUILD START: 12/08/89		ENGINEER: R.Bolton			
BUILD #1: 28		BUILD COMPLETE: 12/18/89		TECHNICIAN: C.Wolfe/W.Smith			
COMPONENT	P/N 1015	S/N	DESIGN	ACTUAL	WEIGHT Kg	DATE	TECH COMMENTS
1. HEATER (1632 tubes)	C-0220-F	01	( 1631 tubes)	26.68000	02/18/88	CFW	
2. DISP. CYL. SEAL	D-0060-C		ID 4.5040	4.5040	05/20/85	GDA	
3. REGENERATOR							
Stand off wire 8 ea .032							
Corase screen 1 ea .030	B-0234-B			.06680	07/31/89	WJS	
Brunswick 1 ea .001	C-0218-B			.23300	07/31/89	WJS	
Fine screen 4 ea .010	B-0233-B			.01600	07/31/89	WJS	
Brunswick 1 ea .291	C-0218-B			.02400	07/31/89	WJS	
Fine screen 4 ea .010	B-0233-B			.01600	07/31/89	WJS	
Brunswick 1 ea .289	C-0218-B			.23600	07/31/89	WJS	
Coarse screen 1 ea .030	B-0234-B			.06680	07/31/89	WJS	
Stand off wire 8 ea .032							
4. COOLER (1584 tubes)							
5. OUTER VENT ORIFICE	D-0068-E	01	( 1584 tubes)	9.26500	02/16/88	CFW	
6. INNER VENT ORIFICE	B-0147-B		ID 0.006	00.0060	02/16/88	CFW	
7. NUTS (24)	B-0147-B		ID 0.006	00.0060	02/16/88	CFW	
				.30000	04/01/88	CFW	
8. COOLER (I/O FLANGES (2))							
9. BOLTS (8)	C-0130-B	1&2		.69400	05/24/85	JSR	
				.02400	05/24/85	JSR	
10. PRESSURE VESSEL w/STUDS							
11. NUTS (30)	D-0501-A	01		19.09090	11/15/89	CFW	
				.51970	02/19/88	CFW	
12. ALT. COOLER JACKET							
13. BOLTS (4)	C-0123-C	01		5.85500	03/31/88	CFW	
14. SPACERS (4)	B-0301-A	1-4		.06400	03/28/88	CFW	
				.03000	03/28/88	CFW	
15. DISP. DOME ASSEMBLY *1							
16. FORWARD G.S. SEAL			ID 3.3514	3.3514	08/10/89	SRI	
17. DISPLACER EXP/CMP SEAL			ID 4.5000	4.50015	08 10/89	SRI	

Note: All length units are in inches.

# SPRE INSPECTION AND BUILD SUMMARY

PAGE 2

ENGINE #:	2	BUILD START: 12/08/89	ENGINEER: R. Bolton					
BUILD #:	28	BUILD COMPLETE: 12/18/89	TECHNICIAN: C. Wolfe/W. Smith					
COMPONENT	P/N	1015	S/N	DESIGN	ACTUAL	WEIGHT Kg	DATE	TECH COMMENTS
18. DISPLACER ROD #1	D-0070-H							
19. BOLTS & WASHERS (4) *1						.02954	09/27/89	CFW
20. DISP. ROD BRG./SEAL				OD 1.8000	1.8000		08/18/89	TB
21. GAS SPRING PISTON #1	D-0595-A		01-P3			.25764	09/27/89	CFW
22. BOLTS & WASHERS (4) *1						.01554	09/27/89	CFW
23. GAS SPRING PISTON SEAL				OD 3.2640	3.2648		09/05/89	TB
24. F/P W/INSTRUMENTATION	D-0113-D		03			9.31600	02/18/88	CFW
25. BORE/BEARING SEAL				ID 1.8010	1.8010		10/19/87	DNS
26. G.S. SEAL				OD 3.3500	3.3500		10/19/87	DNS
27. FIXTURE BOLTS (4)						.02900	10/19/87	DNS
28. GAS SPRING CYLINDER	D-0106-C		01-P3			3.70300	10/19/87	DNS
29. BOLTS (8)						.04900	10/19/87	DNS
30. AFT G.S. SEAL				ID 3.2659	3.2666		10/19/87	DNS
31. STUFFER VOLUME				( 6.3060 in**3)			05/27/87	JSR
32. JOIN'N RING W/INST&STUDS	D-0504-A		01			29.91477	11/17/89	CFW
33. PISTON CYLINDER W/PLUGS	D-0502-A		01					
34. INNER STATOR & NUTS	D-0488-A		01					
35. BOLTS (9)						.07200	04/25/85	JSR
36. G.S. BRG. SUPPLY PORT PLUG				X OPEN	CLSD		03/20/89	CFW
37. BRG. RET. ORIFICE				ID 0.0200		.03000	04/01/88	CFW
38. CYLINDER BORE				ID 5.7000	5.7014		12/16/87	CFW
39. POWER PISTON W/STUDS #2	D-0088-C		01					
40. PISTON BRG. SEAL				06 Ports Open			12/16/87	CFW
41. PLENUM COV/ARM MNT				OD 5.7000	5.7003			
42. BOLTS (18)	D-0276-D		01			1.26200	03/30/88	CFW
						.03530	03/30/88	CFW

Note: All length units are in inches.



# SPRE INSPECTION AND BUILD SUMMARY

PAGE 3

ENGINE #:	2	BUILD START:	12/08/89	ENGINEER:	R.Bolton			
BUILD #:	28	BUILD COMPLETE:	12/18/89	TECHNICIAN:	C.Wolfe/W.Smith			
COMPONENT	P/N	1015	S/N	DESIGN	ACTUAL	WEIGHT Kg	DATE	TECH COMMENTS
43. STATOR MTG. RING	E-0277-E	01				2.43230	03/30/88	CFW
44. BOLTS (12)						.03500	03/30/88	CFW
45. ALTERNATOR PLUNGER *2	D-0036-C	02				4.18950	02/19/88	CFW
46. NUTS (18) *2						.02500	02/19/88	CFW
47. MAGNET DIAMETER				ID 8.367	8.3600		02/19/88	CFW
48. MAGNET DIAMETER				OD 8.940	8.9700		02/19/88	CFW
49. OUTER ALTERNATOR STATOR W/STUDS & NUTS	D-0284-B	02				26.60000	02/19/88	CFW
50. STATOR ID				ID 9.0000	9.0000		02/19/88	CFW
BEARING CLEARANCES								
51. DISPLACER ROD				0.0010	0.0010			
52. POWER PISTON				0.0010	0.0011			
SEAL CLEARANCES								
53. DISPLACER EXP/CMP (2,18)				0.0040	0.0041			
54. FWD DISPLACER G.S. DISPLACER (16,26)				0.0014	0.0012			
55. FWD DISPLACER G.S. PISTON (20,25)				0.0010	0.0010			
56. AFT DISPLACER G.S. PISTON (23,30)				0.0014	0.0016			
57. AFT DISPLACER G.S. ROD (20,25)				0.0010	0.0010			
58. PISTON CMP. SPACE (38,40)				0.0010	0.0011			
59. PISTON GAS SPRING (38,40)				0.0010	0.0011			
ALTERNATOR PLUNGER CLEARANCES								
60. INNER GAP				0.060	0.0600			
61. OUTER GAP				0.060	0.0300			

Note: All length units are in inches.

SPRE INSPECTION AND BUILD SUMMARY

PAGE 4

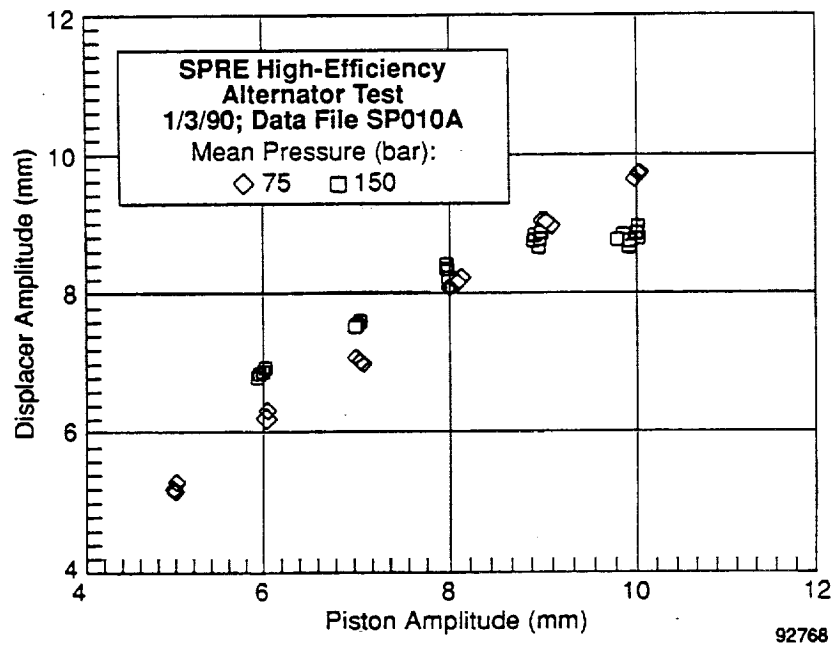
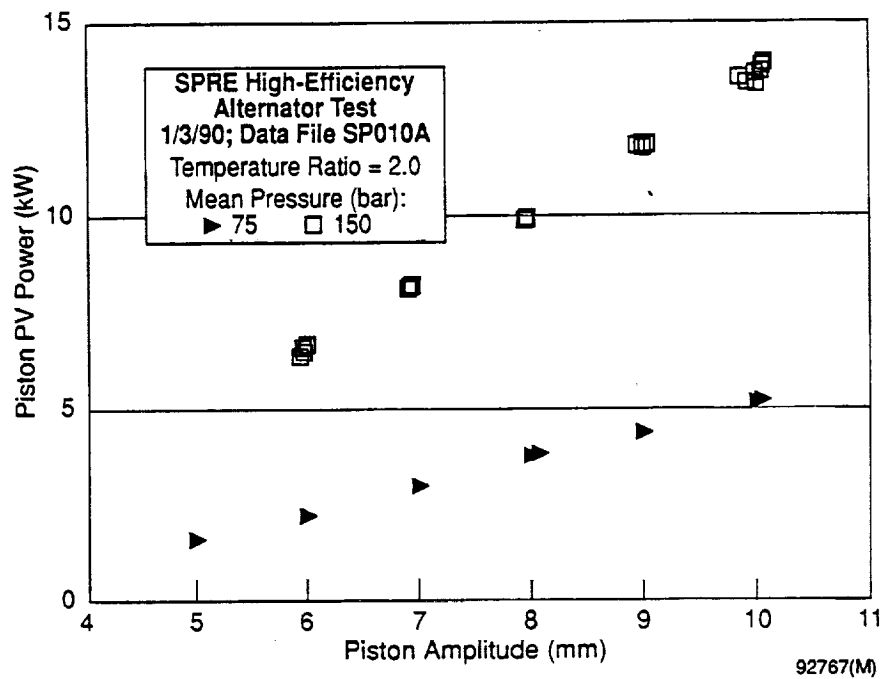
ENGINE #:	2	BUILD START:	12/08/89	ENGINEER:	R. Bolton			
BUILD #:	28	BUILD COMPLETE:	12/18/89	TECHNICIAN:	C.Wolfe/W.Smith			
COMPONENT	P/N	1015	S/N	DESIGN	ACTUAL	WEIGHT	DATE	TECH COMMENTS
TOTAL DYNAMIC MASS								
62. PISTON ASSEMBLY DYNAMIC MASS								
63. DISPLACER ASSEMBLY DYNAMIC MASS								
64. CASING ASSEMBLY DYNAMIC MASS								
65. TOTAL ENGINE MASS								

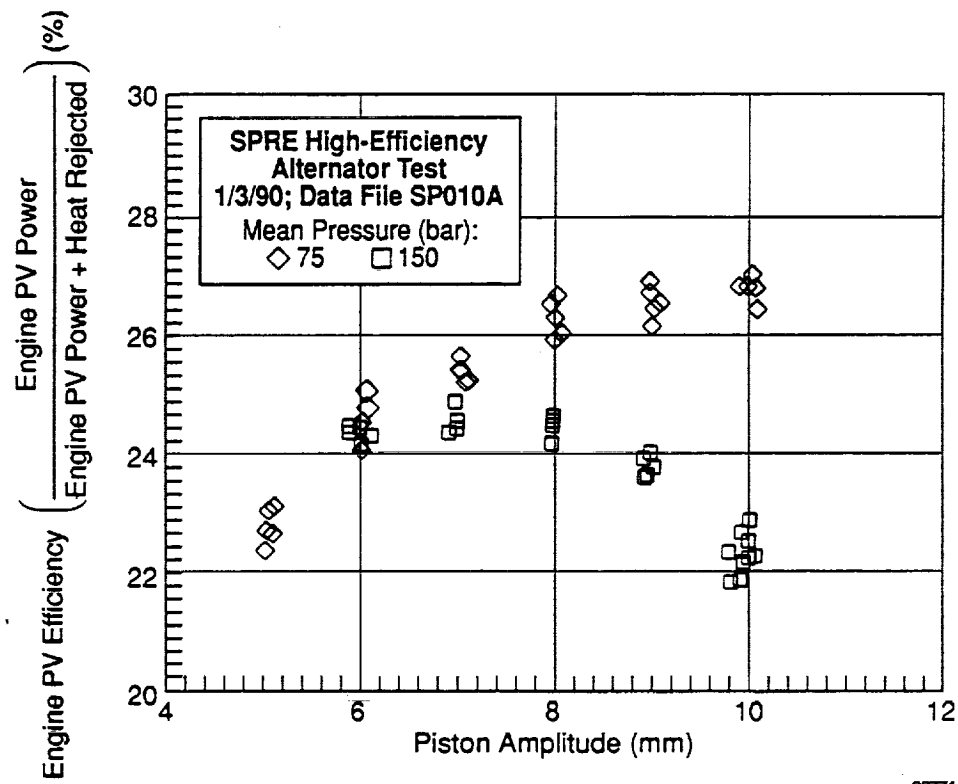
NOTES:

- \*1 DISPLACER MASS COMPONENTS
- \*2 PISTON MASS COMPONENTS

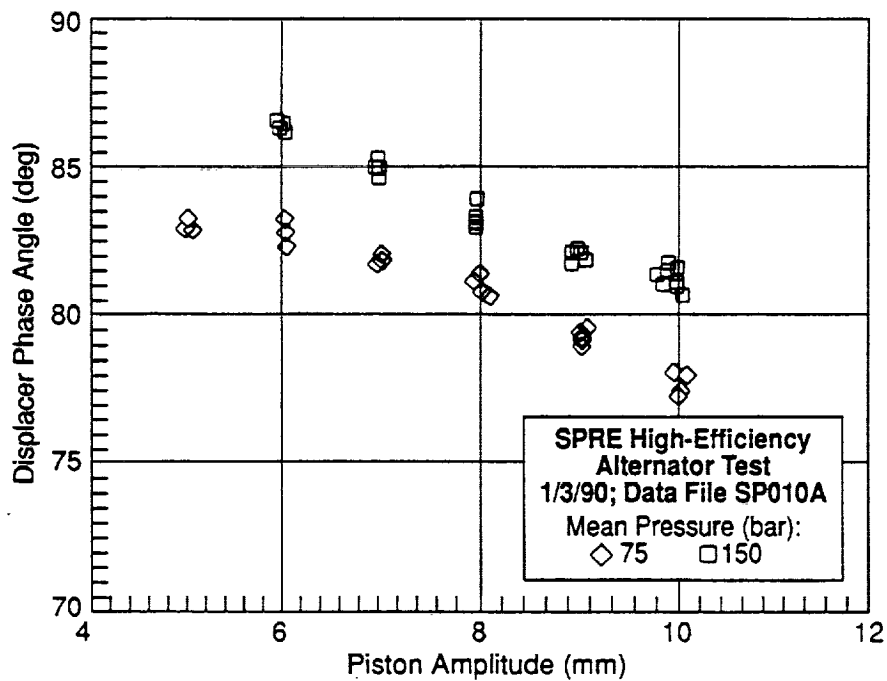
A.C. LOAD  
DISPLACER OUTSTOP MODIFICATION (ref. build 12) MOD. HEIGHT FROM.220" TO.160"  
PISTON OUTSTOP .075"  
DISPLACER CENTERING INSTALLED  
ADDED STAND OFF WIRE TO BOTTOM OF COOLER 0.032 in.  
COMPRESSION SPACE TRANSDUCER EXT. TUBE ADDED 5.25"X.126"X.082"  
EXPANDED SPACE PRESS. XDUCER REPLACED BY FOUR TC's -2 on disp. cyl.(top/bot), 2 on post(top/bot)  
REMOVED TC CYL(bot), REPLACED WITH COMP.SPACE TC 3615  
ONE TC (3708) TO DISPLACER APT GAS SPRING  
TACKED FOWARD DISPLACER GAS SPRING TC(3703) TO THE SEAL I.D. WALL. CHANGED TO FWD.DISP. SEAL WALL  
TEMP.  
ADDED 8 TC's TO FLANGE/POST ASSEMBLY; I.D'd 0 & 7-14, READ ON FLUKE 2280B DATA LOGGING SYSTEM. FOR  
LOCATION, SEE ATTACHED ENCLOSURES.  
REMOVED TWO TC's ON DISPLACER CYLINDER 3710 & 3712  
DISPLACER VENT HOLE MOD. TO 1/4-20 TAP, 13.5 MIL HOLE IN 1/4-20 CAPSCREW W/CU. GASKET AS VENT.  
NEW WASHER DESIGN UNDER 4-10-32 X 1 3/4" ROD TO DISPLACER CAPSCREW.  
ONE TIME NOTE; DISPLACER CYLINDER/FLANGE-POST REPINNED. MIN 1mil CLEARANCE ESTABLISHED.

Note: All length units are in inches.

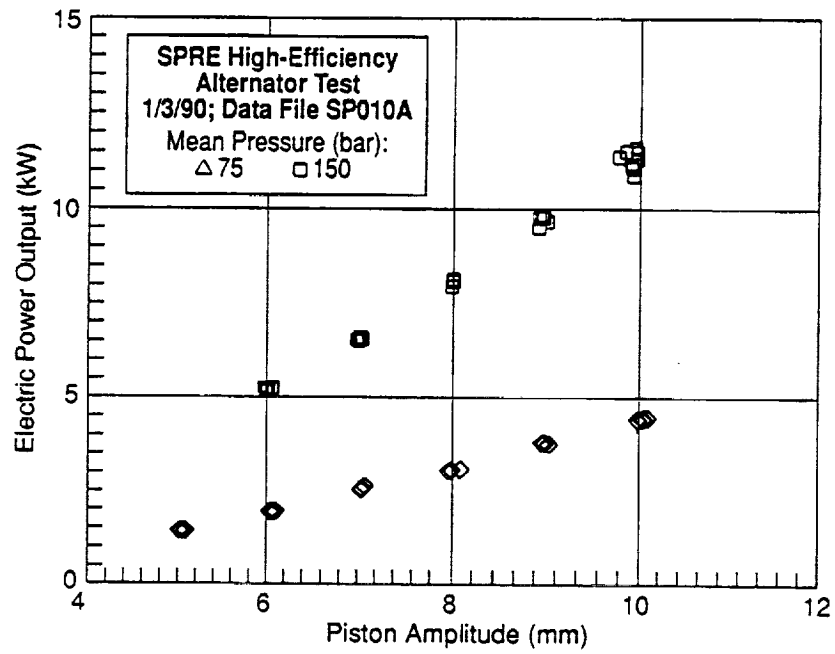




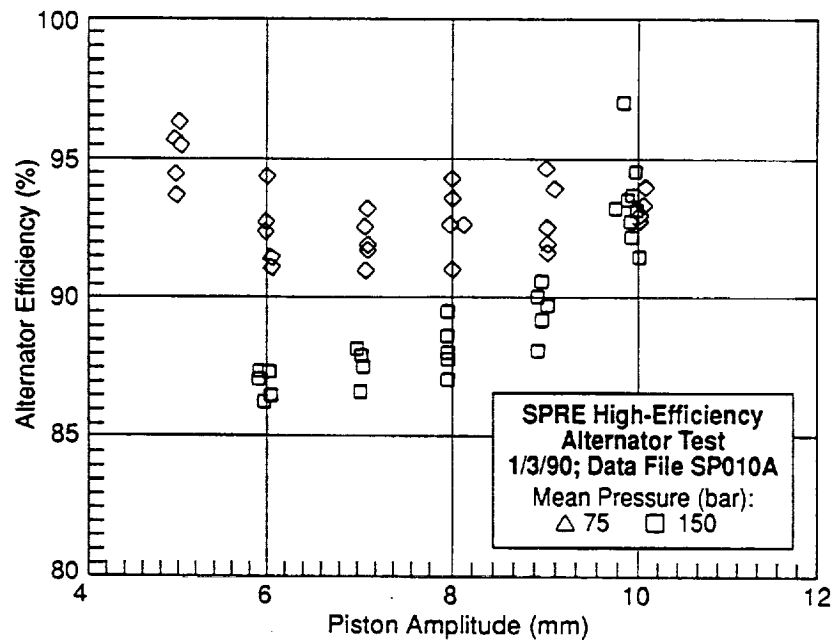
92771



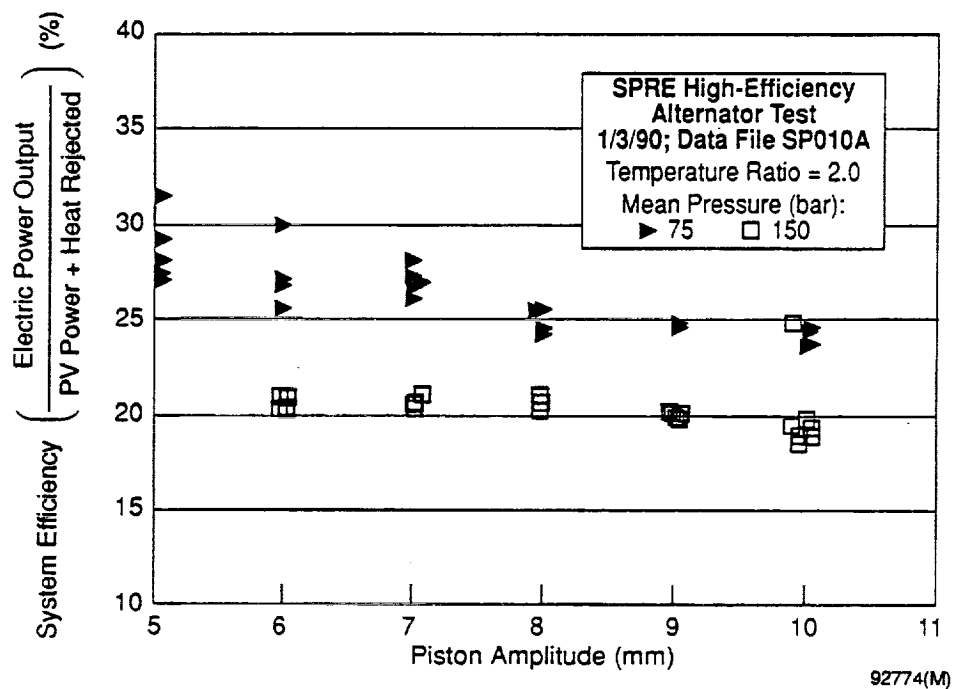
92770



92772



92769



1	0103	1105	7	5093E+06	7	3872E+01	5	0349E-03	5	3855E-03	2	2971E-01	1	6724E+03	1	4983E+03	8	3025E+01	9	5309E-01
2	0103	1106	7	5136E+06	7	3970E+01	5	0194E-03	5	3855E-03	2	2971E-01	1	6724E+03	1	4983E+03	8	3025E+01	9	5309E-01
3	0103	1107	7	5179E+06	7	3878E+01	5	0175E-03	5	3855E-03	2	2971E-01	1	6724E+03	1	4983E+03	8	3025E+01	9	5309E-01
4	0103	1108	7	5205E+06	7	3878E+01	5	0061E-03	5	3855E-03	2	2971E-01	1	6724E+03	1	4983E+03	8	3025E+01	9	5309E-01
5	0103	1109	7	5433E+06	7	3937E+01	5	0039E+00	5	3855E-03	2	2971E-01	1	6724E+03	1	4983E+03	8	3025E+01	9	5309E-01
6	0103	1119	7	5182E+06	7	3785E+01	6	0241E-03	6	1798E-03	6	4530E-01	2	3304E+03	2	0075E+03	8	2819E+01	9	2583E-01
7	0103	1120	7	4896E+06	7	3755E+01	6	0291E-03	6	2389E-03	6	5021E-01	2	3430E+03	2	0099E+03	8	2475E+01	9	1397E-01
8	0103	1121	7	5061E+06	7	3812E+01	6	0046E+00	6	2250E-03	6	4762E-01	2	3668E+03	2	0109E+03	8	2831E+01	9	1560E-01
9	0103	1123	7	5014E+06	7	3825E+01	6	0294E-03	6	1726E-03	6	2449E-01	2	3345E+03	2	0196E+03	8	3183E+01	9	2796E-01
10	0103	1124	7	5173E+06	7	3856E+01	6	0171E-03	6	1662E-03	6	2403E-01	2	3130E+03	2	0070E+03	8	2807E+01	9	4450E-01
11	0103	1131	7	5013E+06	7	3527E+01	7	0456E-03	7	0654E-03	7	5285E-01	2	9908E+03	2	0235E+03	8	2012E+01	9	2299E-01
12	0103	1132	7	4925E+06	7	3719E+01	7	0055E+00	7	0755E-03	7	5285E-01	2	0144E+03	2	0235E+03	8	1895E+01	9	1917E-01
13	0103	1134	7	5037E+06	7	3534E+01	7	0019E+00	7	0495E-03	7	5285E-01	2	0359E+03	2	0235E+03	8	1965E+01	9	1373E-01
14	0103	1135	7	4754E+06	7	3566E+01	7	0194E-03	7	1067E-03	7	5285E-01	2	9908E+03	2	0235E+03	8	1835E+01	9	2277E-01
15	0103	1211	7	5045E+06	7	3674E+01	8	0088E-03	8	0802E-03	8	6215E-01	2	6508E+03	2	0235E+03	8	0946E+01	9	4094E-01
16	0103	1212	7	5163E+06	7	3802E+01	8	0024E+00	8	0408E-03	8	6533E-01	2	7043E+03	2	0235E+03	8	0950E+01	9	2748E-01
17	0103	1213	7	5276E+06	7	3737E+01	8	0046E+00	8	1011E-03	8	6533E-01	2	7043E+03	2	0235E+03	8	0950E+01	9	2748E-01
18	0103	1214	7	4956E+06	7	3685E+01	8	0098E-03	8	0998E-03	8	6025E-01	2	7451E+03	2	0235E+03	8	0807E+01	9	3666E-01
19	0103	1218	7	4824E+06	7	3523E+01	8	0732E-03	8	9597E-03	8	6508E-01	4	4335E+03	4	7722E+03	7	9737E+01	9	4216E-01
20	0103	1220	7	5294E+06	7	3623E+01	9	0232E-03	9	9294E-03	9	6099E-01	4	4390E+03	4	7722E+03	7	9737E+01	9	4770E-01
21	0103	1221	7	5196E+06	7	3696E+01	9	0319E-03	9	9978E-03	9	6833E-01	4	4477E+03	4	7722E+03	7	9655E+01	9	2325E-01
22	0103	1222	7	5108E+06	7	3631E+01	9	0242E-03	9	9240E-03	9	6633E-01	4	4468E+03	4	7722E+03	7	9466E+01	9	2325E-01
23	0103	1223	7	4950E+06	7	3486E+01	9	0032E-03	9	7332E-03	9	6945E-01	4	4577E+03	4	7722E+03	7	7997E+01	9	3339E-01
24	0103	1224	7	5072E+06	7	3517E+01	9	0018E-03	9	7115E-03	9	6799E-01	4	4577E+03	4	7722E+03	7	7997E+01	9	3339E-01
25	0103	1232	7	5206E+06	7	3505E+01	9	0056E-03	9	7344E-03	9	6766E-01	4	4577E+03	4	7722E+03	7	7997E+01	9	3339E-01
26	0103	1233	7	5023E+07	1	0215E+02	6	0233E-03	6	8981E-03	6	4307E-01	6	4892E+03	6	2533E+03	8	6233E+01	8	6721E+01
27	0103	1330	1	5075E+07	1	0221E+02	6	0040E+00	6	8981E-03	6	4307E-01	6	4892E+03	6	2533E+03	8	6233E+01	8	6721E+01
28	0103	1331	1	5004E+07	1	0221E+02	6	0040E+00	6	8981E-03	6	4307E-01	6	4892E+03	6	2533E+03	8	6233E+01	8	6721E+01
29	0103	1332	1	5008E+07	1	0221E+02	6	0040E+00	6	8981E-03	6	4307E-01	6	4892E+03	6	2533E+03	8	6233E+01	8	6721E+01
30	0103	1333	1	4954E+07	1	0208E+02	6	0032E+00	6	8981E-03	6	4307E-01	6	4892E+03	6	2533E+03	8	6233E+01	8	6721E+01
31	0103	1334	1	5027E+07	1	0182E+02	6	0091E+00	6	9713E-03	6	4307E-01	6	4892E+03	6	2533E+03	8	6233E+01	8	6721E+01
32	0103	1340	1	5026E+07	1	0185E+02	6	0082E+00	6	9713E-03	6	4307E-01	6	4892E+03	6	2533E+03	8	6233E+01	8	6721E+01
33	0103	1341	1	5042E+07	1	0185E+02	6	0082E+00	6	9713E-03	6	4307E-01	6	4892E+03	6	2533E+03	8	6233E+01	8	6721E+01
34	0103	1342	1	4984E+07	1	0191E+02	6	0082E+00	6	9713E-03	6	4307E-01	6	4892E+03	6	2533E+03	8	6233E+01	8	6721E+01
35	0103	1343	1	5027E+07	1	0182E+02	6	0091E+00	6	9713E-03	6	4307E-01	6	4892E+03	6	2533E+03	8	6233E+01	8	6721E+01
36	0103	1344	1	5042E+07	1	0185E+02	6	0082E+00	6	9713E-03	6	4307E-01	6	4892E+03	6	2533E+03	8	6233E+01	8	6721E+01
37	0103	1345	1	4984E+07	1	0191E+02	6	0082E+00	6	9713E-03	6	4307E-01	6	4892E+03	6	2533E+03	8	6233E+01	8	6721E+01
38	0103	1346	1	5027E+07	1	0182E+02	6	0091E+00	6	9713E-03	6	4307E-01	6	4892E+03	6	2533E+03	8	6233E+01	8	6721E+01
39	0103	1347	1	5042E+07	1	0185E+02	6	0082E+00	6	9713E-03	6	4307E-01	6	4892E+03	6	2533E+03	8	6233E+01	8	6721E+01
40	0103	1348	1	4984E+07	1	0191E+02	6	0082E+00	6	9713E-03	6	4307E-01	6	4892E+03	6	2533E+03	8	6233E+01	8	6721E+01
41	0103	1350	1	4982E+07	1	0161E+02	6	0047E+00	6	9713E-03	6	4307E-01	6	4892E+03	6	2533E+03	8	6233E+01	8	6721E+01
42	0103	1351	1	5073E+07	1	0159E+02	6	0058E+00	6	9713E-03	6	4307E-01	6	4892E+03	6	2533E+03	8	6233E+01	8	6721E+01
43	0103	1352	1	4948E+07	1	0163E+02	6	0052E+00	6	9713E-03	6	4307E-01	6	4892E+03	6	2533E+03	8	6233E+01	8	6721E+01
44	0103	1353	1	4948E+07	1	0163E+02	6	0052E+00	6	9713E-03	6	4307E-01	6	4892E+03	6	2533E+03	8	6233E+01	8	6721E+01
45	0103	1354	1	5076E+07	1	0162E+02	6	0053E+00	6	9713E-03	6	4307E-01	6	4892E+03	6	2533E+03	8	6233E+01	8	6721E+01
46	0103	1401	1	5026E+07	1	0136E+02	6	0034E+00	6	9384E-03	6	4307E-01	6	4892E+03	6	2533E+03	8	6233E+01	8	6721E+01
47	0103	1402	1	4961E+07	1	0140E+02	6	0043E+00	6	9384E-03	6	4307E-01	6	4892E+03	6	2533E+03	8	6233E+01	8	6721E+01
48	0103	1403	1	5059E+07	1	0131E+02	6	0043E+00	6	9384E-03	6	4307E-01	6	4892E+03	6	2533E+03	8	6233E+01	8	6721E+01
49	0103	1404	1	5022E+07	1	0137E+02	6	0032E+00	6	9384E-03	6	4307E-01	6	4892E+03	6	2533E+03	8	6233E+01	8	6721E+01
50	0103	1405	1	5022E+07	1	0137E+02	6	0032E+00	6	9384E-03	6	4307E-01	6	4892E+03	6	2533E+03	8	6233E+01	8	6721E+01
51	0103	1410	1	4986E+07	1	0127E+02	6	0099E+00	6	9165E-03	6	4307E-01	6	4892E+03	6	2533E+03	8	6233E+01	8	6721E+01
52	0103	1452	1	4986E+07	1	0086E+02	6	0152E+00	6	9065E-03	6	4307E-01	6	4892E+03	6	2533E+03	8	6233E+01	8	6721E+01
53	0103	1456	1	4986E+07	1	0099E+02	6	0099E+00	6	9065E-03	6	4307E-01	6	4892E+03	6	2533E+03	8	6233E+01	8	6721E+01
54	0103	1501	1	5042E+07	1	0083E+02	6	0151E+00	6	9065E-03	6	4307E-01	6	4892E+03	6	2533E+03	8	6233E+01	8	6721E+01
55	0103	1504	1	5022E+07	1	0083E+02	6	0151E+00	6	9065E-03	6	4307E-01	6	4892E+03	6	2533E+03	8	6233E+01	8	6721E+01
56	0103	1504	1	5022E+07	1	0083E+02	6	0151E+00	6	9065E-03	6	4307E-01	6	4892E+03	6	2533E+03	8	6233E+01	8	6721E+01
57	0103	1504	1	5022E+07	1	0083E+02	6	0151E+00	6	9065E-03	6	4307E-01	6	4892E+03	6	2533E+03	8	6233E+01	8	6721E+01
58	0103	1504	1	5022E+07	1	0083E+02	6	0151E+00	6	9065E-03	6	4307E-01	6	4892E+03	6	2533E+03	8	6233E+01	8	6721E+01
59	0103	1504	1	5022E+07	1	0083E+02	6	0151E+00	6	9065E-03	6	4307E-01	6	4892E+03	6	2533E+03	8	6233E+01	8	6721E+01
60	0103	1504	1	5022E+07	1	0083E+02	6	0151E+00	6	9065E-03	6	4307E-01	6	4892E+03	6	2533E+03	8	6233E+01	8	6721E+01
61	0103	1504	1	5022E+07	1	0083E+02	6	0151E+00	6	9065E-03	6	4307E-01	6	4892E+03	6	2533E+03	8	6233E+01	8	6721E+01
62	0103	1504	1	5022E+07	1	0083E+02	6	0151E+00	6	9065E-03	6	4307E-01	6	4892E+03	6	2533E+03	8	6233E+01	8	6721

Data Summary Report from: SP010A at 8:07 AM FRI 5 JAN., 1990 Plot file:

N <sub>0</sub>	Date	Time	PHEAN <sub>3</sub>	FRQ(SUM) <sub>4</sub>	TATQA <sub>5</sub>	XPA <sub>6</sub>	XDA <sub>7</sub>	ETPVC <sub>8</sub>	PUPST <sub>9</sub>	KWALT <sub>10</sub>	XD <sub>11</sub>	3	ETALT <sub>12</sub>
56	0103	1502	1.4967E+07	1.0094E+02	1.9713E+00	9.9233E-03	8.9214E-03	2.121E-01	1.3021E+04	1.0646E+04	8.0733E+01	9.2626E-01	
57	0103	1512	1.5036E+07	1.0094E+02	1.9830E+00	9.9233E-03	8.7880E-03	2.1631E-01	1.3021E+04	1.0646E+04	8.1311E+01	9.1956E-01	
58	0103	1514	1.5036E+07	1.0094E+02	1.9906E+00	9.9233E-03	8.7892E-03	2.1860E-01	1.3033E+04	1.0947E+04	8.1559E+01	9.4064E-01	
59	0103	1516	1.5054E+07	1.0114E+02	1.9982E+00	9.9532E-03	8.8221E-03	2.2177E-01	1.3196E+04	1.1180E+04	8.1225E+01	9.3610E-01	
60	0103	1517	1.5058E+07	1.0099E+02	1.9996E+00	9.9417E-03	8.6599E-03	2.1889E-01	1.3092E+04	1.0927E+04	8.1816E+01	9.2239E-01	
61	0103	1518	1.5116E+07	1.0121E+02	2.0024E+00	9.9338E-03	8.7512E-03	2.2141E-01	1.3307E+04	1.1180E+04	8.1544E+01	9.2688E-01	
62	0103	1519	1.5147E+07	1.0126E+02	2.0037E+00	1.0020E-02	8.6732E-03	2.2298E-01	1.3635E+04	1.1478E+04	8.0829E+01	9.3198E-01	
63	0103	1520	1.5035E+07	1.0138E+02	2.0074E+00	9.8728E-03	8.6571E-03	2.2338E-01	1.3383E+04	1.1341E+04	8.1781E+01	9.2802E-01	
64	0103	1521	1.5068E+07	1.0124E+02	2.0074E+00	1.0015E-02	8.9069E-03	2.2514E-01	1.3695E+04	1.1575E+04	8.1695E+01	9.2313E-01	
66	0103	1522	1.5005E+07	1.0110E+02	2.0095E+00	9.9771E-03	8.8230E-03	2.2676E-01	1.3461E+04	1.1490E+04	8.1053E+01	9.4508E-01	
67	0103	1523	1.4927E+07	1.0108E+02	2.0057E+00	9.9804E-03	8.8461E-03	2.2249E-01	1.3553E+04	1.1427E+04	8.1156E+01	9.3746E-01	
68	0103	1524	1.5053E+07	1.0105E+02	2.0080E+00	1.0016E-02	8.8161E-03	2.2866E-01	1.3615E+04	1.1261E+04	8.1675E+01	9.1473E-01	



No Date Time PNEAN<sub>3</sub> FRQ(SVH)<sub>4</sub> ETSYS<sub>5</sub> PWAPS<sub>6</sub> PALTS<sub>7</sub> XPL<sub>8</sub> 1 XPL<sub>9</sub> 2 XDL<sub>10</sub> 1 XDL<sub>11</sub> 2 PWDGAS<sub>12</sub>

1	0003	1105	7	5093E+06	2	3879E+01	2	7577E-01	1	3200E+02	1	5527E+03	7	5613E-04	0348E-03	5	0194E-03	3	5162E-04	9	7395E+00
2	0003	1106	7	5263E+06	7	3936E+01	7	8233E-01	1	0400E+02	1	5624E+03	7	6663E-04	0194E-03	5	0194E-03	3	5162E-04	9	7395E+00
3	0003	1108	7	5050E+06	7	4078E+01	7	1380E-01	1	1040E+02	1	5885E+03	7	6029E-04	0175E-03	5	0175E-03	3	5443E-04	9	7300E+00
4	0003	1109	7	5433E+06	7	3917E+01	7	7255E-01	1	271E+02	1	5774E+03	7	6250E-04	0463E-03	5	0463E-03	3	0667E-04	9	9000E+00
6	0000	1100	7	5182E+06	7	3789E+01	7	7090E-01	1	502E+02	1	0979E+03	8	8710E-04	0241E-03	6	0241E-03	4	0788E-04	1	3675E+01
7	0000	1101	7	5086E+06	7	3772E+01	7	5671E-01	1	507E+02	1	0933E+03	8	8357E-04	0291E-03	6	0291E-03	4	8636E-04	1	3780E+01
8	0000	1102	7	5061E+06	7	3813E+01	7	6770E-01	1	506E+02	1	0917E+03	8	8343E-04	0294E-03	6	0294E-03	4	9203E-04	1	3702E+01
9	0000	1103	7	5037E+06	7	3855E+01	7	6921E-01	1	504E+02	1	0912E+03	8	8340E-04	0294E-03	6	0294E-03	4	9235E-04	1	3702E+01
10	0000	1104	7	5037E+06	7	3855E+01	7	6921E-01	1	504E+02	1	0912E+03	8	8340E-04	0294E-03	6	0294E-03	4	9235E-04	1	3702E+01
11	0000	1105	7	5013E+06	7	3823E+01	7	7594E-01	2	2300E+02	2	7586E+03	3	5921E-04	0455E-03	7	0455E-03	7	1211E-04	1	8133E+01
12	0000	1106	7	5029E+06	7	3768E+01	7	6850E-01	2	2348E+02	2	7577E+03	3	5921E-04	0455E-03	7	0455E-03	7	1211E-04	1	8133E+01
13	0000	1107	7	5029E+06	7	3768E+01	7	6850E-01	2	2348E+02	2	7577E+03	3	5921E-04	0455E-03	7	0455E-03	7	1211E-04	1	8133E+01
14	0000	1108	7	5029E+06	7	3768E+01	7	6850E-01	2	2348E+02	2	7577E+03	3	5921E-04	0455E-03	7	0455E-03	7	1211E-04	1	8133E+01
15	0000	1109	7	5029E+06	7	3768E+01	7	6850E-01	2	2348E+02	2	7577E+03	3	5921E-04	0455E-03	7	0455E-03	7	1211E-04	1	8133E+01
16	0000	1110	7	5047E+06	7	3674E+01	7	7940E-01	2	2300E+02	2	7586E+03	3	5921E-04	0455E-03	7	0455E-03	7	1211E-04	1	8133E+01
17	0000	1111	7	5047E+06	7	3674E+01	7	7940E-01	2	2300E+02	2	7586E+03	3	5921E-04	0455E-03	7	0455E-03	7	1211E-04	1	8133E+01
18	0000	1112	7	5047E+06	7	3674E+01	7	7940E-01	2	2300E+02	2	7586E+03	3	5921E-04	0455E-03	7	0455E-03	7	1211E-04	1	8133E+01
19	0000	1113	7	5047E+06	7	3674E+01	7	7940E-01	2	2300E+02	2	7586E+03	3	5921E-04	0455E-03	7	0455E-03	7	1211E-04	1	8133E+01
20	0000	1114	7	5047E+06	7	3674E+01	7	7940E-01	2	2300E+02	2	7586E+03	3	5921E-04	0455E-03	7	0455E-03	7	1211E-04	1	8133E+01
21	0000	1115	7	5047E+06	7	3674E+01	7	7940E-01	2	2300E+02	2	7586E+03	3	5921E-04	0455E-03	7	0455E-03	7	1211E-04	1	8133E+01
22	0000	1116	7	5047E+06	7	3674E+01	7	7940E-01	2	2300E+02	2	7586E+03	3	5921E-04	0455E-03	7	0455E-03	7	1211E-04	1	8133E+01
23	0000	1117	7	5047E+06	7	3674E+01	7	7940E-01	2	2300E+02	2	7586E+03	3	5921E-04	0455E-03	7	0455E-03	7	1211E-04	1	8133E+01
24	0000	1118	7	5047E+06	7	3674E+01	7	7940E-01	2	2300E+02	2	7586E+03	3	5921E-04	0455E-03	7	0455E-03	7	1211E-04	1	8133E+01
25	0000	1119	7	5047E+06	7	3674E+01	7	7940E-01	2	2300E+02	2	7586E+03	3	5921E-04	0455E-03	7	0455E-03	7	1211E-04	1	8133E+01
26	0000	1120	7	5047E+06	7	3674E+01	7	7940E-01	2	2300E+02	2	7586E+03	3	5921E-04	0455E-03	7	0455E-03	7	1211E-04	1	8133E+01
27	0000	1121	7	5047E+06	7	3674E+01	7	7940E-01	2	2300E+02	2	7586E+03	3	5921E-04	0455E-03	7	0455E-03	7	1211E-04	1	8133E+01
28	0000	1122	7	5047E+06	7	3674E+01	7	7940E-01	2	2300E+02	2	7586E+03	3	5921E-04	0455E-03	7	0455E-03	7	1211E-04	1	8133E+01
29	0000	1123	7	5047E+06	7	3674E+01	7	7940E-01	2	2300E+02	2	7586E+03	3	5921E-04	0455E-03	7	0455E-03	7	1211E-04	1	8133E+01
30	0000	1124	7	5047E+06	7	3674E+01	7	7940E-01	2	2300E+02	2	7586E+03	3	5921E-04	0455E-03	7	0455E-03	7	1211E-04	1	8133E+01
31	0000	1125	7	5047E+06	7	3674E+01	7	7940E-01	2	2300E+02	2	7586E+03	3	5921E-04	0455E-03	7	0455E-03	7	1211E-04	1	8133E+01
32	0000	1126	7	5047E+06	7	3674E+01	7	7940E-01	2	2300E+02	2	7586E+03	3	5921E-04	0455E-03	7	0455E-03	7	1211E-04	1	8133E+01
33	0000	1127	7	5047E+06	7	3674E+01	7	7940E-01	2	2300E+02	2	7586E+03	3	5921E-04	0455E-03	7	0455E-03	7	1211E-04	1	8133E+01
34	0000	1128	7	5047E+06	7	3674E+01	7	7940E-01	2	2300E+02	2	7586E+03	3	5921E-04	0455E-03	7	0455E-03	7	1211E-04	1	8133E+01
35	0000	1129	7	5047E+06	7	3674E+01	7	7940E-01	2	2300E+02	2	7586E+03	3	5921E-04	0455E-03	7	0455E-03	7	1211E-04	1	8133E+01
36	0000	1130	7	5047E+06	7	3674E+01	7	7940E-01	2	2300E+02	2	7586E+03	3	5921E-04	0455E-03	7	0455E-03	7	1211E-04	1	8133E+01
37	0000	1131	7	5047E+06	7	3674E+01	7	7940E-01	2	2300E+02	2	7586E+03	3	5921E-04	0455E-03	7	0455E-03	7	1211E-04	1	8133E+01
38	0000	1132	7	5047E+06	7	3674E+01	7	7940E-01	2	2300E+02	2	7586E+03	3	5921E-04	0455E-03	7	0455E-03	7	1211E-04	1	8133E+01
39	0000	1133	7	5047E+06	7	3674E+01	7	7940E-01	2	2300E+02	2	7586E+03	3	5921E-04	0455E-03	7	0455E-03	7	1211E-04	1	8133E+01
40	0000	1134	7	5047E+06	7	3674E+01	7	7940E-01	2	2300E+02	2	7586E+03	3	5921E-04	0455E-03	7	0455E-03	7	1211E-04	1	8133E+01
41	0000	1135	7	5047E+06	7	3674E+01	7	7940E-01	2	2300E+02	2	7586E+03	3	5921E-04	0455E-03	7	0455E-03	7	1211E-04	1	8133E+01
42	0000	1136	7	5047E+06	7	3674E+01	7	7940E-01	2	2300E+02	2	7586E+03	3	5921E-04	0455E-03	7	0455E-03	7	1211E-04	1	8133E+01
43	0000	1137	7	5047E+06	7	3674E+01	7	7940E-01	2	2300E+02	2	7586E+03	3	5921E-04	0455E-03	7	0455E-03	7	1211E-04	1	8133E+01
44	0000	1138	7	5047E+06	7	3674E+01	7	7940E-01	2	2300E+02	2	7586E+03	3	5921E-04	0455E-03	7	0455E-03	7	1211E-04	1	8133E+01
45	0000	1139	7	5047E+06	7	3674E+01	7	7940E-01	2	2300E+02	2	7586E+03	3	5921E-04	0455E-03	7	0455E-03	7	1211E-04	1	8133E+01
46	0000	1140	7	5047E+06	7	3674E+01	7	7940E-01	2	2300E+02	2	7586E+03	3	5921E-04	0455E-03	7	0455E-03	7	1211E-04	1	8133E+01
47	0000	1141	7	5047E+06	7	3674E+01	7	7940E-01	2	2300E+02	2	7586E+03	3	5921E-04	0455E-03	7	0455E-03	7	1211E-04	1	8133E+01
48	0000	1142	7	5047E+06	7	3674E+01	7	7940E-01	2	2300E+02	2	7586E+03	3	5921E-04	0455E-03	7	0455E-03	7	1211E-04	1	8133E+01
49	0000	1143	7	5047E+06	7	3674E+01	7	7940E-01	2	2300E+02	2	7586E+03	3	5921E-04	0455E-03	7	0455E-03	7	1211E-04	1	8133E+01
50	0000	1144	7	5047E+06	7	3674E+01	7	7940E-01	2	2300E+02	2	7586E+03	3	5921E-04	0455E-03	7	0455E-03	7	1211E-04	1	8133E+01
51	0000	1145	7	5047E+06	7	3674E+01	7	7940E-01	2	2300E+02	2	7586E+03	3	5921E-04	0455E-03	7	0455E-03	7	1211E-04	1	8133E+01
52	0000	1146	7	5047E+06	7	3674E+01	7	7940E-01	2	2300E+02	2	7586E+03	3	5921E-04	0455E-03	7	0455E-03	7	1211E-04	1	8133E+01
53	0000	1147	7	5047E+06	7	3674E+01	7	7940E-01	2	2300E+02	2	7586E+03	3	5921E-04	0455E-03	7	0455E-03	7	1211E-04	1	8133E+01
54	0000	1148	7	5047E+06	7	3674E+01	7	7940E-01	2	2300E+02	2	7586E+03	3	5921E-04	0455E-03	7	0455E-03	7	1211E-04	1	8133E+01
55	0000	1149	7	5047E+06	7	3674E+01	7	7940E-01	2	2300E+02	2	7586E+03	3	5921E-04	0455E-03	7	0455E-03	7	1211E-04	1	8133E+01
56	0000	1150	7	5047E+06	7	3674E+01	7	7940E-01	2	2300E+02	2	7586E+03	3	5921E-04	0455E-03	7	0455E-03	7	1211E-04	1	8133E+01
57	0000	1151	7	5047E+06	7	3674E+01	7	7940E-01	2	2300E+02	2	7586E+03	3	5921E-04	0455E-03	7	0455E-03	7	1211E-04	1	8133E+01
58	0000	1152	7	5047E+06	7	3674E+01	7	7940E-01	2	2300E+02	2	7586E+03	3	5921E-04	0455E-03	7	0455E-03	7	1211E-04	1	8133E+01
59	0000	1153	7	5047E+06	7	3674E+01	7	7940E-01	2	2300E+02	2	7586E+03	3	5921E-04	0455E-03	7	0455E-03	7	1211E-04	1	8133E+01
60	0000	1154	7	5047E+0																	

Data Summary Report from: SP010A at 8:07 AM FRI. 5 JAN. 1990 Plot file: PF2

No	Date	Time	PMEAN <sub>3</sub>	FRQ(SUM) <sub>4</sub>	ETBS <sub>5</sub>	PWAPS <sub>6</sub>	PALTS <sub>7</sub>	XPL <sub>8</sub>	XPL <sub>9</sub>	XDL <sub>10</sub>	XDL <sub>11</sub>	PWDGAS <sub>12</sub>
54	0103	1509	1.4967E+07	1.0094E+02	1.733E-01	1.151E+03	1.149E+04	-1.302E-03	9.923E-03	-2.291E-04	8.921E-03	8.328E+01
55	0103	1512	1.5029E+07	1.0093E+02	1.858E-01	1.182E+03	1.175E+04	-1.322E-03	9.923E-03	-2.376E-04	8.780E-03	8.162E+01
56	0103	1514	1.5036E+07	1.0094E+02	1.892E-01	1.215E+03	1.163E+04	-1.321E-03	9.923E-03	-2.519E-04	8.782E-03	8.176E+01
57	0103	1516	1.5094E+07	1.0114E+02	1.881E-01	1.169E+03	1.194E+04	-1.308E-03	9.952E-03	-2.485E-04	8.825E-03	8.273E+01
58	0103	1517	1.5058E+07	1.0092E+02	1.850E-01	1.165E+03	1.184E+04	-1.307E-03	9.941E-03	-2.908E-04	8.659E-03	8.087E+01
61	0103	1519	1.5115E+07	1.0121E+02	1.897E-01	1.162E+03	1.206E+04	-1.327E-03	9.938E-03	-2.534E-04	8.751E-03	8.215E+01
62	0103	1519	1.5142E+07	1.0132E+02	1.887E-01	1.137E+03	1.231E+04	-1.357E-03	9.908E-03	-2.224E-04	8.673E-03	8.397E+01
63	0103	1519	1.5035E+07	1.0132E+02	1.945E-01	1.130E+03	1.215E+04	-1.353E-03	9.858E-03	-2.292E-04	8.757E-03	8.154E+01
64	0103	1520	1.5138E+07	1.0120E+02	2.497E-01	1.139E+03	1.187E+04	-1.360E-03	9.870E-03	-2.705E-04	8.857E-03	8.252E+01
65	0103	1521	1.5068E+07	1.0124E+02	1.948E-01	1.183E+03	1.242E+04	-1.297E-03	1.001E-02	-1.825E-04	8.906E-03	8.438E+01
66	0103	1522	1.5005E+07	1.0110E+02	1.987E-01	1.219E+03	1.215E+04	-1.317E-03	9.977E-03	-2.055E-04	8.823E-03	8.281E+01
67	0103	1523	1.4975E+07	1.0108E+02	1.912E-01	1.280E+03	1.231E+04	-1.333E-03	9.904E-03	-2.688E-04	8.864E-03	8.507E+01
68	0103	1524	1.5055E+07	1.0108E+02	1.943E-01	1.230E+03	1.231E+04	-1.335E-03	1.001E-02	-2.816E-04	8.861E-03	8.307E+01

CELL 5 - REGENERATOR TEST - CH0550 091212.1525:  
MEASUREMENT SCAN. 28 1-2, 190 12:29:14 ( FILE SP010A )

DYNAMIC RESULTS FROM SUM'S

NSIG	TITLE	MEAN	AMP	PHASE1	PHASE2
1	XPL	-1.4520E-04	1.0018E-03	0.0000E+00	-7.7559E+01
2	XPL	-3.4069E-03	9.2157E-03	9.7659E+01	-0.0000E+00
3	PCL	7.4566E+04	9.1637E+03	-8.6257E+01	-8.6257E+01
4	PES	-7.9432E+04	5.8468E+03	9.1637E+01	-8.6257E+01
5	PAPSD	-2.0402E+05	3.1892E+03	9.1637E+01	-8.6257E+01
6	PAPSD	-5.4715E+05	3.1892E+03	9.1637E+01	-8.6257E+01
7	PAPSD	-5.0416E+05	1.0020E+03	9.1637E+01	-8.6257E+01
8	ITALD	-5.8586E-02	4.1920E+01	9.1637E+01	-8.6257E+01
9	VLD	-5.4819E-01	2.6628E+02	9.1637E+01	-8.6257E+01
10	UCAPD	-2.2502E-01	2.0818E+02	9.1637E+01	-8.6257E+01
11	ACABE	-1.1162E-01	1.7539E+02	9.1637E+01	-8.6257E+01
12	ACABE	-1.9610E+02	1.9535E-04	9.1637E+01	-8.6257E+01
13	XDCLK	-2.4217E-03	9.2360E-03	9.1637E+01	-8.6257E+01
14	--OPEN--	-2.1301E-10	2.2195E-09	9.1637E+01	-8.6257E+01

STEADY STATE MEASUREMENTS FROM COUNTER & DVM

NSIG	TITLE	FREQ(SUM)	FREQ(DVM)	PMEAN	PBRNGP	PBRNGD
21	XPL	7.3618E+01	2.0000E+15	7.5077E+06	8.2553E+06	8.2553E+06
22	XPL(M)	-1.6550E-03	-2.643E-03	1.5400E-05	1.9942E-02	1.932E-02
23	ACABE	1.3858E+03	4.4354E+03	1.9421E+02	1.2467E+02	1.4689E+02
24	ITAL	2.9617E+01	2.8049E-02	1.3372E+02	4.6000E-01	5.1318E+04
25	FLEH	1.7357E+00	1.1527E+00	3.0720E-01	2.8650E+00	2.9250E+00
26	THTRQ	3.1175E+02	3.0460E+02	2.6860E+01	3.0833E+02	1.0147E+01
27	TPACI	1.0280E+01	1.0283E+01	2.4009E+00	3.6899E+00	3.2310E-01
28	DTAPAC	3.2561E-01	3.0537E+01	2.3154E+00	2.5336E+01	3.084E+02
29	TRECI	1.0200E+01	1.3263E+01	1.0253E+01	1.0299E+01	-3.7869E+00
30	DTRECI	3.4868E+00	6.0726E-01	3.5567E-01	3.7067E-01	2.9527E+02
31	TCSRPE	2.7448E+02	3.0100E+02	-4.3868E+02	1.7911E+01	4.6888E+01
32	TCHRL1	2.5333E+02	2.5701E+02	2.3933E+02	6.0523E+01	4.7486E+01
33	TCCR6	4.5477E+01	5.9894E+00	1.9725E+00	-1.0000E+03	-1.5035E+00
34	TPOST6	8.1579E+00	3.2196E+00	1.7919E+01	1.1397E+01	6.0532E+00
35	TEDSW	1.3606E+01	1.7250E+01	1.0126E+02	6.0176E+00	-2.1459E+01
36	TPOS12	-4.1713E+01	-1.5069E+02	4.0160E-02	0.0000E+00	0.0000E+00

CELL 5 - REGENERATOR TEST - CHN540 (891212 1525  
MEASUREMENT SCAN 67 1-3-1990 15:23:37 (FILE: SP010A )

# DYNAMIC RESULTS FROM SUM'S

NSIG	TITLE	MEAN	AMP	PHASE1	PHASE2
1	XPL	-1.5220E-03	9.9804E-03	0.0000E+00	-8.1356E-01
2	XDL	-2.6829E-04	8.8351E-03	0.0000E+00	-8.0000E+01
3	PCL	-1.4132E-06	2.0357E-06	9.1155E+00	-9.8486E+01
4	PES	-1.0077E+05	1.5800E+03	3.9323E+02	5.8199E+00
5	PAPSP	-2.1909E+06	1.540E+06	1.3544E+01	-3.1977E+00
6	PFSD	-2.1214E+05	2.3571E+05	-1.2886E+02	-2.5922E+02
7	IATD	-2.1214E+05	7.4874E+01	9.3317E+01	-1.7404E+02
8	VALT	-7.1300E-02	4.6912E+02	3.8970E+01	-1.2061E+01
9	ULD	-9.6237E-03	3.0169E+02	3.3110E+01	-1.1954E+01
10	VCAPD	-3.2828E-02	3.9908E+02	2.8260E+00	-7.8330E+01
11	ACASE	-1.9610E+02	2.9590E-04	8.1514E-01	-8.0441E-01
12	XDACK	-2.5131E-04	8.6419E-03	8.1444E+01	-8.8755E-01
13	--OPEN--	1.5064E-10	1.9073E-09	4.2979E+01	0.0000E+00
14					

# STEADY STATE MEASUREMENTS FROM COUNTER & DUM

NSIG	TITLE	MEAN	PMEAN	PBRNGD
21	FRO(DUM)	2.0000E+15	1.4977E+07	1.6039E+07
22	XPL(M)	9.0438E-04	1.4740E-05	1.7590E-02
23	ACCXC(A)	1.1427E+04	3.5654E+02	2.8545E+02
24	IATL	2.7579E-02	1.2187E+02	7.7818E+04
25	FLEH	1.1733E+00	3.012E-01	2.6710E+00
26	THRO	3.6565E+02	2.7914E+01	3.9371E+01
27	TPACI	3.0391E+01	-1.2432E+01	1.1853E+01
28	DIPARC	7.0847E+01	3.8237E+00	2.6333E+01
29	TRECI	3.9908E+01	3.0346E+01	3.0346E+01
30	DIPAC	1.2642E+00	1.4724E+00	1.5756E+00
31	TCSEF2	3.5749E+02	3.2750E+02	3.5228E+02
32	TCSEF1	2.9755E+02	2.5974E+02	3.5228E+02
33	TCSEF	4.2013E+01	3.1461E+01	3.7339E+02
34	TPOST	5.1478E+00	2.6501E+01	8.8480E+01
35	TPDSH	6.7107E+01	-1.2492E+02	4.4771E+01
36	TPDSH12	-9.7478E+02	4.0411E-02	0.0000E+00

## CONSTANTS

CELL 5 - REGENERATOR TEST - CHS60 (891212 1525)  
MEASUREMENT SCAN 67 1-3 1990 15 23 37 ( FILE SP010A )

CALCULATIONS, ΔCELLS REVISION: K									
-1	TPHWH	3.637E+02	3.637E+02	3.637E+02	3.637E+02	3.637E+02	3.637E+02	3.637E+02	3.637E+02
-2	TPHWH	3.637E+02	3.637E+02	3.637E+02	3.637E+02	3.637E+02	3.637E+02	3.637E+02	3.637E+02
-3	TRTOP	4.426E+01	4.426E+01	4.426E+01	4.426E+01	4.426E+01	4.426E+01	4.426E+01	4.426E+01
-4	TRTOP	2.006E+00	2.006E+00	2.006E+00	2.006E+00	2.006E+00	2.006E+00	2.006E+00	2.006E+00
-5	TRTOP	2.077E+00	2.077E+00	2.077E+00	2.077E+00	2.077E+00	2.077E+00	2.077E+00	2.077E+00
-6	TRTOP	1.330E-03	1.330E-03	1.330E-03	1.330E-03	1.330E-03	1.330E-03	1.330E-03	1.330E-03
-7	TRTOP	9.994E+01	9.994E+01	9.994E+01	9.994E+01	9.994E+01	9.994E+01	9.994E+01	9.994E+01
-8	TRTOP	1.269E+03	1.269E+03	1.269E+03	1.269E+03	1.269E+03	1.269E+03	1.269E+03	1.269E+03
-9	TRTOP	2.783E+02	2.783E+02	2.783E+02	2.783E+02	2.783E+02	2.783E+02	2.783E+02	2.783E+02
-10	TRTOP	1.280E+03	1.280E+03	1.280E+03	1.280E+03	1.280E+03	1.280E+03	1.280E+03	1.280E+03
-11	TRTOP	5.978E+04	5.978E+04	5.978E+04	5.978E+04	5.978E+04	5.978E+04	5.978E+04	5.978E+04
-12	TRTOP	5.978E+04	5.978E+04	5.978E+04	5.978E+04	5.978E+04	5.978E+04	5.978E+04	5.978E+04
-13	TRTOP	5.978E+04	5.978E+04	5.978E+04	5.978E+04	5.978E+04	5.978E+04	5.978E+04	5.978E+04
-14	TRTOP	5.978E+04	5.978E+04	5.978E+04	5.978E+04	5.978E+04	5.978E+04	5.978E+04	5.978E+04
-15	TRTOP	5.978E+04	5.978E+04	5.978E+04	5.978E+04	5.978E+04	5.978E+04	5.978E+04	5.978E+04
-16	TRTOP	5.978E+04	5.978E+04	5.978E+04	5.978E+04	5.978E+04	5.978E+04	5.978E+04	5.978E+04
-17	TRTOP	5.978E+04	5.978E+04	5.978E+04	5.978E+04	5.978E+04	5.978E+04	5.978E+04	5.978E+04
0	DRD	4.572E-02	4.572E-02	4.572E-02	4.572E-02	4.572E-02	4.572E-02	4.572E-02	4.572E-02
0	HP1ST	9.968E+00	9.968E+00	9.968E+00	9.968E+00	9.968E+00	9.968E+00	9.968E+00	9.968E+00
0	PCG	5.000E-01	5.000E-01	5.000E-01	5.000E-01	5.000E-01	5.000E-01	5.000E-01	5.000E-01
0	1.953E+01	5.330E+02	5.330E+02	5.330E+02	5.330E+02	5.330E+02	5.330E+02	5.330E+02	5.330E+02

## REFERENCES

- Brown, A. "Space Power Demonstrator Engine - Phase I Final Report." NASA Contractor Report No. 179555, MTI Report No. 87TR36 (May 1987).
- Dochat, G. "Stirling Space Power Demonstrator Engine Test/Analytical Comparison." ACTA Astronautica 15, no. 6/7 (1987): 341-46.
- Dochat, G. "Development Status: Stirling Space Power Demonstrator Engine." AIAA Paper 86-1167-CP, Space System Technology Conference, San Diego, CA (June 1986).
- Hull, D. R., Alger, D. L., Moore, T. J., and Scheuermann, C. M. "Fatigue Failure of Regenerator Screens in a High-Frequency Stirling Engine." NASA TM 88974 (March 1987).
- Rauch, J., Bolta, R., and Short, H. "SPRE Alternator Dynamometer Test." NASA Contractor Report No. 182251, MTI Report No. 90TR15 (February 1990).
- Rauch, J. "SPRE-I Acceptance Test". MTI Report No. 87TR59 (July 1987).
- Spelter, S., and Dhar, M. "Space Power Research Engine Power Piston Hydrodynamic Bearing Technology Development." NASA Contractor Report 182136, MTI Report No. 88TR32 (December 1989).

REPORT DOCUMENTATION PAGE			Form Approved OMB No. 0704-0188	
Public reporting burden for this collection of information is estimated to average 1 hour per response, including the time for reviewing instructions, searching existing data sources, gathering and maintaining the data needed, and completing and reviewing the collection of information. Send comments regarding this burden estimate or any other aspect of this collection of information, including suggestions for reducing this burden, to Washington Headquarters Services, Directorate for Information Operations and Reports, 1215 Jefferson Davis Highway, Suite 1204, Arlington, VA 22202-4302, and to the Office of Management and Budget, Paperwork Reduction Project (0704-0188), Washington, DC 20503.				
1. AGENCY USE ONLY (Leave blank)		2. REPORT DATE September 1993		3. REPORT TYPE AND DATES COVERED Final Contractor Report
4. TITLE AND SUBTITLE  SPDE/SPRE Final Summary Report			5. FUNDING NUMBERS  WU-590-13-11 C-NAS3-23883	
6. AUTHOR(S)  George Dochat				
7. PERFORMING ORGANIZATION NAME(S) AND ADDRESS(ES)  Mechanical Technology Incorporated 968 Albany-Shaker Road Latham, New York 12110			8. PERFORMING ORGANIZATION REPORT NUMBER  E-8126	
9. SPONSORING/MONITORING AGENCY NAME(S) AND ADDRESS(ES)  National Aeronautics and Space Administration Lewis Research Center Cleveland, Ohio 44135-3191			10. SPONSORING/MONITORING AGENCY REPORT NUMBER  NASA CR-187086	
11. SUPPLEMENTARY NOTES  Project Manager, James E. Dudenhofer, Power Technology Division, (216) 977-1146.				
12a. DISTRIBUTION/AVAILABILITY STATEMENT  Unclassified - Unlimited Subject Category 20			12b. DISTRIBUTION CODE	
13. ABSTRACT (Maximum 200 words)  Mechanical Technology Incorporated (MTI) performed acceptance testing on the Space Power Research Engine (SPRE), which demonstrated satisfactory operation and sufficient reliability for delivery to NASA Lewis Research Center. The unit produced 13.5 kW PV power with an efficiency of 22% versus design goals of 28.8 kW PV power and efficiency of 28%. Maximum electric power was only 8 kW <sub>e</sub> due to lower alternator efficiency. One of the major shortcomings of the SPRE was linear alternator efficiency, which was only 70% compared to a design value of 90%. It was determined from static tests that the major cause for the efficiency shortfall was the location of the magnetic structure surrounding the linear alternator. Testing of an alternator configuration without a surrounding magnetic structure on a linear dynamometer confirmed earlier static test results. Linear alternator efficiency improved from 70% to over 90%. Testing of the MTI SPRE was also performed with hydrodynamic bearings and achieved full-stroke, stable operation. This testing indicated that hydrodynamic bearings may be useful in free-piston Stirling engines. An important factor in achieving stable operation at design stroke was isolating a portion of the bearing length from the engine pressure variations. In addition, the heat pipe heater head design indicates that integration of a Stirling engine with a heat source can be performed via heat pipes. This design will provide a baseline against which alternative designs can be measured.				
14. SUBJECT TERMS  Stirling; Space power; Free piston			15. NUMBER OF PAGES 111	
			16. PRICE CODE A06	
17. SECURITY CLASSIFICATION OF REPORT Unclassified	18. SECURITY CLASSIFICATION OF THIS PAGE Unclassified	19. SECURITY CLASSIFICATION OF ABSTRACT Unclassified	20. LIMITATION OF ABSTRACT	